ALMA MATER STUDIORUM · UNIVERSITÀ DI BOLOGNA

FACOLTÀ DI SCIENZE MATEMATICHE, FISICHE E NATURALI

Dottorato di ricerca in matematica

XXI ciclo

Settore Scientifico-Disciplinare: MAT/03

Shape from Functions: Enhancing Geometrical-Topological Descriptors

Tesi di Dottorato

di

Barbara Di Fabio

Relatori:
Prof. Massimo Ferri
D.ssa Claudia Landi

Coordinatore:
Prof. Alberto Parmeggiani

Parole chiave: Shape comparison, size function, natural pseudo-distance, persistent homology module, Čech homology, shape occlusion.

ESAME FINALE ANNO 2009

A zia Laura

Introduction

Outline. “Shape from X” is a common expression in computer vision and pattern recognition that means extracting knowledge, about the shape of an object in the scene, from some of the features of its image(s), be it shading, texture, disparity, motion, etc. In this thesis we focus on a class of methods for shape understanding whose main peculiarity consists in linking the concept itself of shape to perceptual instances relative to the observer [6]. Mathematically, these are formalized as particular functions defined on the shape, whence the neologism we have chosen: *shape from functions*.

Shape analysis and understanding are very hot research topics for the disciplines of computer vision, computer graphics and pattern recognition, finding their motivations in diverse application areas, such as geometric modeling, visual perception, medical imaging, and structural molecular biology.

The last decade has been characterized by an explosion in the number of methods proposed for solving problems related to shape recognition, classification and matching, because of an incremental growth of digital models. The most popular recognition techniques can be mainly divided into two classes: model-based and aspect-based techniques [61]. Model-based techniques are object-centered and are focused on the *representation* of a shape looking for effective and perceptually important shape features based on either shape boundary information or boundary plus interior content. Aspect-based techniques are viewer-centered and are focused on the *description* of a shape on the basis of its shape features perceived by the viewer.

Recently, the research interest in Computer Graphics has gradually moved from methods to *represent* shapes towards methods to *describe* shapes. Indeed, the representation of an object is detailed and accurate, but it does not explicitly contain any high-level information on the shape of the object. Conversely, the description is concise but conveys an elaborate and composite view of the object identity.

A variety of methods have been proposed in the literature to deal with the problem of shape description and reasoning. To this scope mathematics has been confirmed to provide a suitable setting for formalizing and solving several problems related to shape description, analysis and understanding. In particular, the potential of approaches based on differential topology have been recently recognized by researchers in computer graphics, who gave birth to a new branch of computational mathematics: *computational topology* [5]. It denotes research activities involving both mathematics and computer science, in order to study the computational aspects of problems with a topological flavour, and to formalize and solve topological problems in computer applications, without neglecting the feasibility or the computational complexity of the problem. The key idea is that many classical concepts in mathematics can be re-interpreted in a computational context, thus furnishing powerful tools also in a discrete setting.

In this context, the classical Morse Theory [51] plays an important role, offering a series of techniques and measures with an extremely high abstraction power. This fact has lead, today, to an increasing interest towards a class of methods finding their roots in it. The common idea underlying these methods, indeed, is to perform a topological exploration of the shape according to some quantitative geometric properties provided by a real-valued function defined on the shape and chosen to extract shape features.

Note that the term *geometrical-topological* used in the title of this manuscript is meant to underline that both levels of information content are relevant for the applications of a shape description: geometrical properties are crucial for characterizing specific instances of features, while topological attributes are necessary to abstract and classify shapes according to invariant aspects of their geometry.

The added value of these approaches, that from now on we will call *shape-from-functions methods*, is in the possibility of adopting different functions as shape descriptors according to the properties and invariants that one wishes to analyze. In this sense, Morse Theory allows one to construct a general framework for shape characterization, parameterized with respect to the mapping function used, and possibly the space associated with the shape. The mapping function plays the role of a lens through which we look at the properties of the shape, and different functions provide different insights. Another attractive feature of shape-from-functions methods is that they concisely capture shape information in a manner that can be robust to deformation while being able to cope with changes in object viewpoint at a multiresolution level. All these facts make understandable the increasing research interest in enhancing the tools provided by these approaches for solving problems of shape description and comparison.

We devoted a large part of the Ph. D. study developing this class of methods in different directions, taking into account both their intrinsic advantages and their weak points.

As for advantages of shape-from-functions methods, certainly one of the most important is their high modularity, provided by the possibility to describe different shape features by choosing different functions. Accordingly, the observation that a shape of an object can be more thoroughly characterized by means of $\mathbb{R}^n$-valued functions, whose n components investigate at the same time different shape features, has lead us to explore the multidimensional setting. The framework we have chosen is that of Persistent Homology Theory, that belongs to the approaches grounding in Morse Theory with the study of the variations of topological features of the lower-level sets of the function on the shape. In this treatment, we will describe the theoretical results that lead to construct concise and complete shape descriptors also in a multidimensional case, and to define a stable distance which favours their comparison.

As far as weak points are concerned, shape-from-functions methods belong to a class of techniques that have been defined as *global object methods* in [57], i.e. methods working on the shape in its whole. An important drawback of all these methods is that in general they do not result to be robust against noise and occlusion, so failing in supporting more elaborate shape comparisons, such as partial matching or sub-part correspondence. With regard to these observations, and considering that a common requirement for shape descriptors is the robustness against partial occlusions, caused by foreground objects overlapping the object under investigations, we have decided to investigate the behavior of size functions in the presence of occlusions. Size functions are geometrical-topological descriptors provided by Size Theory in order to analyze the variations of connected components of the lower-level sets of a mapping function ranging on the shape. In this exposition, we will show the robustness of these descriptors under occlusions from both a theoretical and an experimental point of view.

The thesis is intended to describe all the above results, starting from a detailed mathematical background in a manner to render the exposition as clear and self-contained as possible. In particular, it is organized as follows.

Chapter 1 provides a brief overview on the approaches to the problem of shape understanding offered by shape-from-functions methods, sketching each of them in its main aspects and application environments. Particular attention is devoted to providing the reader with a necessary mathematical background on Size Theory and Persistent Homology Theory, in order to facilitate his access to individual topics.

Chapter 2 deals with our approach to the problem of multidimensional Persistent Homology Theory. In particular, we will show that the comparison between multidimensional rank invariants can be reduced to the 1-dimensional case by partitioning their domain into half-planes. The basic idea is to demonstrate that a multidimensional persistent homology module to these half-planes turns out to be a 1-dimensional persistent homology module. This important result allows one to use all the instruments available in the 1-dimensional setting in the multidimensional one.

In Chapter 3 we study the behavior of size functions in the presence of occlusion, and their ability to preserve not only global, but also local information. The main result is that an occluded object and a fully visible object share a set of common features in the corresponding size functions. This property can be exploited to support recognition in the presence of occlusions, as shown by the experiments we present here.

We conclude by discussing the main results achieved and our research activity planned for the future developments of shape-from-functions methods.

For the convenience of the reader, Appendices A and B contain a brief summary on Čech Homology Theory, a useful tool in Chapter 3.

From the results obtained in Chapters 2 and 3 we have realized two papers [9, 22] that, at the present time are available as preprint.

Contents

List of Figures

List of Tables

Chapter 1

Shape from functions

This chapter is intended to provide the reader with a necessary mathematical background on shape-from-functions methods, to facilitate his access to the individual topics.

It is organized as follows. In Section 1.1 we briefly sketch all these techniques, underlining only their characterizing aspects. The rest of the chapter is devoted to a detailed exposition of methods developed in this thesis: Size Theory and Persistent Homology Theory. Section 1.2 summarizes the history of the concept of *persistence*, that can be seen as the link between these two approaches. Section 1.3 is devoted to an overview on Size Theory, with a particular attention to the theoretical results concerning size functions. Section 1.4 contains a detailed exposition on Persistent Homology Theory and related concepts.
The most important definitions and results concerning these theories are exposed, connected and organized together, and some examples are inserted to facilitate the comprehension of the fundamental concepts.

1.1 Shape-from-functions methods

Shape-from-functions methods are geometrical-topological approaches to the problems of shape description and comparison, increasingly studied in computer vision, computer graphics and pattern recognition.

The common approach of all these methods to the problem of shape analysis is provided by the classical Morse Theory. Indeed, the intuition behind Morse Theory is that of combining the topological exploration of a space S with quantitative measurements of its geometrical properties provided by a mapping function f defined on S. So, for these methods, a shape is mathematically identified with a pair (S, f) and its description is translated into an analysis of the behavior of f on S. Analyzing the behavior of such a function on the space associated with the shape means studying either the properties, the configuration, or the evolution of its critical points. In fact, critical points are associated with the features of interest that one wishes to extract, and the configuration, or evolution, of these critical points captures a global description of the shape.

The different approaches can be divided into three main groups:

- methods studying the configuration of critical points on the space boundary (*Morse* and *Morse-Smale complexes*);
- methods studying the evolution of level sets of f (*contour trees* and *Reeb graphs*);
- methods studying the evolution of lower-level sets of f (*Size Theory*, *persistent homology* and *Morse shape descriptor*).

Intuitively, Morse and Morse-Smale complexes provide a view of shape properties from the perspective of the gradient of the mapping function. Their aim is to describe the shape by decomposing it into cells of uniform behavior of the gradient flow. This decomposition can be interpreted as having been obtained by a network on the surface that joins the critical points of the mapping function f through lines of steepest ascent, or descent, of the gradient.

Contour trees describe the shape of a scalar field f by analyzing the evolution of its level sets, as f spans the range of its possible values: components of level sets may appear, disappear, join, split, touch the boundary, or change genus. The contour tree stores this evolution and provides a compact description of the properties and structure of the scalar field. The generalization of a contour tree is given by Reeb graphs [3], even if their definition and theoretical study date back to 1946, thanks to the research work of a French mathematician, George Reeb. A Reeb graph is the quotient space defined by the equivalence relation that identifies the points belonging to the same connected component of each level set of f. Today it represents a suitable tool in computer graphics to solve problems related to shape matching, morphing and coding. Reeb graphs can be considered the first example of a fully modular framework for studying the shape of a manifold: here the shape exists by itself and the function used to study it can be arbitrarily chosen.

Beside the possibility of adopting different functions for describing shapes, at a higher level of abstraction, the modularity of the approaches based on Morse Theory can be extended to the choice of the space used to represent the shape, or phenomenon, under study. Size Theory and Persistent Homology Theory fall into this last group, with the study of topological attributes of lower-level sets of the mapping function. The Morse shape descriptor differs from the other two as it makes use of the theory of relative homology groups to define a shape description [1].

For technical details on shape-from-functions methods we refer the reader to the survey [6].

1.2 Topological persistence

Topological Persistence started *ante litteram* at the beginning of the 1990s under the name of Size Theory, with the idea of defining a suitable mathematical setting for the problem of shape comparison, supported by the adoption of suitable mathematical tools: the natural pseudo-distance (Subsection 1.3.1) and the size function (Subsection 1.3.2). This was actually the origin of rather large experimental research, beginning with [62, 60, 64]. Size functions were generalized by the same School in two directions: Size Homotopy Groups [38] and Size Functor [8] (see Subsection 1.3.6 for more details). Approximately ten years later, Persistent Homology Theory was independently introduced, re-proposing some ideas from a homological point of view (see [27] for a survey on this topic).

The high modularity of such approaches is given by the possibility to choose arbitrarily both the mapping functions and the underlying space. This possibility supplies them with an important advantage with respect to other methods of pattern recognition: they capture qualitative aspects of shape in a quantitative way, turning out to be particularly suited to the analysis of "natural" shapes (blood cells [32], signatures [25], gestures

[48, 59], melanocytic lesions [54], proteins [2], . . .).

Comparing these two methodologies, the reader will be able to observe the affinities characterizing them. Retrospectively, indeed, a size function (Definition 1.3) can be identifiable with the 0-th rank invariant (Definition 1.14), the value of a size function in a point of Δ^+ with the rank of a 0-th persistent homology module (or 0-th persistent Betti number) (Definition 1.10), the first persistent homology module with the Abelianization of the first size homotopy group [38], and the size functor [8] with a functorial formalization of the direct sum of persistent homology modules. On the other hand, Persistent Homology Theory is not properly an extension of Size Theory to all homology degrees. In fact, some restrictive conditions are imposed by the former. For example, Size Theory requires only the continuity of the measuring functions, while Persistent Homology Theory also requires their tameness, that is the presence of a finite number of homological critical values (Definitions 1.8 and 1.9). Moreover, size functions are computed in terms of connected components instead of arcwise connected components as singular homology does.

Different terms have been used to denote the same mathematical constructs, which often overwhelm the understanding of the underlying common framework. Therefore, to avoid confusion, we will expose the relevant material on both the approaches, setting a coherent notation and terminology.

1.3 Size Theory

Size Theory has been developed since the beginning of the 1990s (with the papers [33], [34] and [64]) in order to provide a geometrical-topological approach to the comparison of shapes.

The basic notion behind size theory is the abstraction of the similarity between shapes in terms of a pseudo-distance between the topological spaces representing the shapes. Accordingly, the degree of similarity (or dissimilarity) between shapes is expressed in terms of variations in the measure of the properties described by the measuring functions when we move from one shape to another. In this setting, shapes are considered similar if there exists a homeomorphism preserving the properties conveyed by the functions.

The formalization of this approach leads us to the introduction of the *natural pseudo-distance*, defined as the infimum of the variation of the values of the chosen functions, when we move from one space to the other through homeomorphisms, if possible. Therefore, two objects have the same shape if they share the same shape properties, expressed by the functions' values, that is, their natural pseudo-distance vanishes.

In order to effectively estimate the natural pseudo-distance and compare shapes, *size functions* are introduced. They are shape descriptors that analyze the variation of the number of connected components of lower-level sets with respect to the real function describing the shape properties we are interested in.

This theoretical approach is quite general and flexible, and, recently, has been extended to multivariate functions. Indeed, the observation that a shape of an object can be more thoroughly characterized by means of measuring functions, each investigating specific shape features, has lead to the extension of Size Theory to a multidimensional setting [4, 14]. Therefore, in the following subsections, the overview on this theory will be exposed in terms of multivariate functions. The fundamental results holding in the 1-dimensional case will be pointed out, when not available in the multidimensional setting.

1.3.1 Natural pseudo-distance

The main idea in Size theory is to compare shapes via the comparison of shape properties, that are described by $\mathbb{R}^n$-valued functions defined on topological spaces associated with the objects to be studied. This leads us to define a shape as a pair $(X,\vec{\varphi})$, called a *size pair*, where X is a non-empty, compact, locally connected, Hausdorff topological space and $\vec{\varphi} = (\varphi_1,\ldots,\varphi_n) : X \to \mathbb{R}^n$ is a continuous function, called an (*n-dimensional*) *measuring function*. Moreover, let us denote by *Size* the collection of all the size pairs.

When two objects must be compared, the first step is to find the "right" set of corresponding properties, that is, of size pairs $(X,\vec{\varphi}),(Y,\vec{\psi})$. The chosen topological spaces do not necessarily coincide with the objects we are referring to. For example, we can consider as a topological space the boundary of the object, or its projection onto a line, or its skeleton, and so on. The choice depends on the kind of comparison we are interested in. As for measuring functions, their choice is driven by the set of properties that one wishes to capture. Particular classes of functions have been singled out as better suited than others to deal with specific problems, such as obtaining invariance under groups of transformations [21, 37, 58], or working with particular classes of objects [13, 62]. Nevertheless, the choice of the most appropriate functions for a particular application is not fixed a priori, but can be changed up to the problem at hand.

The next step in the comparison process is to consider the natural pseudo-distance d, whose formal definition is the following.

Definition 1.1. *Let* $(X,\vec{\varphi}),(Y,\vec{\psi})$ *be two size pairs. We shall call* natural pseudo-distance *the pseudo-distance* $d : Size \times Size \to \mathbb{R}\cup\{+\infty\}$ *defined as*

$$d\left((X,\vec{\varphi}),(Y,\vec{\psi})\right) = \begin{cases} \inf\limits_{f\in H(X,Y)} \max\limits_{P\in X} \|\vec{\varphi}(P)-\vec{\psi}(f(P))\|_\infty & \textit{if } H(X,Y)\neq\emptyset \\ +\infty & \textit{otherwise,} \end{cases}$$

where $H(X,Y)$ *denotes the set of all homeomorphisms from* X *to* Y.

It should be noted that the existence of homeomorphisms is not required for the two compared objects but for the associated topological spaces. Moreover, observe that the term pseudo-distance means that d can vanish even if $(X,\vec{\varphi})$ and $(Y,\vec{\psi})$ do not coincide; in that case, X and Y are only sharing the same shape properties with respect to the chosen functions $\vec{\varphi}$ and $\vec{\psi}$, respectively.

Since the set of homeomorphisms between two topological spaces is rarely tractable, simpler mathematical tools are required to estimate the natural pseudo-distance. To this end, the main mathematical tool introduced in Size Theory is given by size functions, which provide a lower bound for the natural pseudo-distance.

1.3.2 Size functions

Size functions are shape descriptors that analyze the variation of the number of connected components of the lower-level sets of the studied space with respect to the chosen measuring function.

Formally, let $\mathbb{R}^n$ be endowed with the usual max-norm, $||(u_1,\ldots,u_n)||_\infty = \max\limits_{1\le i\le n}|u_i|$. Moreover, define the following relations $\preceq$, $\prec$ in $\mathbb{R}^n$: for $\vec{u}=(u_1,\ldots,u_n)$ and $\vec{v}=$

$(v_1,\ldots,v_n)$, we shall say $\vec{u} \preceq \vec{v}$ (resp. $\vec{u} \prec \vec{v}$) if and only if $u_i \le v_i$ (resp. $u_i < v_i$) for $i = 1,\ldots,n$.

Given a size pair $(X,\vec{\varphi})$, for every n-tuple $\vec{u} = (u_1,\ldots,u_n) \in \mathbb{R}^n$, let us denote by $X\langle\vec{\varphi} \preceq \vec{u}\rangle$ the lower-level set $\{P \in X, \vec{\varphi}(P) \preceq \vec{u}\}$.

Definition 1.2. *Let $(X,\vec{\varphi})$ be a size pair. For every $\vec{u} \in \mathbb{R}^n$, we shall say that two points $P,Q \in X$ are $\langle\vec{\varphi} \preceq \vec{u}\rangle$*-connected *if and only if a connected subset of $X\langle\vec{\varphi} \preceq \vec{u}\rangle$ exists, containing both P and Q.*

The relation of $\langle\vec{\varphi} \preceq \vec{u}\rangle$-connectedness is an equivalence relation. If two points $P,Q \in X$ are $\langle\vec{\varphi} \preceq \vec{u}\rangle$-connected we shall write $P \sim_{\langle\vec{\varphi}\preceq\vec{u}\rangle} Q$.

In what follows, when no confusion arises about the measuring function we are referring to, we will denote the lower-level set $X\langle\vec{\varphi} \preceq \vec{u}\rangle$ simply by $X_{\vec{u}}$, and the connectedness relation between $P,Q \in X$, $P \sim_{\langle\vec{\varphi}\preceq\vec{u}\rangle} Q$, simply by $P \sim_{\vec{u}} Q$.

Eventually, let Δ^+ be the open set $\{(\vec{u},\vec{v}) \in \mathbb{R}^n \times \mathbb{R}^n : \vec{u} \prec \vec{v}\}$, while $\Delta = \partial\Delta^+$.

Definition 1.3. *The* size function *associated with the size pair $(X,\vec{\varphi})$ is the function $\ell_{(X,\varphi)} : \Delta^+ \to \mathbb{N}$ such that, for every $(\vec{u},\vec{v}) \in \Delta^+$, $\ell_{(X,\varphi)}(\vec{u},\vec{v})$ is equal to the number of equivalence classes into which the set $X\langle\vec{\varphi} \preceq \vec{u}\rangle$ is divided by the relation of $\langle\vec{\varphi} \preceq \vec{v}\rangle$-connectedness.*

In other words, $\ell_{(X,\vec{\varphi})}(\vec{u},\vec{v})$ is equal to the number of connected components in $X\langle\vec{\varphi} \preceq \vec{v}\rangle$ containing at least one point of $X\langle\vec{\varphi} \preceq \vec{u}\rangle$. The finiteness of this number is a consequence of the compactness and local connectedness of X, and the continuity of $\vec{\varphi}$.

In the following subsections on Size Theory, we will show the main results involving 1-dimensional size functions (that, for conciseness, will be often called simply size functions).

1.3.3 An example of 1-dimensional size function

First of all, we want to give a simple example of a 1-dimensional size function to facilitate comprehension of the reader. In this example, displayed in Figure 1.1, we consider the size pair (X,φ), where X is the curve of $\mathbb{R}^2$, represented by a solid line in

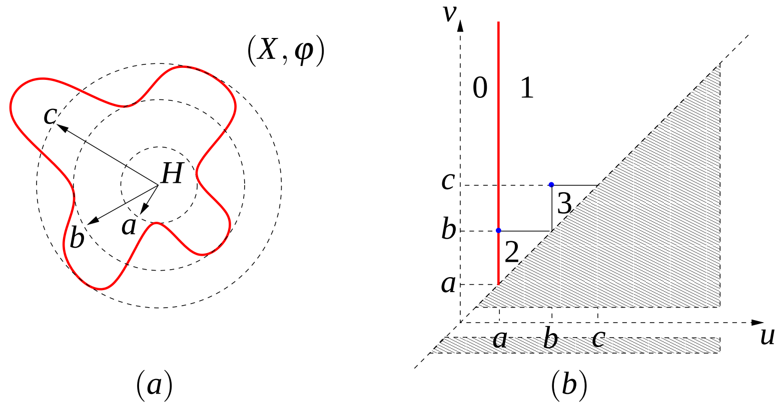

Figure 1.1: (b) The size function of the size pair (X,φ), where X is the curve represented by a solid line in (a), and $\varphi : X \to \mathbb{R}$ is the function "Euclidean distance from the point H".

Figure 1.1 (a), and $\varphi : X \to \mathbb{R}$ is the function "Euclidean distance from the point H". The size function associated with (X,φ) is shown in Figure 1.1 (b). Here, the domain of the size function, $\Delta^+ = \{(u,v) \in \mathbb{R}^2, u < v\}$, is divided by solid lines, representing the discontinuity points of the size function. These discontinuity points divide Δ^+ into regions where the size function is constant. The value displayed in each region is the value taken by the size function in that region.

For instance, for $a \le u < b$, the set X_u has two connected components contained in different connected components of X_v, when $u < v < b$. Therefore, $\ell_{(X,\varphi)}(u,v) = 2$ for $a \le u < b$ and $u < v < b$. When $a \le u < b$ and $v \ge b$, all the connected components of X_u are contained in the same connected component of X_v. Therefore, $\ell_{(X,\varphi)}(u,v) = 1$ for $a \le u < b$ and $v \ge b$. When $b \le u < c$ and $u < v < c$, the three connected components of X_u persist in X_v, so $\ell_{(X,\varphi)}(u,v) = 3$ for such values; while for $b \le u < c$ and $v \ge c$, all of the three connected components of X_u belong to the same connected component of X_v, implying that in this case $\ell_{(X,\varphi)}(u,v) = 1$.

As for the values taken on the discontinuity lines, they are easily obtained by observing that size functions are right-continuous, both in the variable u and in the variable v.

We point out that in less recent papers about size functions one encounters a slightly different definition of size function. In fact, the original definition of size function was based on the relation of arcwise-connectedness. The definition used here, based on connectedness, was introduced in [20]. This change of definition is theoretically motivated, since it implies the right-continuity of size functions, not only in the variable u but also in the variable v. As a consequence, many results can be stated more neatly.

1.3.4 Algebraic representation of 1-dimensional size functions

In [35] a new kind of representation of size functions was introduced, based on the fact that they can always be seen as linear combinations of characteristic functions of triangles (possibly unbounded triangles with vertices at infinity), with a side lying on the diagonal of $\mathbb{R}^2$, and the other sides parallel to the coordinate axes. For example, in Figure 1.1 (b), the depicted size function is the sum of the characteristic functions of the two triangles with right angles at vertices (a,b) and (b,c), respectively, plus the characteristic function of the infinite triangle defined by the vertical line $u=a$. This observation suggested the important property for which the size functions are always representable as collections of vertices and lines (called proper cornerpoints and cornerpoints at infinity, respectively). The main reference here is [36].

Roughly speaking, a proper cornerpoint for $\ell_{(X,\varphi)}$ is a point of $(u,v)\in\Delta^+$ encoding the level u at which a new connected component is born and the level v at which it gets merged to another connected component. Formally, a proper cornerpoint can be defined as follows.

Definition 1.4. *For every point $p=(u,v)\in\Delta^+$ and for every positive real number ε with $u+\varepsilon<v-\varepsilon$, let us define the number $\mu^{\varepsilon}_{(X,\varphi)}(p)$ as*

$$\ell_{(X,\varphi)}(u+\varepsilon,v-\varepsilon)-\ell_{(X,\varphi)}(u-\varepsilon,v-\varepsilon)-\ell_{(X,\varphi)}(u+\varepsilon,v+\varepsilon)+\ell_{(X,\varphi)}(u-\varepsilon,v+\varepsilon).$$

The finite number $\mu_{(X,\varphi)}(p)=\lim_{\varepsilon\to0^+}\mu^{\varepsilon}_{(X,\varphi)}(p)$ will be called multiplicity *of p for $\ell_{(X,\varphi)}$. Moreover, we shall call* proper cornerpoint *for $\ell_{(X,\varphi)}$ any point $p\in\Delta^+$ such that the number $\mu(p)$ is strictly positive.*

A cornerpoint at infinity, instead, encodes the level u at which a new connected component of X is born, and such that no level v, $v>u$, exist at which this connected component gets merged to another one. In particular, it as been proved [36, Prop. 9] that the number of cornerpoints at infinity corresponds to the number of connected components of X, and their abscissas to the level at which they are born. Formally a cornerpoint at infinity can be defined as follows.

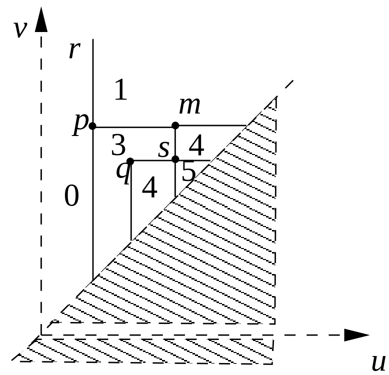

Figure 1.2: Cornerpoints of a size function: in this example, p, q and m are the only proper cornerpoints, and have multiplicity equal to 2 (p) and 1 (m,q). The point s is not a cornerpoint, since its multiplicity vanishes. The line r is the only cornerpoint at infinity and it has multiplicity equal to 1.

Definition 1.5. *For every vertical line r, with equation $u = k$, and for every positive real number ε with $k+\varepsilon < 1/\varepsilon$, let us identify r with the pair (k,∞), and define the number $\mu^{\varepsilon}_{(X,\varphi)}(r)$ as*

$$\ell_{(X,\varphi)}(k+\varepsilon, 1/\varepsilon) - \ell_{(X,\varphi)}(k-\varepsilon, 1/\varepsilon).$$

When the finite number $\mu_{(X,\varphi)}(r) = \lim_{\varepsilon\to 0^+} \mu^{\varepsilon}_{(X,\varphi)}(r)$, called multiplicity of r *for $\ell_{(X,\varphi)}$, is strictly positive, we shall call the line r a* cornerpoint at infinity *for the size function.*

As an example of cornerpoints in size functions, in Figure 1.2 we see that the proper cornerpoints of the depicted size function are the points p, q and m (with multiplicity 2, 1 and 1, respectively). The line r is the only cornerpoint at infinity (with multiplicity 1): this means that the underlying topological space is connected.

The importance of cornerpoints is revealed by the next result, showing that cornerpoints, with their multiplicities, uniquely determine size functions.

Let us denote by Δ^* the open half-plane Δ^+, extended by the points at infinity of the kind (k,∞), i.e.

$$\Delta^* := \Delta^+ \cup \{(k,\infty) : k \in \mathbb{R}\}.$$

Theorem 1.3.1. *For every $(\overline{u},\overline{v}) \in \Delta^+$ we have*

$$\ell_{(X,\varphi)}(\overline{u},\overline{v}) = \sum_{\substack{(u,v)\in\Delta^* \\ u\le\overline{u},\, v>\overline{v}}} \mu_{(X,\varphi)}\big((u,v)\big). \tag{1.1}$$

The equality (1.1) can be checked in the example of Figure 1.2. The points where the size function takes value 0 are exactly those for which there is no cornerpoint (either proper or at infinity) lying to the left and above them. Let us take a point in the region of the domain where the size function takes the value 3. According to the above theorem, the value of the size function at that point must be equal to $\mu(r)+\mu(p)=3$.

The result stated in Theorem 1.3.1 implies that it is possible to represent any size function by a formal series of points and lines of the real plane, i.e. by means of its proper cornerpoints and cornerpoints at infinity, counted with their multiplicities.

1.3.5 Distances between 1-dimensional size functions

The possibility to express size functions as formal series of points provides a simple and concise representation of this shape descriptor, and enables one to compare size functions using distances between sets of points [24], such as the Hausdorff metric or the matching distance (see e.g. [16, 19, 20, 35, 44]).

The definition of Hausdorff distance between two size functions is the following.

Definition 1.6. *Let (X,φ) and (Y,ψ) be two size pairs, with X and Y having the same number of connected components. Let A_1 (resp. A_2) be the set of all cornerpoints for $\ell_{(X,\varphi)}$ (resp. $\ell_{(Y,\psi)}$), augmented by adding a countable infinity of points of the diagonal $\Delta=\{(u,v)\in\mathbb{R}^2, u=v\}$. The* Hausdorff distance *between the size functions $\ell_{(X,\varphi)}$ and $\ell_{(Y,\psi)}$ is defined as*

$$d_H(\ell_{(X,\varphi)},\ell_{(Y,\psi)})=\max\{\max_{p\in A_1}\min_{q\in A_2}\|p-q\|_\infty,\max_{q\in A_2}\min_{p\in A_1}\|q-p\|_\infty\}.$$

In other words, the Hausdorff distance is the maximum between the distance of A_1 from A_2 and that of A_2 from A_1. The distance of A_i from A_j is computed as the largest among all the minimum distances of each point of A_i from all the points of A_j.

Hausdorff distance is stable with respect to perturbations of the measuring functions and, in experimental frameworks, its computational complexity is low. Nevertheless, it does not seem to be a suitable metric for the computation of the distance between size functions, because it does not take into account the multiplicities of cornerpoints. Accordingly, in [20] the matching distance between size functions was introduced. It can be defined in the following way.

Definition 1.7. *Let (X,φ) and (Y,ψ) be two size pairs, with X and Y having the same number of connected components. Let C_1 (resp. C_2) be the multiset of all cornerpoints for $\ell_{(X,\varphi)}$ (resp. $\ell_{(Y,\psi)}$) counted with their multiplicities, augmented by adding a countable infinity of points of the diagonal $\Delta = \{(u,v) \in \mathbb{R}^2, u = v\}$. The* matching distance *between $\ell_{(X,\varphi)}$ and $\ell_{(Y,\psi)}$ is given by*

$$d_{match}(\ell_{(X,\varphi)}, \ell_{(Y,\psi)}) = \min_{\sigma} \max_{p \in C_1} \delta(p, \sigma(p)),$$

where σ varies among all the bijections between C_1 and C_2 and

$$\delta((u,v),(u',v')) = \min\left\{\max\{|u-u'|,|v-v'|\}, \max\left\{\frac{v-u}{2}, \frac{v'-u'}{2}\right\}\right\}.$$

The adopted convention about ∞ is that $\infty - v = v - \infty = \infty$ for $v \neq \infty$, $\infty - \infty = 0$, $\frac{\infty}{2} = \infty$, $|\infty| = \infty$, $\min\{\infty, c\} = c$, $\max\{\infty, c\} = \infty$.

Roughly speaking, the matching distance d_{match} between two size functions is the minimum, over all the matchings between the cornerpoints of the two size functions, of the maximum of the L_∞-distances between two matched cornerpoints. Since two size functions can have a different number of proper cornerpoints, these can be also matched to points of the diagonal. An example of computation of matching distance is illustrated in Figure 1.3. A size function, representable as the formal series of three proper cornerpoints, a, b, c, and one cornerpoint at infinity, r (Figure 1.3, (a)), is compared with a size function having two proper cornerpoints, a', c', and one cornerpoint at infinity, r' (Figure 1.3, (b)). The cost of the optimal matching between cornerpoints of the two size functions (that is of the matching that minimizes the dissimilarity measure between the two point sets) equals the cost of moving the cornerpoint b onto the diagonal.

The stability of this representation has been studied in [18, 19]. In particular, it has been proved that the matching distance is continuous with respect to the measuring functions (in the sense of L_∞-topology), guaranteeing a property of perturbation robustness.

Theorem 1.3.2. *Let (X,φ) be a size pair. For every real number $\varepsilon \geq 0$ and for every measuring function $\psi : X \to \mathbb{R}$, such that $\max_{P \in X} |\varphi(P) - \psi(P)| \leq \varepsilon$, we have*

$$d_{match}(\ell_{(X,\varphi)}, \ell_{(X,\psi)}) \leq \varepsilon.$$

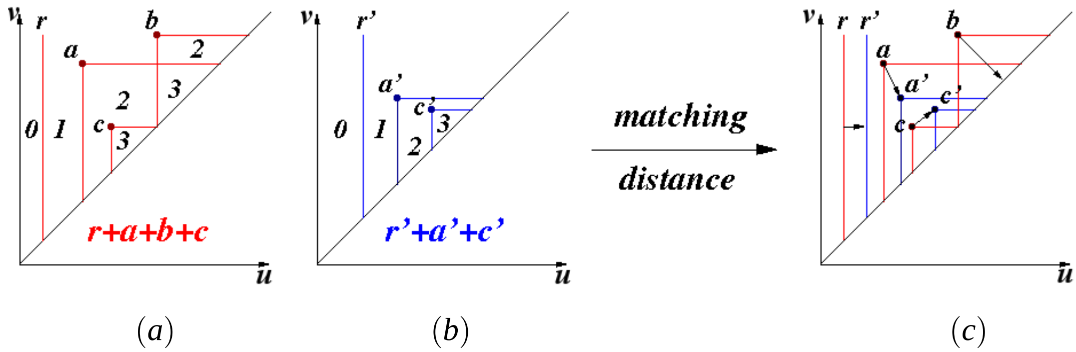

Figure 1.3: Two size functions can be described by cornerpoints (proper and at infinity) and compared by the matching distance.

Moreover, in [19] it has been shown that the matching distance between size functions produces a sharp lower bound for the natural pseudo-distance between size pairs.

Theorem 1.3.3. *Let* $\varepsilon \geq 0$ *be a real number and let* (X, φ) *and* (Y, ψ) *be two size pairs with* X *and* Y *homeomorphic. Then*

$$d_{match}\left(\ell_{(X,\varphi)}, \ell_{(Y,\psi)}\right) \leq d((X, \varphi), (Y, \psi)),$$

where d *is the natural pseudo-distance between* (X, φ) *and* (Y, ψ).

In addition, in [19] it has been proved that the matching distance gives the best lower bound for the natural pseudo-distance, in the sense that any other distance between size functions, such as that given in [23], would yield a worse bound. These results guarantee a link between the comparison of size functions and the comparison of shapes [20].

1.3.6 Algebraic topology in Size Theory

Size functions are not the sole tool introduced in Size Theory. Indeed, algebraic topology has been used to obtain generalizations of size functions that give a more complete description of a size pair (X, φ), since they take into account not only the number of connected components, but also the presence of other features such as holes, tunnels and voids. The first development in this sense can be found in [38], where *size homotopy groups* are introduced (already in a multidimensional setting), inspired by the classical mathematical notion of homotopy group. They have been shown to provide a lower bound for the natural pseudo-distance, much in the same way as size functions do.

The study of size functions in the algebraic topological setting was also developed in [8], by observing that, if (X,φ) is a size pair with X a closed smooth manifold and $\varphi : X \to \mathbb{R}$ a Morse function, the value of $\ell_{(X,\varphi)}$ at a point $(u,v) \in \Delta^+$, computed in terms of arcwise connected components (instead of connected components), equals the rank of the image of $\iota_0^{u,v} : H_0(X_u) \to H_0(X_v)$, where $\iota_0^{u,v}$ is the homomorphism between 0th singular homology groups over a field $\mathbb{K}$ induced by the inclusion of X_u in X_v. This observation has led to the definition of *size functor*, which studies the maps $\iota_k^{u,v} : H_k(X_u) \to H_k(X_v)$, for every $k \in \mathbb{Z}$. In other words, it studies the process of birth and death of homology classes as lower-level sets change. The size functor can be described by oriented trees, called H_k – *trees* (see [8, 10]).

Another topological interpretation of size functions, again computed in terms of arcwise connected components, is that given by Allili et al. in [1]: given a size pair (X,φ) with X a closed smooth manifold and $\varphi : X \to \mathbb{R}$ a Morse function, the value of $\ell_{(X,\varphi)}$ at a point $(u,v) \in \Delta^+$ is equal to the difference between the rank of $H_0(X_v)$ and that of $H_0(X_v, X_u)$. These two topological interpretations of size functions will be recuperated in Chapter 3 for proving analogous results involving the new definition of size functions in terms of connected components (see Section 3.1).

1.4 Persistent Homology Theory

The theory of persistent homology was introduced about nine years ago [28, 29], providing an algebraic method for measuring topological features of shapes and of functions. The authors follows a similar approach to Size Theory introducing the paradigm of *persistence*, which grows a space incrementally and analyzes the topological changes that occur during this growth. In particular, they produce a tool, called *persistent homology*, for controlling the placement of topological events (such as the merging of connected components or the filling of holes) within the history of this growth. The aim is to furnish a scale to assess the relevance of topological attributes. Indeed, the main assumption of persistence is that longevity is equivalent to significance. In other words, a significant topological attribute must have a long lifetime in a growing complex. In this way, one is able to distinguish the essential features from the fine details. In experimental frameworks, this theoretical procedure can be translated into the following: topological events having a long lifetime in the growing complex are considered structural shape features; those whose lifetime is short are identified with noise.

The two fundamental ingredients in persistent homology theory are the filtration of a space and the pairing of homological critical values. Roughly speaking, the filtration is a sequence of nested subspaces; pairing homological critical values means linking the critical level that mark the appearance of a topological event (birth) with the critical level that mark its disappearance (death). These concepts will be illustrated in Subsection 1.4.2.

As for the assumptions on the pair (X,φ) defining the shape of an object, in literature one can find different kinds of request involving both the space X and the function $\varphi : X \to \mathbb{R}$ [27]. In this treatment we require X to be a triangulable space and φ a continuous tame function (Definition 1.9), in agreement with [16]. We recall that a topological space is *triangulable* if there exist a finite simplicial complex with homeomorphic underlying space.

1.4.1 1-dimensional persistent homology modules

First of all, we restate two definitions from [16] (according with our notations), that introduce two important concepts in this theoretical setting. The first one is the concept of homological critical value, representing a level at which new topological attributes are born or existing topological attributes die. The second one introduces the concept of *tameness*.

Definition 1.8. *Let X be a triangulable topological space, $\varphi : X \to \mathbb{R}$ a continuous real function on X and $k \in \mathbb{Z}$. A* homological k-critical value *of φ is a real number w such that, for every sufficiently small $\varepsilon > 0$, the map $\iota_k^{w-\varepsilon,w+\varepsilon} : H_k(X_{w-\varepsilon}) \to H_k(X_{w+\varepsilon})$ induced by the inclusion of $X\langle\varphi \le w-\varepsilon\rangle$ in $X\langle\varphi \le w+\varepsilon\rangle$ is not an isomorphism.*

This is called a *k-essential critical value* in the previously quoted paper [8, Def. 2.6] (see Subsection 1.3.6).

In the following the values that are not k-critical for any $k \in \mathbb{Z}$ will be called *k-regular values*.

Definition 1.9. *Let X be a triangulable topological space. A continuous function $\varphi : X \to \mathbb{R}$ is* tame *if it has a finite number of homological k-critical values for every $k \in \mathbb{Z}$, and the homology modules $H_k(X\langle\varphi \le w\rangle)$ are finite-dimensional for all $k \in \mathbb{Z}$ and $w \in \mathbb{R}$.*

In other words, a function is tame if the homology modules of each lower-level set have finite ranks and there exist only finitely many values w at which the homology modules change.

Examples of tame functions are Morse functions on closed smooth manifolds and piecewise linear functions on triangulable topological spaces.

From now on, a pair (X,φ) with X a triangulable space and φ a tame function, will be called a *tame pair*.

Definition 1.10. *Let (X,φ) be a tame pair and let $u,v \in \mathbb{R}$ with $u < v$. The k*th persistent homology module *$H_k^{u,v}(X,\varphi)$ is the image of the homomorphism $\iota_k^{u,v} : H_k(X\langle\varphi \le u\rangle) \to H_k(X\langle\varphi \le v\rangle)$ induced by the inclusion mapping of $X\langle\varphi \le u\rangle$ into $X\langle\varphi \le v\rangle$, that is $H_k^{u,v}(X,\varphi) = \operatorname{im} \iota_k^{u,v}$.*

For every $k \in \mathbb{Z}$, the rank of the image of $\iota_k^{u,v}$ is called the *k-persistent Betti number* and is denoted by $\beta_k^{u,v}(X,\varphi)$. It counts the number of k-dimensional homology classes that are born at or before u and are still alive at v.

In the following, when no confusion arises in terms of the measuring function φ we are considering, for conciseness we will denote $H_k^{u,v}(X,\varphi)$ simply by $H_k^{u,v}(X)$, and $\beta_k^{u,v}(X,\varphi)$ by $\beta_k^{u,v}(X)$.

1.4.2 Barcodes, persistence diagrams and bottleneck distance

Now, we are ready to introduce the *filtration* of X defined by the lower-level sets of φ.

By Definition 1.9, the choice of a topological space X endowed with a tame real function φ implies, for every $k \in \mathbb{Z}$, the existence of a finite number of homological k-critical values, say $w_1,\dots,w_m$. Then, choosing $m+1$ k-regular values $s_0,\dots,s_m$ such that $s_{i-1} < w_i < s_i$ for $1 \leq i \leq m$, a filtration of X can be defined as a finite sequence of nested subspaces $\{X_{s_i}\}_{i=0,\dots,m}$, that is $X_{s_0} \subset X_{s_1} \subset \ldots \subset X_{s_m}$. Set also $s_{-1} = w_0 = -\infty$ and $w_{m+1} = s_{m+1} = +\infty$. We say that a homology class α is born at X_{s_i} if it does not come from a class in $X_{s_{i-1}}$. Moreover, if α is born at X_{s_i}, we say it dies entering X_{s_j} if the image of the map induced by $X_{s_{i-1}} \subset X_{s_{j-1}}$ does not contain the image of α but the image of the map induced by $X_{s_{i-1}} \subset X_{s_j}$ does.

Following the above-described procedure, the homological critical values can be paired by the following rule. Through the filtration of X a homological critical value w_i, corresponding to the birth of a non trivial homological cycle, is paired with the homological critical value (if there exists) $w_j > w_i$ corresponding to the death of the same cycle, that is when the cycle becomes a boundary. The persistence of the cycle is computed in terms of the difference between the paired homological critical values, and its lifetime can be graphically described by an open interval $[w_i, w_j)$. The cycles that do not die during the filtration are called *essential classes* of (X, φ) and are represented by open intervals of type $[w, \infty)$. Therefore, the persistent homology of a filtered topological space can be portrayed as a collection of open intervals, called *persistence intervals* or *barcode* [11, 39] (see Figure 1.4, bottom).

More recently, a new kind of description of barcode has been introduced [16]. The pairs (w_i, w_j), with $w_i < w_j$, are represented as points with multiplicities in the extended plane, and this set of points is called a *persistence diagram*.

Definition 1.11. *The* persistence diagram $\mathrm{Dgm}_k(X, \varphi) \subseteq \Delta^*$ *associated with the pair* (X, φ) *is a multiset of points* (w_i, w_j) *counted with multiplicity*

$$\mu_k^{w_i,w_j}(X,\varphi) = \beta_k^{s_i,s_{j-1}}(X,\varphi) - \beta_k^{s_{i-1},s_{j-1}}(X,\varphi) - \beta_k^{s_i,s_j}(X,\varphi) + \beta_k^{s_{i-1},s_j}(X,\varphi)$$

for $0 \leq i < j \leq m+1$, $k \in \mathbb{Z}$, *together with all points on the diagonal, counted with infinite multiplicity.*

By convention, $H_k^{u,v}(X,\varphi) = \{0\}$ whenever u or v is infinite. Therefore, in Definition 1.11, $\beta_k^{s_{-1},s_i}(X,\varphi) = \beta_k^{s_i,s_{m+1}} = 0$ for every $i \in \{-1,\dots,m+1\}$ and $k \in \mathbb{Z}$.

Let us denote $\mu_k^{w_i,w_j}(X,\varphi)$ simply by $\mu_k^{w_i,w_j}$ and $\beta_k^{s_i,s_j}(X,\varphi)$ by $\beta_k^{s_i,s_j}$, and write the multiplicity of a point (w_i, w_j) as the following difference between two differences

$$\mu_k^{w_i,w_j} = (\beta_k^{s_i,s_{j-1}} - \beta_k^{s_i,s_j}) - (\beta_k^{s_{i-1},s_{j-1}} - \beta_k^{s_{i-1},s_j}).$$

Recalling that $\beta_k^{s_i,s_{j-1}}$ represents the number of homology classes in $X_{s_{j-1}}$ born before s_i, it holds that the first difference, $\beta_k^{s_i,s_{j-1}} - \beta_k^{s_i,s_j}$, counts the classes in $X_{s_{j-1}}$ born before s_i, that die before s_j; while the second difference, $\beta_k^{s_{i-1},s_{j-1}} - \beta_k^{s_{i-1},s_j}$, counts the classes in $X_{s_{j-1}}$ born before s_{i-1}, that die before s_j. Thus, $\mu_k^{w_i,w_j}$ counts the classes born between s_{i-1} and s_i, that die between s_{j-1} and s_j.

The total multiplicity of the persistence diagram minus the diagonal is

$$\sharp(\mathrm{Dgm}_k(X,\varphi) - \Delta) = \sum_{\substack{i<j \\ k\in\mathbb{Z}}} \mu_k^{w_i,w_j}.$$

Persistence diagrams can be compared by stable distances, such as the Hausdorff distance and the *bottleneck distance*.The last one is defined in the following manner.

Definition 1.12. *The* bottleneck distance *between* $\mathrm{Dgm}_k(X,\varphi)$ *and* $\mathrm{Dgm}_k(X,\psi)$ *is given by*

$$d_B(\mathrm{Dgm}_k(X,\varphi), \mathrm{Dgm}_k(X,\psi)) = \inf_{\sigma} \sup_{p\in \mathrm{Dgm}_k(X,\varphi)} \|p - \sigma(p)\|_\infty,$$

where σ ranges over all the bijections between $\mathrm{Dgm}_k(X,\varphi)$ *and* $\mathrm{Dgm}_k(X,\psi)$.

In [16] it has been proved that, using the bottleneck distance, persistence diagrams are robust against small perturbations of real functions.

Theorem 1.4.1. *Let X be a triangulable space endowed with continuous tame functions $\varphi,\psi : X \to \mathbb{R}$. Then, for every $k \in \mathbb{Z}$, the persistence diagrams satisfy*

$$d_B(\mathrm{Dgm}_k(X,\varphi), \mathrm{Dgm}_k(X,\psi)) \le \|\varphi - \psi\|_\infty,$$

where $\|\varphi - \psi\|_\infty = \max_{P\in X} |\varphi(P) - \psi(P)|$.

Note that persistence diagrams essentially play the same role as cornerpoints in size functions (see Chapter 3, Subsection 3.1.1 and [14] for more details). Therefore, looking at these points as vertices of triangular regions (with a finite or infinite area), a generalization of a size function to all homology degrees is obtained. This kind of representation is the graph of a function, called *rank invariant*, and defined as $\rho_k^{X,\varphi} : \Delta^+ \to \mathbb{N}$ such that $\rho_k^{X,\varphi}(u,v) = rank(H_k^{u,v}(X,\varphi))$ (see the following section for its general definition). An example is given in Figure 1.4 (center).

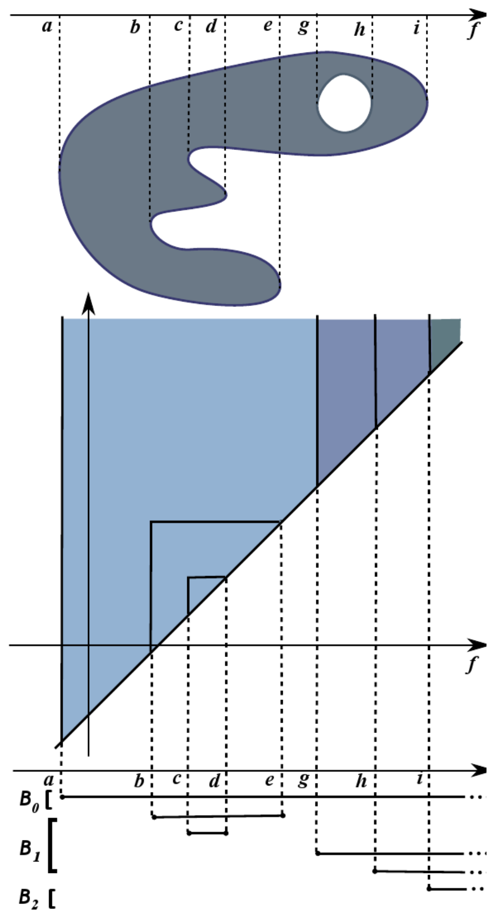

Figure 1.4: Top: a surface studied with respect to the height function f in the horizontal direction. Center and bottom: the associated rank invariants and persistence intervals representing the 0th (light blue), 1st (middle blue) and 2nd (dark blue) persistent Betti numbers, respectively.

1.4.3 Multifiltrations and persistence modules

The most general setting for Topological Persistence has been recently proposed by G. Carlsson and A. Zomorodian in [12], where an extension of the theory to a multidimensional setting is exposed. The main concept introduced by the authors is that of *multifiltration* of a space, that would be the suitable tool to model richer structures parameterizable along multiple geometric dimensions.

Let $\vec{u},\vec{v} \in \mathbb{N}^n$. We write $\vec{u} \preceq \vec{v}$ if $u_j \leq v_j$ for $j = 1,\ldots,n$. The formal definition of a multifiltration is the following.

Definition 1.13. *A topological space X is* multifiltered *if we are given a family* (multifiltration) *of subspaces $\{X^{(\vec{v})} \subseteq X\}_{\vec{v}\in\mathbb{N}^n}$ with inclusions $X^{(\vec{u})} \subseteq X^{(\vec{w})}$ whenever $\vec{u} \preceq \vec{w}$, so that the diagrams*

$$\begin{array}{ccc} X^{(\vec{u})} & \longrightarrow & X^{(\vec{v}_1)} \\ \downarrow & & \downarrow \\ X^{(\vec{v}_2)} & \longrightarrow & X^{(\vec{w})} \end{array} \tag{1.2}$$

commute for $\vec{u} \preceq \vec{v}_1, \vec{v}_2 \preceq \vec{w}$.

The generality of the above definition is given by the fact that neither conditions on the topological space X are imposed nor requirements on the construction of its subspaces $X^{(\vec{v})}$ are made.

Given a multifiltered space X, the homology of each subspace $X^{(\vec{v})}$ over a field $\mathbb{K}$ is a vector space. Moreover, there exist inclusion maps relating the subspaces, inducing maps at homology level.

Figure 1.1 (a) displays an example of a bifiltration. The input is a finite triangle K along with a function $F : \mathbb{R}^2 \to K$ that gives a subcomplex $K^{(\vec{v})}$ for any value $\vec{v} \in \mathbb{R}^2$. To convert this input to a multifiltered complex, it is sufficient to take into account only the finite set of critical coordinates $C = \{\vec{v}_i \in \mathbb{R}^2\}_i$ at which new simplices enter the complex. So, we can reduce ourself to consider a finite number of critical values, such that diagrams (1.2) commute in the discrete set of $\mathbb{N}^2$. Figure 1.1 (b) shows a commutative diagram isomorphic to the zeroth homology vector spaces of the bifiltered triangle.

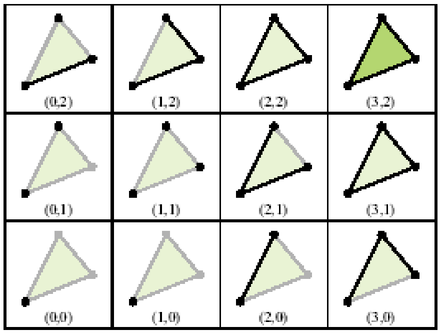

$$\begin{tikzcd}
\mathbb{K}^2 \arrow[r] & \mathbb{K} \arrow[r] & \mathbb{K} \arrow[r] & \mathbb{K} \\
\mathbb{K}^2 \arrow[r] \arrow[u] & \mathbb{K}^3 \arrow[r] \arrow[u] & \mathbb{K} \arrow[r] \arrow[u] & \mathbb{K} \arrow[u] \\
\mathbb{K} \arrow[r] \arrow[u] & \mathbb{K} \arrow[r] \arrow[u] & \mathbb{K} \arrow[r] \arrow[u] & \mathbb{K} \arrow[u]
\end{tikzcd}$$

(a) (b)

Table 1.1: (a) A bifiltration of a triangle. (b) The commutative diagram of zeroth homology vector spaces associated with the subspaces of the bifiltered complex, and their maps induced by the inclusion maps relating the subspaces.

The homology of a multifiltration in each degree can be described by a discrete invariant called *rank invariant*.

Definition 1.14. *Let* $X = \{X^{(\vec{v})}\}_{\vec{v}\in\mathbb{N}^n}$ *be a multifiltration. We define* $\rho_{X,k} : \{(\vec{u},\vec{v}) \in \mathbb{N}^n \times \mathbb{N}^n, \vec{u} \preceq \vec{v}\} \to \mathbb{N}$ *over a field* $\mathbb{K}$ *to be*

$$\rho_{X,k}(\vec{u},\vec{v}) = \mathrm{rank}(H_k(X^{(\vec{u})}) \to H_k(X^{(\vec{v})})).$$

Retrospectively, mathematical tools provided by Size Theory and Persistent Homology Theory can be considered particular examples of those presented in this section. In particular, the concept of multifiltration of a space in a n-dimensional setting (or that of filtration in a 1-dimensional one) used by these theories is always defined by a mapping function ranging on the space.
Indeed, to be more precise, in [12] it has also been introduced the concept of *kth persistence module*. The homology of a multifiltration in each degree is a particular persistence module. The multidimensional persistent homology is the homology of a particular multifltration: the multifiltration defined by the lower-level sets of a multidimensional measuring function varying on the space.

Chapter 2

Stability for rank invariants of multidimensional persistent homology

The interest in extending shape-from-functions techniques to a multidimensional setting, in the sense of extracting knowledge from high-dimensional data by means of functions with values in $\mathbb{R}^n$, is increasing. One of the main reasons for such a generalization is that certain shape features (such as color) are characterized by a multidimensional nature whose description can be achieved necessarily by a multivalued function. Moreover, another advantage of working with $\mathbb{R}^n$-valued functions is that shapes can be simultaneously investigated by n different real-valued functions.

Topological persistence approaches are moving towards this direction with the aim to enhance the ability of their descriptors in recognizing a shape by enhancing the ability of measuring functions in capturing a greater quantity of shape information. However, in spite of the potentiality of the n-dimensional setting, some objective obstacles, concerning, above all, the lack of an efficient computational approach, make it difficult to purse such a research line. Indeed, a direct approach to the multidimensional case forces to work in subsets of $\mathbb{R}^{2n}$, implying higher computational costs in evaluating and comparing shape descriptors, because of the absence of a representation by means of multisets of points, analogous to persistence diagrams.

As for Persistence Homology Theory, these obstacles in treating the multidimensional setting appear in the approach proposed by Carrlson and Zomorodian in [12].

Indeed, the authors concluded that paper claiming that multidimensional persistence has an essentially different character from its 1-dimensional version, since their approach does not seem to lead to a complete, stable descriptor in the multidimensional case. The rank invariant, introduced to describe a multifiltration of a space (see Subsection 1.4.3), represents a practical tool for robust estimation of the Betti numbers in a multifiltration, but it results to be a complete discrete invariant only in the 1-dimensional setting [12, Thm. 5].

Recently, Size Theory has been developed in the n-dimensional framework [4, 14] in a manner to pave a way out of all the above-mentioned difficulties, and providing a concise, complete and stable (though not discrete) shape descriptor also in the multidimensional context, that inherits the good properties of 1-dimensional size functions. The strategy proposed is the reduction of multidimensional size functions to 1-dimensional ones by a suitable change of variables. In particular, a suitable planes' foliation of $\Delta^+ = \{(\vec{u},\vec{v}) \in \mathbb{R}^{2n}, \vec{u} \prec \vec{v}\}$ is defined to make an n-dimensional size function, associated with a topological space endowed with an n-dimensional measuring function, equal to a 1-dimensional size function, associated with the same topological space endowed with a 1-dimensional measuring function, in correspondence of each half-plane [4]. The importance of this result resides in the fact that, on each leaf of the foliation, it is possible to translate and use all the results conveyed in the last years for 1-dimensional size functions. In particular, on each half-plane, multidimensional size functions can be expressed as formal series of cornerpoints, making their comparison possible through the matching distance. So,even if, unfortunately, cornerpoints do not form, in general, discrete sets in the multidimensional case, this approach makes it possible to find them "slice by slice" with the familiar discrete technique of dimension one. A practical use is for sampling of the sets of leaves, so getting bounds for a stable distance between size functions. Experimental results shown in [4] have validated this approach and demonstrated the higher discriminatory power achieved using n-dimensional measuring functions, by blending the information conveyed by their n components.

Our purpose, in this chapter, is to show analogous positive results for Multidimensional Persistent Homology, by extending the approach of Size Theory to all homology degrees. In particular a reduction theorem, asserting the coincidence between a

n-dimensional kth persistent homology module and a 1-dimensional one on each leaf of the foliation of Δ^+, represents the main tool for the construction of a stable multidimensional bottleneck distance between n-dimensional kth rank invariants.

The chapter is structured as follows. Section 2.1 provides the necessary tools for our goal, concerning the foliation of Δ^+. In Section 2.2 we give a new definition of multidimensional kth persistent homology modules (Definition 2.3), in terms of max-tame size pairs (Definition 2.2). Moreover, our reduction theorem (Theorem 2.2.1) is stated and proved. Section 2.3 is devoted to define and show properties of the multidimensional bottleneck distance. In a 1-dimensional setting, it is redefined in terms of rank invariants (Definition 2.5), instead of persistence diagrams (Definition 1.12), leading us to its extension to a multidimensional context (Definition 2.6). In Section 2.4 we describe two examples demonstrating the higher discriminatory power of multidimensional persistence than 1-dimesional and expose further observations on the cooperation of measuring functions. A brief discussion on the results achieved and open problems concludes the chapter.

2.1 A suitable foliation of Δ^+

In this section we show how it is possible to define a foliation of $\Delta^+ \subset \mathbb{R}^n \times \mathbb{R}^n$ suitable to reduce computation of persistent homology from the multidimensional to the 1-dimensional case. Its construction depends on so-called "admissible" vector pairs.

Definition 2.1. *For every unit vector $\vec{l} = (l_1, \ldots, l_n)$ in $\mathbb{R}^n$ such that $l_j > 0$ for $j = 1, \ldots, n$, and for every vector $\vec{b} = (b_1, \ldots, b_n)$ in $\mathbb{R}^n$ such that $\sum_{j=1}^{n} b_j = 0$, we shall say that the pair $(\vec{l}, \vec{b})$ is* admissible. *We shall denote the set of all admissible pairs in $\mathbb{R}^n \times \mathbb{R}^n$ by Adm_n. Given an admissible pair $(\vec{l}, \vec{b})$, we define the half-plane $\pi_{(\vec{l},\vec{b})}$ in $\mathbb{R}^n \times \mathbb{R}^n$ by the following parametric equations:*

$$\begin{cases} \vec{u} = s\vec{l} + \vec{b} \\ \vec{v} = t\vec{l} + \vec{b} \end{cases}$$

for $s, t \in \mathbb{R}$, with $s < t$.

For every $(\vec{u},\vec{v}) \in \Delta^+$, there exists exactly one admissible pair $(\vec{l},\vec{b})$ such that $(\vec{u},\vec{v}) \in \pi_{(\vec{l},\vec{b})}$ [4, Prop.1].

The following proposition is substantially contained in the proof of [4, Thm. 3] and represents the fundamental ingredient for proving our reduction theorem (Theorem 2.2.1). Indeed, Proposition 2.1.1 asserts that, fixed an admissible pair, a multidimensional measuring function can be replaced by a 1-dimensional one, in such a way that their lower-level sets coincide on the corresponding leaf of the foliation.

Proposition 2.1.1. *Let $(X,\vec{\varphi})$ be a size pair. Let $(\vec{l},\vec{b})$ be an admissible pair, and let $F^{\vec{\varphi}}_{(\vec{l},\vec{b})} : X \to \mathbb{R}$ be defined by setting*

$$F^{\vec{\varphi}}_{(\vec{l},\vec{b})}(P) = \max_{j=1,\ldots,n} \left\{ \frac{\varphi_j(P) - b_j}{l_j} \right\},$$

for every $P \in X$. Then, for every $(\vec{u},\vec{v}) = (s\vec{l}+\vec{b}, t\vec{l}+\vec{b}) \in \pi_{(\vec{l},\vec{b})}$, the following equalities hold:

$$X\langle\vec{\varphi} \preceq \vec{u}\rangle = X\langle F^{\vec{\varphi}}_{(\vec{l},\vec{b})} \leq s\rangle, \qquad X\langle\vec{\varphi} \preceq \vec{v}\rangle = X\langle F^{\vec{\varphi}}_{(\vec{l},\vec{b})} \leq t\rangle.$$

Proof. For every $\vec{u} = (u_1,\ldots,u_n) \in \mathbb{R}^n$, with $u_j = sl_j + b_j$, $j = 1,\ldots,n$, it holds that

$$\begin{aligned}
X\langle\vec{\varphi} \preceq \vec{u}\rangle &= \{P \in X : \varphi_j(P) \leq u_j, j = 1,\ldots,n\} \\
&= \{P \in X : \varphi_j(P) \leq sl_j + b_j, j = 1,\ldots,n\} \\
&= \left\{P \in X : \frac{\varphi_j(P) - b_j}{l_j} \leq s, j = 1,\ldots,n\right\} \\
&= X\langle F^{\vec{\varphi}}_{(\vec{l},\vec{b})} \leq s\rangle.
\end{aligned}$$

Analogously, for every $\vec{v} = (v_1,\ldots,v_n) \in \mathbb{R}^n$, with $v_j = tl_j + b_j$, $j = 1,\ldots,n$, it can be proved that $X\langle\vec{\varphi} \preceq \vec{v}\rangle = X\langle F^{\vec{\varphi}}_{(\vec{l},\vec{b})} \leq t\rangle$. $\square$

Note that the above result holds for an arbitrarily size pair $(X,\vec{\varphi})$.

For our purpose, we need the following further condition: $\varphi_1,\ldots,\varphi_n : X \to \mathbb{R}$ shall be tame functions (Definition 1.9). In agreement with this hypothesis, throughout all the chapter, a size pair $(X,\vec{\varphi})$ such that all the components of $\vec{\varphi}$ are tame will be called a *tame size pair*.

2.2 Homological 1-dimensional reduction

The results shown in the previous section do not constitute the sole instruments leading to the definition of a stable distance between multidimensional rank invariants. So, in this section, we investigate further fundamental tools for our goal.

A necessary requirement for our reduction theorem, is that, given $\vec{\varphi} : X \to \mathbb{R}^n$, both $\varphi_j : X \to \mathbb{R}$ for $j = 1, \ldots, n$, and $F^{\vec{\varphi}}_{(\vec{l},\vec{b})} : X \to \mathbb{R}$ are tame functions, and the following remark states that this condition is not always fullfilled.

Remark 1. *The maximum of two tame functions is not necessarily a tame function.*

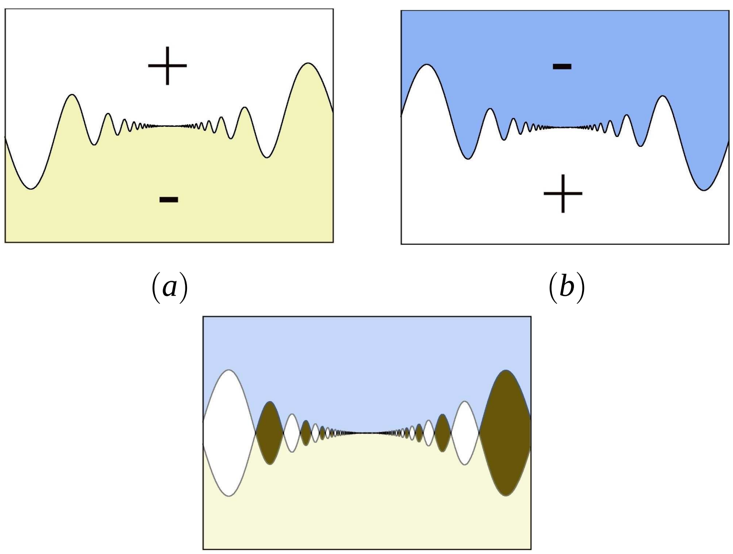

(a) (b) (c)

Figure 2.1: In (a) the lower-level set $\mathbb{R}^2\langle f_1 \leq 0\rangle$ (yellow area - one connected component). In (b) lower-level set $\mathbb{R}^2\langle f_2 \leq 0\rangle$ (blue area - one connected component). In (c) lower-level set $\mathbb{R}^2\langle f \leq 0\rangle$ (dark zone - infinitely many connected components).

As an example, let $f_1, f_2 : \mathbb{R}^2 \to \mathbb{R}$ be two tame functions defined as

$$f_1(u,v) = \begin{cases} v - u^2 \sin(\frac{1}{u}) & u \neq 0 \\ v & u = 0 \end{cases}, \quad f_2(u,v) = \begin{cases} -v - u^2 \sin(\frac{1}{u}) & u \neq 0 \\ -v & u = 0 \end{cases}$$

and consider the function

$$f = \max(f_1, f_2).$$

Figure 2.1 shows the sets where f_1 ((a), yellow area), f_2 ((b), blue area) and f ((c), dark areas), respectively, take a value smaller or equal to 0. It is easily seen that, even if f_1 and f_2 are tame functions, with $\mathbb{R}^2\langle f_1 \leq 0\rangle$ and $\mathbb{R}^2\langle f_2 \leq 0\rangle$ connected lower-level sets, f does not result to be tame, since $H_0(\mathbb{R}^2\langle f \leq 0\rangle)$ is not a finitely generated module.

Given this fault related to tame functions, a preliminary solution we propose is to introduce the following concept.

Definition 2.2. *Let $(X,\vec{\varphi})$ be a tame size pair. We shall say that $(X,\vec{\varphi})$ is a* max-tame size pair *if, for every admissible pair $(\vec{l},\vec{b})$, the function $F^{\vec{\varphi}}_{(\vec{l},\vec{b})} : X \to \mathbb{R}$ such that $F^{\vec{\varphi}}_{(\vec{l},\vec{b})}(P) = \max_{j=1,\dots,n}\left\{\frac{\varphi_j(P)-b_j}{l_j}\right\}$ for every $P \in X$, is tame.*

Let us redefine multidimensional persistent homology modules in view of the above definition.

Definition 2.3. *Let $(X,\vec{\varphi})$ be a max-tame size pair. For $(\vec{u},\vec{v}) \in \Delta^+$, let $\iota_k^{\vec{u},\vec{v}} : H_k(X\langle\vec{\varphi} \preceq \vec{u}\rangle) \to H_k(X\langle\vec{\varphi} \preceq \vec{v}\rangle)$ be the map induced by inclusion of the lower-level set of $\vec{u}$ in that of $\vec{v}$, for a fixed integer k. We call* multidimensional kth-persistent homology module *of $(X,\vec{\varphi})$ the image of such a homomorphism, and write $H_k^{\vec{u},\vec{v}}(X,\vec{\varphi}) = \mathrm{im}\,\iota_k^{\vec{u},\vec{v}}$.*

Now we can state and prove the theorem which, in analogy with the main result of [4], enables us to reduce the computation of multidimensional persistent homology modules to the 1-dimensional case. This is important, not so much for finding the homology modules themselves point by point, but much more for finding points of change of the modules. However, before its formulation, the introduction of some notations would be necessary.

Given $F^{\vec{\varphi}}_{(\vec{l},\vec{b})}(P) = \max_{j=1,\dots,n}\left\{\frac{\varphi_j(P)-b_j}{l_j}\right\}$ for a fixed $(\vec{l},\vec{b}) \in Adm_n$, let $\kappa_k^{s,t} : H_k(X\langle F^{\vec{\varphi}}_{(\vec{l},\vec{b})} \leq s\rangle) \to H_k(X\langle F^{\vec{\varphi}}_{(\vec{l},\vec{b})} \leq t\rangle)$ for $s,t \in \mathbb{R}$, $s < t$ and $k \in \mathbb{Z}$, be the map induced by inclusion of the lower-level set of s in that of t, and denote by $H_k^{s,t}(X,F^{\vec{\varphi}}_{(\vec{l},\vec{b})}) = \mathrm{im}\,\kappa_k^{s,t}$ the kth persistent homology module of $(X,F^{\vec{\varphi}}_{(\vec{l},\vec{b})})$.

Theorem 2.2.1. *Let $(X,\vec{\varphi})$ be a max-tame size pair. Let $(\vec{l},\vec{b})$ be an admissible pair. Then, for every $(\vec{u},\vec{v}) = (s\vec{l}+\vec{b},t\vec{l}+\vec{b}) \in \pi_{(\vec{l},\vec{b})}$, the equality*

$$H_k^{\vec{u},\vec{v}}(X,\vec{\varphi}) = H_k^{s,t}(X,F^{\vec{\varphi}}_{(\vec{l},\vec{b})})$$

holds for every $k \in \mathbb{Z}$ and $s,t \in \mathbb{R}$ with $s < t$.

Proof. By Lemma 2.1.1, we have the equalities $X\langle\vec{\varphi} \preceq \vec{u}\rangle = X\langle F^{\vec{\varphi}}_{(\vec{l},\vec{b})} \leq s\rangle$ and $X\langle\vec{\varphi} \preceq \vec{v}\rangle = X\langle F^{\vec{\varphi}}_{(\vec{l},\vec{b})} \leq t\rangle$ for every $(\vec{u},\vec{v}) = (s\vec{l}+\vec{b}, t\vec{l}+\vec{b}) \in \pi_{(\vec{l},\vec{b})}$. They obviously imply that, for every $k \in \mathbb{Z}$, $H_k(X\langle\vec{\varphi} \preceq \vec{u}\rangle) = H_k(X\langle F^{\vec{\varphi}}_{(\vec{l},\vec{b})} \leq s\rangle)$ and $H_k(X\langle\vec{\varphi} \preceq \vec{v}\rangle) = H_k(X\langle F^{\vec{\varphi}}_{(\vec{l},\vec{b})} \leq t\rangle)$, respectively. Thus, since $\iota_k^{\vec{u},\vec{v}} : H_k(X\langle\vec{\varphi} \preceq \vec{u}\rangle) \to H_k(X\langle\vec{\varphi} \preceq \vec{v}\rangle)$ and $\kappa_p^{s,t} : H_k(X\langle F^{\vec{\varphi}}_{(\vec{l},\vec{b})} \leq s\rangle) \to H_k(X\langle F^{\vec{\varphi}}_{(\vec{l},\vec{b})} \leq t\rangle)$ are homomorphisms induced by inclusion, having the same domain and codomain, it necessarily follows that $\operatorname{im} \iota_k^{\vec{u},\vec{v}} = \operatorname{im} \kappa_p^{s,t}$, and the claim is proved. $\square$

2.3 Multidimensional bottleneck distance

This section deals with the construction of the bottleneck distance between multidimensional rank invariants, by mimicking the theoretical approach of Size Theory with regard to the generalization of the matching distance shown in [4]. In particular, after a reformulation of the 1-dimensional bottleneck distance d_B in terms of rank invariants (Definition 2.5), instead of persistence diagrams (Definition 1.12), we will prove that, using this distance, on each leaf of the foliation rank invariants result stable under small perturbations of 1-dimensional measuring functions (with respect to the max-norm) (Proposition 2.3.2), and under small perturbations of the leaves (Proposition 2.3.3), respectively. Moreover, we will extend d_B to a multidimensional distance D_B (Definition 2.6), and prove that the latter is still a lower bound for the natural pseudo-distance (Theorem 2.3.4). Eventually, in Proposition 2.3.5, we prove the higher discriminatory power of the multidimensional bottleneck distance than the 1-dimensional one, showing that the former gives a better lower bound for the natural pseudo-distance than the latter.

First of all, according to the general Definition 1.14, let us define an n-dimensional kth rank invariant describing the homology of a multifiltration that is defined by the variation of an n-dimensional measuring function, with tame components.

Definition 2.4. *Let $(X,\vec{\varphi})$ be a tame size pair. For every $(\vec{u},\vec{v}) \in \Delta^+$ and $k \in \mathbb{Z}$, we define*

$\rho_k^{(X,\vec{\varphi})}: \Delta^+ \to \mathbb{N}$ *over a field* $\mathbb{K}$ *to be*

$$\rho_k^{(X,\vec{\varphi})}(\vec{u},\vec{v}) = \mathrm{rank} H_k^{\vec{u},\vec{v}}(X,\vec{\varphi}).$$

Let us observe that, in the 1-dimensional setting, the existing relation between persistence diagrams and rank invariants is analogous to the relation between cornerpoints and size functions. Therefore, rank invariants associated with 1-dimensional persistent modules can be compared through the bottleneck distance (Definition 1.12).

Definition 2.5. *Let* (X,φ), (Y,ψ) *be two tame size pairs, and let* $k \in \mathbb{Z}$ *such that* $\beta_k(X) = \beta_k(Y)$. *Moreover, let* $\rho_k^{(X,\varphi)}$ *and* $\rho_k^{(Y,\psi)}$ *be the respective 1-dimensional kth rank invariants. Let* C_1 *(resp.* C_2*) be the multiset of all pairs of homological critical values counted with their multiplicities, together with all points on the diagonal* Δ *counted with infinite multiplicity. The* bottleneck distance *between* $\rho_k^{(X,\varphi)}$ *and* $\rho_k^{(Y,\psi)}$ *is given by*

$$d_B\left(\rho_k^{(X,\varphi)}, \rho_k^{(Y,\psi)}\right) = \inf_{\sigma} \sup_{p\in C_1} \|p-\sigma(p)\|_\infty$$

where σ *ranges over all the bijections between* C_1 *and* C_2.

The above definition is more general than the one involving persistence diagrams (Definition 1.12). Indeed, in this new version, the bottleneck distance between kth rank invariants can be computed also when the involved size pairs have different spaces. Naturally, the two definitions coincide when the spaces coincide. This fact extends the validity of Theorem 1.4.1 on the bottleneck stability.

In the sequel, let us consider two max-tame size pairs $(X,\vec{\varphi})$, $(Y,\vec{\psi})$, associated with $\rho_k^{(X,\vec{\varphi})}$, $\rho_k^{(Y,\vec{\psi})}$ respectively, for $k \in \mathbb{Z}$. Furthermore, let an admissible pair $(\vec{l},\vec{b})$ be fixed, and let $F_{(\vec{l},\vec{b})}^{\vec{\varphi}}: X \to \mathbb{R}$, $F_{(\vec{l},\vec{b})}^{\vec{\psi}}: Y \to \mathbb{R}$ be defined as before.

An easy corollary of our Theorem 2.2.1 is the following, which is the higher degree version of [4, Cor. 1]. It states that, for fixed $k \in \mathbb{Z}$, two multidimensional kth rank invariants coincide if and only if the corresponding 1-dimensional kth rank invariants associated with each admissible pair $(\vec{l},\vec{b})$ coincide; so, the set of 1-dimensional rank invariants $\rho_k^{(X,F_{(\vec{l},\vec{b})}^{\vec{\varphi}})}$, as $(\vec{l},\vec{b})$ varies in Adm_n, completely characterizes $\rho_k^{(X,\vec{\varphi})}$.

Corollary 2.3.1. *For each* $k \in \mathbb{Z}$ *the identity* $\rho_k^{(X,\vec{\varphi})} \equiv \rho_k^{(Y,\vec{\psi})}$ *holds if and only if, for every admissible pair* $(\vec{l},\vec{b})$, $d_B\left(\rho_k^{(X,F_{(\vec{l},\vec{b})}^{\vec{\varphi}})}, \rho_k^{(Y,F_{(\vec{l},\vec{b})}^{\vec{\psi}})}\right) = 0$.

The persistence diagrams are known to be stable under possibly small perturbations of 1-dimensional measuring functions (Theorem 1.4.1). In the multidimensional setting, the stability of rank invariants under perturbations of 1-dimensional measuring functions on each leaf of the foliation is stated by the following proposition.

Proposition 2.3.2. *Let $(X,\vec{\varphi})$, $(X,\vec{\psi})$ be two max-tame size pairs with $\|\vec{\varphi}-\vec{\psi}\|_\infty \le \varepsilon$. Then, for every admissible pair $(\vec{l},\vec{b})$ and for each $k\in\mathbb{Z}$, it holds that*

$$d_B\left(\rho_k^{(X,F^{\vec{\varphi}}_{(\vec{l},\vec{b})})},\rho_k^{(X,F^{\vec{\psi}}_{(\vec{l},\vec{b})})}\right)\le\frac{\varepsilon}{\min\limits_{j=1,\dots,n} l_j}.$$

Proof. First of all, let us recall that

$$\|\vec{\varphi}-\vec{\psi}\|_\infty=\max_{P\in X}\|\vec{\varphi}(P)-\vec{\psi}(P)\|_\infty=\max_{P\in X}\max_{j=1,\dots,n}|\varphi_j(P)-\psi_j(P)|.$$

Moreover, since $(X,\vec{\varphi})$ $(X,\vec{\psi})$ have the same support, we can apply Theorem 1.4.1, for which it holds that

$$d_B\left(\rho_k^{(X,F^{\vec{\varphi}}_{(\vec{l},\vec{b})})},\rho_k^{(X,F^{\vec{\psi}}_{(\vec{l},\vec{b})})}\right)\le\max_{P\in X}|F^{\vec{\varphi}}_{(\vec{l},\vec{b})}(P)-F^{\vec{\psi}}_{(\vec{l},\vec{b})}(P)|.$$

Fix now $P\in X$ and denote by $\hat{j}$ the index for which $\max\limits_j\frac{\varphi_j(P)-b_j}{l_j}$ is attained. By the definition of $F^{\vec{\varphi}}_{(\vec{l},\vec{b})}$ and $F^{\vec{\psi}}_{(\vec{l},\vec{b})}$, it holds that

$$\begin{aligned}
F^{\vec{\varphi}}_{(\vec{l},\vec{b})}(P)-F^{\vec{\psi}}_{(\vec{l},\vec{b})}(P) &= \max_j\frac{\varphi_j(P)-b_j}{l_j}-\max_j\frac{\psi_j(P)-b_j}{l_j}\\
&= \frac{\varphi_{\hat{j}}(P)-b_{\hat{j}}}{l_{\hat{j}}}-\max_j\frac{\psi_j(P)-b_j}{l_j}\\
&\le \frac{\varphi_{\hat{j}}(P)-b_{\hat{j}}}{l_{\hat{j}}}-\frac{\psi_{\hat{j}}(P)-b_{\hat{j}}}{l_{\hat{j}}}\\
&= \frac{\varphi_{\hat{j}}(P)-\psi_{\hat{j}}(P)}{l_{\hat{j}}}\le\frac{\|\vec{\varphi}(P)-\vec{\psi}(P)\|_\infty}{\min\limits_{j=1,\dots,n} l_j}.
\end{aligned}$$

In an analogous way, we obtain that $F^{\vec{\psi}}_{(\vec{l},\vec{b})}(P)-F^{\vec{\varphi}}_{(\vec{l},\vec{b})}(P)\le\frac{\|\vec{\varphi}(P)-\vec{\psi}(P)\|_\infty}{\min\limits_{j=1,\dots,n} l_j}$. Therefore, if

$\max_{P\in X}\|\vec{\varphi}(P)-\vec{\psi}(P)\|_\infty \le \varepsilon$, then

$$\begin{aligned}\max_{P\in X}\left|F^{\vec{\varphi}}_{(\vec{l},\vec{b})}(P)-F^{\vec{\psi}}_{(\vec{l},\vec{b})}(P)\right| &\le \max_{P\in X}\frac{\|\vec{\varphi}(P)-\vec{\psi}(P)\|_\infty}{\min_{j=1,\ldots,n} l_j}\\ &\le \frac{\varepsilon}{\min_{j=1,\ldots,n} l_j}.\end{aligned}$$

□

Proposition 2.3.3 ensures the robustness of the rank invariant under small changes of the leaves in the foliation. Roughly speaking, it asserts that small changes in the admissible pair $(\vec{l},\vec{b})$ with respect to the max-norm induce small changes of the rank invariant $\rho_k^{(X,F^{\vec{\varphi}}_{(\vec{l},\vec{b})})}$ with respect to the bottleneck distance.

Proposition 2.3.3. *If $(X,\vec{\varphi})$ is a max-tame size pair and $(\vec{l},\vec{b})$, $(\vec{l}',\vec{b}')$ are admissible pairs with $\|\vec{l}-\vec{l}'\|_\infty \le \varepsilon$, $\|\vec{b}-\vec{b}'\|_\infty \le \varepsilon$ and $\varepsilon < \min_{j=1,\ldots,n}\{l_j\}$, it holds that*

$$d_B\left(\rho_k^{(X,F^{\vec{\varphi}}_{(\vec{l},\vec{b})})},\rho_k^{(X,F^{\vec{\varphi}}_{(\vec{l}',\vec{b}')})}\right) \le \varepsilon\cdot\frac{\max_{P\in X}\|\vec{\varphi}(P)\|_\infty+\|\vec{l}\|_\infty+\|\vec{b}\|_\infty}{\min_{j=1,\ldots,n}\{l_j(l_j-\varepsilon)\}}.$$

Proof. From the bottleneck stability stated in Theorem 1.4.1, we have

$$d_B\left(\rho_k^{(X,F^{\vec{\varphi}}_{(\vec{l},\vec{b})})},\rho_k^{(X,F^{\vec{\varphi}}_{(\vec{l}',\vec{b}')})}\right) \le \max_{P\in X}|F^{\vec{\varphi}}_{(\vec{l},\vec{b})}(P)-F^{\vec{\varphi}}_{(\vec{l}',\vec{b}')}(P)|.$$

Fix now $P\in X$, and denote by $\hat{j}$ the index for which $\max_j\frac{\varphi_j(P)-b_j}{l_j}$ is attained. By the definition of $F^{\vec{\varphi}}_{(\vec{l},\vec{b})}$ and $F^{\vec{\varphi}}_{(\vec{l}',\vec{b}')}$, it follows that

$$\begin{aligned}
F^{\vec{\varphi}}_{(\vec{l},\vec{b})}(P) - F^{\vec{\varphi}}_{(\vec{l}',\vec{b}')}(P) &= \max_j \frac{\varphi_j(P)-b_j}{l_j} - \max_j \frac{\varphi_j(P)-b'_j}{l'_j} \\
&= \frac{\varphi_{\hat{j}}(P)-b_{\hat{j}}}{l_{\hat{j}}} - \max_j \frac{\varphi_j(P)-b'_j}{l'_j} \\
&\leq \frac{\varphi_{\hat{j}}(P)-b_{\hat{j}}}{l_{\hat{j}}} - \frac{\varphi_{\hat{j}}(P)-b'_{\hat{j}}}{l'_{\hat{\imath}}} \\
&= \frac{(l'_{\hat{j}}-l_{\hat{j}})\varphi_{\hat{j}}(P) - l'_{\hat{j}}b_{\hat{j}} + l_{\hat{j}}b'_{\hat{j}}}{l_{\hat{j}}l'_{\hat{j}}} \\
&= \frac{(l'_{\hat{j}}-l_{\hat{j}})\varphi_{\hat{j}}(P) + l_{\hat{j}}(b'_{\hat{j}}-b_{\hat{j}}) + b_{\hat{j}}(l_{\hat{j}}-l'_{\hat{j}})}{l_{\hat{j}}l'_{\hat{j}}} \\
&\leq \frac{|l'_{\hat{j}}-l_{\hat{j}}||\varphi_{\hat{j}}(P)| + |l_{\hat{j}}||b'_{\hat{j}}-b_{\hat{j}}| + |b_{\hat{j}}||l_{\hat{j}}-l'_{\hat{j}}|}{l_{\hat{j}}l'_{\hat{j}}} \\
&\leq \frac{\varepsilon(\|\vec{\varphi}(P)\|_\infty + \|\vec{l}\|_\infty + \|\vec{b}\|_\infty)}{l_{\hat{j}}(l_{\hat{j}}-\varepsilon)} \\
&\leq \frac{\varepsilon(\|\vec{\varphi}(P)\|_\infty + \|\vec{l}\|_\infty + \|\vec{b}\|_\infty)}{\min\limits_{j=1,\ldots,n}\{l_j(l_j-\varepsilon)\}}.
\end{aligned}$$

In the same manner we can see that $F^{\vec{\varphi}}_{(\vec{l}',\vec{b}')}(P) - F^{\vec{\varphi}}_{(\vec{l},\vec{b})}(P) \leq \frac{\varepsilon(\|\vec{\varphi}(P)\|_\infty + \|\vec{l}\|_\infty + \|\vec{b}\|_\infty)}{\min_{j=1,\ldots,n}\{l_j(l_j-\varepsilon)\}}$. Therefore,

$$\max_{P\in X}\left|F^{\vec{\varphi}}_{(\vec{l},\vec{b})}(P) - F^{\vec{\varphi}}_{(\vec{l}',\vec{b}')}(P)\right| \leq \varepsilon \cdot \frac{\max\limits_{P\in X}\|\vec{\varphi}(P)\|_\infty + \|\vec{l}\|_\infty + \|\vec{b}\|_\infty}{\min\limits_{j=1,\ldots,n}\{l_j(l_j-\varepsilon)\}}$$

and the claim is proved. □

Definition 2.6. *Let $(X,\vec{\varphi})$, $(Y,\vec{\psi})$ be two max-tame size pairs, with $\beta_k(X)=\beta_k(Y)$ for a fixed $k\in\mathbb{Z}$. Then the k*th multidimensional bottleneck distance *between $\rho_k^{(X,\vec{\varphi})}$ and $\rho_k^{(Y,\vec{\psi})}$ is defined by*

$$D_B\left(\rho_k^{(X,\vec{\varphi})}, \rho_k^{(Y,\vec{\psi})}\right) = \sup_{(\vec{l},\vec{b})\in Adm_n} \min_{j=1,\ldots,n} l_j \cdot d_B\left(\rho_k^{(X,F^{\vec{\varphi}}_{(\vec{l},\vec{b})})}, \rho_k^{(Y,F^{\vec{\psi}}_{(\vec{l},\vec{b})})}\right).$$

Note that D_B is by construction a global distance, i.e. not depending on $(\vec{l},\vec{b})$, but since the coefficients l_j are always < 1, there might be distances d_B, for particular admissible pairs, which take greater values. On the other hand, the definition above implies that each 1-dimensional bottleneck distance obtained in correspondence of an admissible pair yields a lower bound for the multidimensional bottleneck distance; so, it suffices a fine sampling by admissible pairs to produce approximations of arbitrary precision of D_B.

The next two results show that, for every homology degree $k \in \mathbb{Z}$, the multidimensional bottleneck distance $D_B\left(\rho_k^{(X,\vec{\varphi})}, \rho_k^{(Y,\vec{\psi})}\right)$ provides a lower bound for the multidimensional natural pseudo-distance $d((X,\vec{\varphi}),(Y,\vec{\psi}))$ (Theorem 2.3.4), and that this lower-bound is better than the one provided by the 1-dimensional bottleneck distance $d_B\left(\rho_k^{(X,\varphi_i)}, \rho_k^{(X,\psi_i)}\right)$ for $i = 1,\ldots,n$ (Proposition 2.3.5), respectively.

Theorem 2.3.4. *Let $(X,\vec{\varphi})$, $(Y,\vec{\psi})$ be two max-tame size pairs, with X,Y homeomorphic topological spaces. Let $d((X,\vec{\varphi}),(Y,\vec{\psi}))$ be the natural pseudo-distance between $(X,\vec{\varphi})$ and $(Y,\vec{\psi})$. Then*

$$D_B\left(\rho_k^{(X,\vec{\varphi})}, \rho_k^{(Y,\vec{\psi})}\right) \le d((X,\vec{\varphi}),(Y,\vec{\psi}))$$

for every $k \in \mathbb{Z}$.

Proof. Let us recall that, by Definition 1.1, the condition X, Y homeomorphic implies that $d((X,\vec{\varphi}),(Y,\vec{\psi})) = \inf_f \max_{P\in X} \|\vec{\varphi}(P) - \vec{\psi}(f(P))\|_\infty$, where f varies among all the homomorphisms in $H(X,Y)$. Moreover, the condition X, Y homeomorphic also implies that $\beta_k(X) = \beta_k(Y)$, for every $k \in \mathbb{Z}$. So, for any such $f \in H(X,Y)$ and any $k \in \mathbb{Z}$, it holds that $\rho_k^{(Y,F^{\vec{\psi}}_{(\vec{l},\vec{b})})} \equiv \rho_k^{(X,F^{\vec{\psi}}_{(\vec{l},\vec{b})}\circ f)}$. By applying Proposition 2.3.2, with $\vec{\psi}$ replaced by $\vec{\psi}\circ f$ and ε by $\max_{P\in X} \|\vec{\varphi}(P) - \vec{\psi}(f(P))\|_\infty$, and observing that $F^{\vec{\psi}}_{(\vec{l},\vec{b})} \circ f \equiv F^{\vec{\psi}\circ f}_{(\vec{l},\vec{b})}$, it follows that

$$\min_{j=1,\ldots,n} l_j \cdot\ d_B\left(\rho_k^{(X,F^{\vec{\varphi}}_{(\vec{l},\vec{b})})}, \rho_k^{(Y,F^{\vec{\psi}\circ f}_{(\vec{l},\vec{b})})}\right) \le \max_{P\in X} \|\vec{\varphi}(P) - \vec{\psi}(f(P))\|_\infty$$

for every admissible pairs $(\vec{l},\vec{b})$ and $k \in \mathbb{Z}$. Furthermore, since it is true for each homeomorphism f between X and Y, the claim immediately follows. $\square$

By the same argument of the analogous Proposition 4 in [4], it is easy to prove the following inequality between the multidimensional bottleneck distance and the 1-

dimensional one obtained by considering the components of the measuring functions. That this inequality can be strict, is shown in an example described in Section 2.4.

Proposition 2.3.5. *Let $(X,\vec{\varphi}),(Y,\vec{\psi})$ be two max-tame size pairs such that $\beta_k(X)=\beta_k(Y)$ for a fixed integer k. Then, for every $i=1,\ldots,n$, it holds that*

$$d_B\left(\rho_k^{(X,\varphi_i)},\rho_k^{(Y,\psi_i)}\right)\ \le\ D_B\left(\rho_k^{(X,\vec{\varphi})},\rho_k^{(Y,\vec{\psi})}\right).$$

Proof. Let $\mu=\max_{P\in X}\|\vec{\varphi}(P)\|_\infty$ and $\nu=\max_{Q\in Y}\|\vec{\psi}(Q)\|_\infty$. For $i=1,\ldots,n$, consider the admissible pair $(\vec{l}^i,\vec{b}^i)$, where $\vec{l}^i=(l_1^i,\ldots,l_n^i)$ and $\vec{b}^i=(b_1^i,\ldots,b_n^i)$ are defined in the following way

$$l_j^i=\tfrac{1}{\sqrt{n}},\quad \text{for } j=1,\ldots,n,$$

$$b_j^i=\begin{cases}-\frac{2(n-1)}{n}\max\{\mu,\nu\}, & \text{if } i=j;\\ \frac{2}{n}\max\{\mu,\nu\}, & \text{if } i\neq j.\end{cases}$$

From Theorem 2.2.1, for every $(\vec{u},\vec{v})=(s\vec{l}^i+\vec{b}^i,t\vec{l}^i+\vec{b}^i)\in\pi_{(\vec{l}^i,\vec{b}^i)}$ and for every $k\in\mathbb{Z}$, it holds that $H_k^{\vec{u},\vec{v}}(X,\vec{\varphi})=H_k^{s,t}(X,F^{\vec{\varphi}}_{(\vec{l}^i,\vec{b}^i)})$, $H_k^{\vec{u},\vec{v}}(Y,\vec{\psi})=H_k^{s,t}(Y,F^{\vec{\psi}}_{(\vec{l}^i,\vec{b}^i)})$, with $F^{\vec{\varphi}}_{(\vec{l}^i,\vec{b}^i)}(P)=\max_{j=1,\ldots,n}\left\{\frac{\varphi_j(P)-b_j^i}{l_j^i}\right\}=\sqrt{n}(\varphi_i(P)-b_i^i)$ for every $P\in X$, and
$F^{\vec{\psi}}_{(\vec{l}^i,\vec{b}^i)}(Q)=\max_{j=1,\ldots,n}\left\{\frac{\psi_j(Q)-b_j^i}{l_j^i}\right\}=\sqrt{n}(\psi_i(Q)-b_i^i)$ for every $Q\in Y$. Then

$$\begin{aligned}d_B\left(\rho_k^{(X,F^{\vec{\varphi}}_{(\vec{l}^i,\vec{b}^i)})},\rho_k^{(Y,F^{\vec{\psi}}_{(\vec{l}^i,\vec{b}^i)})}\right) &= d_B\left(\rho_k^{(X,\sqrt{n}(\varphi_i-b_i^i))},\rho_k^{(Y,\sqrt{n}(\psi_i-b_i^i))}\right)\\ &= \sqrt{n}\cdot d_B\left(\rho_k^{(X,\varphi_i-b_i^i)},\rho_k^{(Y,\psi_i-b_i^i)}\right)\\ &= \sqrt{n}\cdot d_B\left(\rho_k^{(X,\varphi_i)},\rho_k^{(Y,\psi_i)}\right)\end{aligned}$$

and hence, using the above definition of l_j^i, $j=1,\ldots,n$, it holds that

$$\begin{aligned}\min_{j=1,\ldots,n} l_j^i\cdot d_B\left(\rho_k^{(X,F^{\vec{\varphi}}_{(\vec{l}^i,\vec{b}^i)})},\rho_k^{(Y,F^{\vec{\psi}}_{(\vec{l}^i,\vec{b}^i)})}\right) &= \frac{1}{\sqrt{n}}\cdot d_B\left(\rho_k^{(X,F^{\vec{\varphi}}_{(\vec{l}^i,\vec{b}^i)})},\rho_k^{(Y,F^{\vec{\psi}}_{(\vec{l}^i,\vec{b}^i)})}\right)\\ &= d_B\left(\rho_k^{(X,\varphi_i)},\rho_k^{(Y,\psi_i)}\right)\end{aligned}$$

Finally, the claim immediately follows from the definition of $D_B\left(\rho_k^{(X,\vec{\varphi})},\rho_k^{(Y,\vec{\psi})}\right)$. $\square$

2.4 Examples and remarks

This section provides two simple examples of shape comparison. Their aim is to demonstrate that the discriminatory power derivable from one comparison between n-dimensional persistent homology modules, i.e. computed with respect to an n-dimensional measuring function is higher than the one achievable in n comparisons between the collection of the 1-dimensional persistent homology modules computed with respect to each component.

The first example concerns the comparison of two different size pairs having the same support.

Let X be the ellipse embedded in $\mathbb{R}^3$ defined by the equations

$$\begin{cases} u^2+v^2=1 \\ v=w \end{cases} \quad \text{or parameterized as} \quad \begin{cases} u=\cos\theta \\ v=\sin\theta \\ w=\sin\theta. \end{cases}$$

Let $\vec{\varphi}=(\varphi_1,\varphi_2), \vec{\psi}=(\psi_1,\psi_2) : X \to \mathbb{R}^2$ be defined as follows: $\varphi_1=u,\ \psi_1=v,\ \varphi_2=\psi_2=w$. Then, it is easily seen that the persistent homology modules of (X,φ_1), (X,ψ_1), $(X,\varphi_2)=(X,\psi_2)$ are identical, while the persistent homology (in degree zero, so the size function) of $(X,\vec{\varphi})$ differs from the one of $(X,\vec{\psi})$. Indeed, while the lower-level sets of $\vec{\psi}$ are always either empty or connected, the lower-level sets $\vec{\varphi} \preceq (\overline{u},\overline{w})$, with $0<\overline{u}<1, \sqrt{1-\overline{u}^2} \le \overline{w} < 1$ consist of two connected components.

The second example we propose is the comparison of two shapes defined by two different topological spaces endowed with the same $\mathbb{R}^2$-valued measuring function. The dissimilarity of these shapes is computed in terms of the bottleneck distance between the respective rank invariants.

In $\mathbb{R}^3$ consider the set $\Omega=[-1,1]\times[-1,1]\times[-1,1]$ and the sphere $\mathcal{S}$ of equation $u^2+v^2+w^2=1$. Let also $\vec{\chi}=(\chi_1,\chi_2):\mathbb{R}^3\to\mathbb{R}^2$ be a continuous function, defined as $\vec{\chi}(u,v,w)=(|u|,|v|)$. In this setting, consider the size pairs $(\mathcal{C},\vec{\varphi})$ and $(\mathcal{S},\vec{\psi})$, where $\mathcal{C}=\partial\Omega$ and $\vec{\varphi}$ and $\vec{\psi}$ are respectively the restrictions of $\vec{\chi}$ to $\mathcal{C}$ and $\mathcal{S}$.

In order to compare the persistent homology modules of $\mathcal{C}$ and $\mathcal{S}$ defined by $\vec{\chi}$, we are interested in studying the half-planes' foliation of $\Delta^+\subset\mathbb{R}^4$, where $\vec{l}=(\cos\theta,\sin\theta)$

with $\theta \in (0, \frac{\pi}{2})$, and $\vec{b} = (a, -a)$ with $a \in \mathbb{R}$. Any such half-plane is parameterized as

$$\begin{cases} u_1 = s\cos\theta + a \\ u_2 = s\sin\theta - a \\ v_1 = t\cos\theta + a \\ v_2 = t\sin\theta - a \end{cases}$$

with $s, t \in \mathbb{R}, s < t$.

For example, focusing on the plane defined by choosing $\theta = \frac{\pi}{4}$ and $a = 0$, i.e. $\vec{l} = (\frac{\sqrt{2}}{2}, \frac{\sqrt{2}}{2})$ and $\vec{b} = (0,0)$, we obtain that

$$F^{\vec{\varphi}}_{(\vec{l},\vec{b})} = \sqrt{2}\max\{\varphi_1, \varphi_2\} = \sqrt{2}\max\{|u|, |v|\},$$
$$F^{\vec{\psi}}_{(\vec{l},\vec{b})} = \sqrt{2}\max\{\psi_1, \psi_2\} = \sqrt{2}\max\{|u|, |v|\}.$$

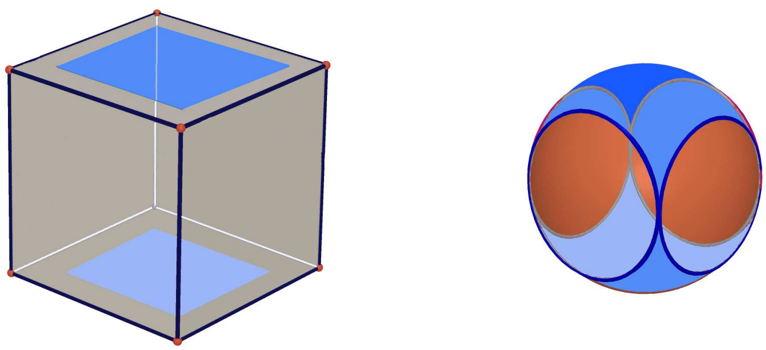

Figure 2.2: Lower-level sets $F^{\vec{\varphi}}_{(\vec{l},\vec{b})} \leq 1$ and $F^{\vec{\psi}}_{(\vec{l},\vec{b})} \leq 1$.

Moreover, for every $k \in \mathbb{Z}$, denoting by $H_k^{s,t}(\mathcal{C})$ and $H_k^{s,t}(\mathcal{S})$ the kth persistent homology modules of the pairs $(\mathcal{C}, F^{\vec{\varphi}}_{(\vec{l},\vec{b})})$ and $(\mathcal{S}, F^{\vec{\psi}}_{(\vec{l},\vec{b})})$, respectively, and by $\rho_k^{(\mathcal{C},F^{\vec{\varphi}}_{(\vec{l},\vec{b})})}, \rho_k^{(\mathcal{S},F^{\vec{\psi}}_{(\vec{l},\vec{b})})}$ the respective kth rank invariants, and observing that $\beta_k(\mathcal{C}) = \beta_k(\mathcal{S})$, for every $k \in \mathbb{Z}$, by Definition 2.5, the bottleneck distance $d_B\left(\rho_k^{(\mathcal{C},F^{\vec{\varphi}}_{(\vec{l},\vec{b})})}, \rho_k^{(\mathcal{S},F^{\vec{\psi}}_{(\vec{l},\vec{b})})}\right)$ is finite for every $k \in Z$. In particular, we have

$$H_0^{s,t}(\mathcal{C}) = \begin{cases} 0, & s,t<0 \\ \mathbb{K}^2, & 0 \le s < t < \sqrt{2} \\ \mathbb{K}, & \text{otherwise} \end{cases}$$

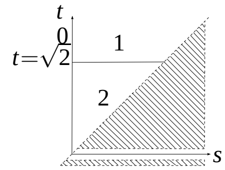

$$H_0^{s,t}(\mathcal{S}) = \begin{cases} 0, & s,t<0 \\ \mathbb{K}^2, & 0 \le s < t < 1 \\ \mathbb{K}, & \text{otherwise} \end{cases}$$

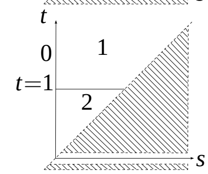

$$\Rightarrow$$

$$\Rightarrow \ D_B\left(\rho_0^{(\mathcal{C},\vec{\varphi})},\rho_0^{(\mathcal{S},\vec{\psi})}\right) \ge \tfrac{\sqrt{2}}{2} d_B\left(\rho_0^{\left(\mathcal{C},F^{\vec{\varphi}}_{(\vec{l},\vec{b})}\right)},\rho_0^{\left(\mathcal{S},F^{\vec{\psi}}_{(\vec{l},\vec{b})}\right)}\right) = \tfrac{\sqrt{2}}{2}(\sqrt{2}-1)$$

$$H_1^{s,t}(\mathcal{C}) = \ 0, \quad \text{for all}\, s,t \in \mathbb{R}$$

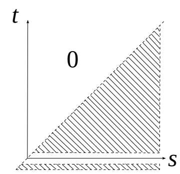

$$H_1^{s,t}(\mathcal{S}) = \begin{cases} \mathbb{K}^3, & 1 \le s < t < \sqrt{2} \\ 0, & \text{otherwise} \end{cases}$$

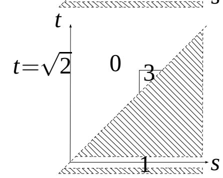

$$\Rightarrow$$

$$\Rightarrow \ D_B\left(\rho_1^{(\mathcal{C},\vec{\varphi})},\rho_1^{(\mathcal{S},\vec{\psi})}\right) \ge \tfrac{\sqrt{2}}{2} d_B\left(\rho_1^{\left(\mathcal{C},F^{\vec{\varphi}}_{(\vec{l},\vec{b})}\right)},\rho_1^{\left(\mathcal{S},F^{\vec{\psi}}_{(\vec{l},\vec{b})}\right)}\right) = \tfrac{\sqrt{2}}{2}\left(\tfrac{\sqrt{2}-1}{2}\right)$$

$$H_2^{s,t}(\mathcal{C}) = \begin{cases} \mathbb{K}, & \sqrt{2} \le s < t \\ 0, & \text{otherwise} \end{cases}$$

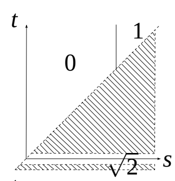

$$H_2^{s,t}(\mathcal{S}) = \begin{cases} \mathbb{K}, & \sqrt{2} \le s < t \\ 0, & \text{otherwise} \end{cases}$$

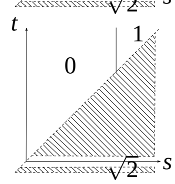

$$\Rightarrow$$

$$\Rightarrow \ D_B\left(\rho_2^{(\mathcal{C},\vec{\varphi})},\rho_2^{(\mathcal{S},\vec{\psi})}\right) \ge \tfrac{\sqrt{2}}{2} d_B\left(\rho_2^{\left(\mathcal{C},F^{\vec{\varphi}}_{(\vec{l},\vec{b})}\right)},\rho_2^{\left(\mathcal{S},F^{\vec{\psi}}_{(\vec{l},\vec{b})}\right)}\right) = 0$$

In other words, the multidimensional persistent homology, with respect to $\vec{\varphi}$ and $\vec{\psi}$, is able to discriminate the cube and the sphere, while the 1-dimensional persistent homology, with respect to φ_1, φ_2 and ψ_1, ψ_2, cannot do that. In fact, for both surfaces the lower-level sets of the single components (i.e. 1-dimensional measuring functions) are homeomorphic for all values: they are topologically either circles, or annuli, or spheres.

This last example suggests also some other considerations on the cooperation of measuring functions.

A first remark regards the possibility to consider *Jacobi sets* [26] on $\mathcal{C}$ and $\mathcal{S}$. Loosely speaking, the Jacobi set of two Morse functions defined on a common manifold is a set of critical points of the restrictions of one function to the level sets of the other function. In our case, neither the components of $\vec{\chi} : \mathbb{R}^3 \to \mathbb{R}^2$ (that we recall to ba the function whose restrictions on $\mathcal{C}$ and $\mathcal{S}$ are $\vec{\varphi}$ and $\vec{\psi}$, respectively) are Morse functions, nor $\mathcal{C}$ is a manifold; nevertheless, considerations in this direction can be done. Indeed, note that, although the persistent homology on single components of $\vec{\chi}$ cannot distinguish the two spaces, the persistent homology on χ_1, for example, if restricted to lower-level sets of χ_2 can, as shown in what follows. Consider again the sphere $\mathcal{S}$ and $\vec{\psi} = \vec{\chi}_{|\mathcal{S}}$. The value $1/\sqrt{2}$ (corresponding to the homological critical value 1 of $F^{\vec{\psi}}_{(\vec{l},\vec{b})}$) is not critical for the maps ψ_1, ψ_2 on $\mathcal{S}$ itself, but it is indeed critical for ψ_2 restricted to $\mathcal{S}\langle \psi_1 \leq 1/\sqrt{2} \rangle$. We believe that , for every $k \in \mathbb{Z}$, homological k-critical values of the 1-dimensional reduction of multidimensional measuring functions are always clues of such phenomena (the case $k = 0$ has already been treated in [14]).

A further speculation on the use of cooperating measuring functions — from a completely different viewpoint than the one developed in the previous sections — is the following. A problem in 1-dimensional persistent homology is the computation of homological k-critical values for $k > 0$. A possibility is the use of several, independent measuring functions for lowering k, i.e. the degree at which the passage through the critical value causes a homology change. Lowering k is important, since homological 0-critical values are easily detected by graph-theoretical techniques [17]. The following example shows that a suitable choice of a second, auxiliary measuring function may actually take homological 1-critical values to 0-critical ones.

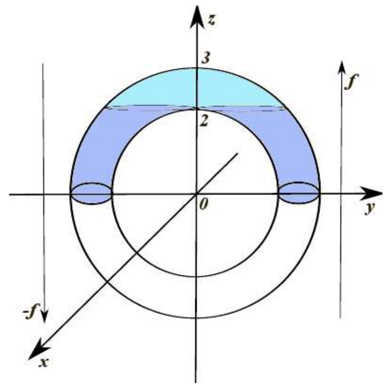

Figure 2.3: An example of cooperating measuring functions.

In $\mathbb{R}^3$, let $\mathcal{T}$ be a torus of revolution around the x axis, with the innermost parallel circle of radius 2, the outermost of radius 3 (see Figure 2.3). On $\mathcal{T}$ define $(f,-f)=(z,-z)$. Suppose we are interested in the persistent homology of the size pair $(\mathcal{T},f)$. Then $z=2$ is a homological 1-critical value for f, i.e. it is a level at which 1-degree homology changes. The same level is a homological 0-critical value for its restriction to $\mathcal{T}\langle -f\leq 0\rangle$, so it can be recovered by the standard graph-theoretical techniques used in degree 0, that is for size functions. The two functions need not be so strictly related: for example, $-f$ could be replaced by the Euclidean distance from $(0,0,3)$ with the same effect. We conjecture that — at least whenever torsion is not involved — one can recursively take the homological k-critical values of a measuring function to homological $(k-1)$-critical ones, down to (easily computable) homological 0-critical values by means of other (auxiliary) measuring functions, as in this example.

2.5 Discussion

The need to extend persistent homology to the multidimensional case is a rather widespread belief, confirmed by simple examples (Section 2.4). The present research shows the possibility of reducing the computation of persistent homology, with respect to multidimensional measuring functions, to the 1-dimensional case, following the line of thought of an analogous extension devised for size functions in [4]. This reduction also yields a stable distance for the rank invariants of size pairs.

In the next future, we plan to characterize the multidimensional max-tame measuring functions in such a way that the reduction to the 1-dimensional case makes the specific features of persistent homology modules hold steady. It also would be our concern to give a rigorous definition of *multidimensional homological k-critical values* of a max-tame function and to relate them to the homological k-critical values of the maximum of its components. Moreover, experimental results would be desirable to analyze the potential of our theoretical approach.

Eventually, in relation to our conjecture about homological k-critical values (see Section 2.4), we plan to build an algorithm to recursively reduce homological k-critical values of a measuring function to homological 0-critical ones.

Chapter 3

The robustness of size functions against partial occlusions

Shape matching and retrieval are key aspects in the design of search engines based on visual, rather than keyword, information. Generally speaking, shape matching methods rely on the computation of a shape description, also called a signature, that effectively captures some essential features of the object. The ability to perform not only global matching, but also partial matching, is regarded as one of the most meaningful properties in order to evaluate the performance of a shape matching method (cf., e.g., [63]). Basically, the interest in robustness against partial occlusions is motivated by the problem of recognizing an object partially hidden by some other foreground object in the same image. However, there are also other situations in which partial matching is useful, such as when dealing with the problem of identifying similarities between different configurations of articulated objects, or when dealing with unreliable object segmentation from images. For these reasons, the ability to recognize shapes, even when they are partially occluded by another pattern, has been investigated in the computer vision literature by various authors, with reference to a variety of shape recognition methods.

In particular, as far as point based representations of shape are concerned, works on the topic include the partial Hausdorff distance [44] by Huttenlocher et al. to compare portions of point sets, and Wolfson and Rigoutsos' use of geometric hashing [66] applied to point features. For shapes encoded as polylines, the Tanase and Veltkamp's approach

[56] is that of computing the dissimilarity between multiple polylines and a polygon using the turning function, while Latecki et al. [50] propose a method based on removing certain parts of a polyline and see whether the objects become more similar without them. As for the region-based shape descriptors, Höynck and Ohm show that using central moments instead of the angular radial transform to extract features improves robustness to occlusions [43]. Regarding the shape-from-functions methods, Biasotti et al. [7] automatically identify similar sub-parts exploiting a graph-matching technique applied to Reeb graphs.

As explained in Chapter 1, size functions belong to a class of methods for shape description, characterized by the study of the topological changes in the lower-level sets of a real valued function defined on the shape to derive its signature (cf., e.g., [6, 46]). Here we want to investigate the behavior of size functions in the presence of partial occlusions. Previous works have already assessed the robustness of size functions with respect to continuous deformations of the shape [20], the conciseness of the descriptor [36], the invariance of the descriptor to transformation groups [21, 58], that are further properties recognized as important for shape matching methods. Size functions, like all shape-from-functions methods, work on a shape as a whole. In general, it is argued that global object methods are not robust against occlusions, whereas methods based on computing local features may be more suited to this task. Our aim is to show that size functions are able to preserve local information, so that they can manage uncertainty due to the presence of occluded shapes.

We model the presence of occlusions in a shape as follows. The visible object is a locally connected compact Hausdorff space X. The object of interest A is occluded by an object B, so that $X = A \cup B$. In particular, A and B have the topology induced from X and are assumed to be locally connected. The shapes of X, A, and B are analyzed through the size functions $\ell_{(X,\varphi)}$, $\ell_{(A,\varphi_{|A})}$, and $\ell_{(B,\varphi_{|B})}$, respectively, where $\varphi : X \to \mathbb{R}$ is the continuous function chosen to extract the shape features.

The starting point of this research is the fact that the size function $\ell_{(X,\varphi)}$, evaluated at a point (u,v) of $\mathbb{R}^2$, with $u < v$, is equal to the rank of the image of the homomorphism induced by inclusion between the Čech homology groups $\check{H}_0(X_u)$ and $\check{H}_0(X_v)$, where $X_u = \{p \in X : \varphi(p) \leq u\}$ and $X_v = \{p \in X : \varphi(p) \leq v\}$.

Our main result establishes a necessary and sufficient condition so that the equality

$$\ell_{(X,\varphi)}(u,v) = \ell_{(A,\varphi_{|A})}(u,v) + \ell_{(B,\varphi_{|B})}(u,v) - \ell_{(A\cap B,\varphi_{|A\cap B})}(u,v) \tag{3.1}$$

holds. This is proved using the Mayer-Vietoris sequence of Čech homology groups.

From this result we can deduce that the size function of X contains features of the size functions of A and B. In particular, when size functions are represented as a formal series of points in the plane through their *cornerpoints* (Definitions 1.4 and 1.5), relation (3.1) allows us to prove that the set of cornerpoints of $\ell_{(X,\varphi)}$ contains a subset of cornerpoints of $\ell_{(A,\varphi_{|A})}$. These are a kind of "fingerprint" of the presence of A in X. In other words, size functions are able to detect a partial matching between two shapes by showing a common subset of cornerpoints.

The chapter is organized as follows. In Section 3.1 some general results concerning the link between size functions and Čech homology are proved, with a particular emphasis on the relation existing between discontinuities of size functions and homological critical values. The reader not familiar with Čech homology can find a brief survey of the subject in Appendices A and B. However, we use Čech homology only for technical reasons, so that, after establishing that all the ordinary homological axioms (Eilenberg-Steenrod) hold in our setting, also for Čech homology groups, we can use them as ordinary (singular) homology groups. Therefore, the reader acquainted with ordinary homology can easily go through the next sections. In Section 3.2 we prove our main result concerning the relationship (3.1) between the size function of A, B and $A \cup B$. The relation we obtain holds, subject to a homological condition derived from the Mayer-Vietoris sequence of Čech homology. In the same section we also investigate this homological condition in terms of size functions. Moreover, we introduce the Mayer-Vietoris sequence of persistent Čech homology groups. Section 3.3 is devoted to the consequent relationship between cornerpoints for $\ell_{(A,\varphi|_A)}$, $\ell_{(B,\varphi|_B)}$ and $\ell_{(X,\varphi)}$ in terms of their coordinates and multiplicities. Before concluding the chapter with a brief discussion of our results, we show some experimental applications in Section 3.4, demonstrating the potential of our approach.

3.1 The link between size functions and Čech homology

In this section we prove that values of size functions can be computed in terms of rank of Čech homology groups. We then analyze the links between homological critical values and size functions.

As recalled in Subsection 1.3.6, the idea of relating size functions to homology groups is not a new one. Already in [8], introducing the concept of *size functor*, this link was recognized, when the space X is a smooth manifold and φ is a Morse function. Roughly speaking, the size functor associated with the pair (X,φ) takes a pair of real numbers $(u,v) \in \Delta^+$ to the image of the homomorphism from $H_k(X_u)$ to $H_k(X_v)$, induced by the inclusion of X_u into X_v. Here homology means singular homology. This also shows a link between size functions and 0th persistent homology groups [29]. Later, the relation between size functions and singular homology groups of closed manifolds endowed with Morse functions emerged again in [1], studying the *Morse shape descriptor*.

The reason for further exploring the homological interpretation of size function in the present chapter is technical. As explained in Section 1.3, our definition of size function is based on the relation of connectedness (cf. Definition 1.3). This implies that singular homology, whose 0th group detects the number of arcwise-connected components, is no longer suited to dealing with size functions. Adding further assumptions on X, so that connectedness and arcwise-connectedness coincide on X, such as asking X to be locally arcwise-connected, is not sufficient to solve the problem. Indeed, we emphasize the fact that in the definition of $\ell_{(X,\varphi)}$ we count the components not of the space X itself, but those of the lower-level sets of X with respect to the continuous function φ, and it is not guaranteed that locally arcwise-connectedness is inherited by lower-level sets.

The tool we need for counting connected components instead of arcwise-connected components is Čech homology (a brief review of this subject can be found in Appendix A). Indeed, in [65] the following result is proved, under the assumption that X is a compact Hausdorff space.

Theorem 3.1.1 ([65], Thm. V 11.3a)**.** *The number of connected components of a space X is exactly the rank of the* 0*th Čech homology group.*

One of the main problems in the use of Čech homology is that, in general, the long sequence of the pair may fail to be exact. However, the exactness of this sequence holds, provided that some assumptions are satisfied: the space must be compact and the group G must be either a compact Abelian topological group or a vector space over a field (see Appendix B). In view of establishing a connection between size functions and Čech homology, it is important to recall that when (X,φ) is a size pair, X is assumed to be compact and Hausdorff and φ is continuous. Therefore, the lower-level sets X_u are themselves Hausdorff and compact spaces. In order that the Čech homology sequence of the pair be available, we will take G to be a vector space over a field. Therefore, from now on, we will take the Čech homology sequence of the pair for granted and we will denote the Čech homology groups of X over G simply by $\check{H}_k(X)$, maintaining the notation $H_k(X)$ for ordinary homology. From [30] we know that $\check{H}_k(X)$ is a vector space over the same field.

We shall first furnish a link between size functions and relative Čech homology groups. We need the following preliminary results.

Definition 3.1 ([65], Def. I 12.2)**.** *If X is a space, and $x,y \in X$, then a finite collection of sets X^1, X^2, ..., X^n will be said to form a* simple chain *of sets from x to y if (1) X^i contains x if and only if $i=1$; (2) X^i contains y if and only if $i=n$; (3) $X^i \cap X^j \neq \emptyset$, $i<j$, if and only if $j=i+1$.*

Proposition 3.1.2 ([65], Cor. I 12.5)**.** *A space X is connected if and only if, for arbitrary $x,y \in X$ and covering $\mathcal{U}$ of X by open sets, $\mathcal{U}$ contains a simple chain from x to y.*

Following the proof used in [65] for proving Theorem 3.1.1, we can interpret also relative homology groups in terms of the number of connected components.

Lemma 3.1.3. *For every pair of spaces (X,A), with X a compact Hausdorff space and A a closed subset of X, the number of connected components of X that do not meet A is equal to the rank of $\check{H}_0(X,A)$.*

Proof. When A is empty, the claim reduces to Theorem 3.1.1. In case A is non-empty, if X is connected then $\check{H}_0(X,A)=0$. Indeed, under these assumptions, let $z_0=\{z_0(\mathcal{U})\}$ be a Čech cycle in X relative to A, with $z_0(\mathcal{U})=\sum_{j=1}^k a_j \cdot U_j$, $a_j \neq 0$. Since $A \subseteq X$ is non-empty, there is an open set $\bar{U} \in \mathcal{U}$ such that $\bar{U} \in \mathcal{U}_A$. Now we can use Proposition 3.1.2

to show that, for every $1 \leq j \leq k$, there exists a sequence $\mathcal{S}_j$ of elements of $\mathcal{U}$, beginning with U_j and ending with $\bar{U}$. So, associated with $\mathcal{S}_j$, there is a 1-chain c_1^j such that $\partial c_1^j = U_j - \bar{U}$. Hence, $\partial \sum_{j=1}^k a_j \cdot c_1^j = \sum_{j=1}^k a_j \cdot U_j - \sum_{j=1}^k a_j \cdot \bar{U} = z_0(\mathcal{U}) - \sum_{j=1}^k a_j \cdot \bar{U}$, proving that $z_0(\mathcal{U})$ is homologous to 0 in $Z_0(X,A)$. By the arbitrariness of $\mathcal{U}$, each coordinate of z_0 is homologous to 0, implying that $\check{H}_0(X,A) = 0$.

In general, if X is not connected, then the preceding argument shows that only those connected components of X that do not meet A contain a non-trivial Čech cycle relative to A. So the claim follows from Theorem 3.1.1. □

As an immediate consequence of Lemma 3.1.3, we have the following link between size functions and relative Čech homology groups. It is analogous to the link given in [1] using singular homology for size functions, defined in terms of the arcwise-connectedness relation. Before exposing it, we need a further assumption on (X,φ): $\check{H}_0(X_u)$ shall be finitely generated for every $u \in \mathbb{R}$. The importance of the following result in our investigation makes this condition necessary throughout the chapter.

Corollary 3.1.4. *For every size pair (X,φ), and every $(u,v) \in \Delta^+$, it holds that the value $\ell_{(X,\varphi)}(u,v)$ equals the rank of $\check{H}_0(X_v)$ minus the rank of $\check{H}_0(X_v,X_u)$.*

Proof. The claim follows from Lemma 3.1.3, observing that $\ell_{(X,\varphi)}(u,v)$ is equal to the number of connected components of X_v that meet X_u. □

We now show that the size function can also be expressed as the rank of the image of the homomorphism between Čech homology groups, induced by the inclusion of X_u into X_v. This link is analogous to the existing one between the size functor and size functions, defined using the arcwise-connectedness relation [8].

Given a size pair (X,φ), and $(u,v) \in \Delta^+ \subset \mathbb{R}^2$, we denote by $\iota^{u,v}$ the inclusion of X_u into X_v. This mapping induces a homomorphism of Čech homology groups $\iota_k^{u,v}$: $\check{H}_k(X_u) \to \check{H}_k(X_v)$ for each integer $k \geq 0$.

Analogously to what is done in [29], we can define the persistent Čech homology groups.

Definition 3.2. *Given a size pair (X,φ) and a point $(u,v) \in \Delta^+$, the k*th persistent Čech homology group $\check{H}_k^{u,v}(X,\varphi)$ *is the image of the homomorphism $\iota_k^{u,v}$ induced between the kth Čech homology groups by the inclusion mapping of X_u into X_v: $\check{H}_k^{u,v}(X,\varphi) = \operatorname{im} \iota_k^{u,v}$.*

From now on, for simplicity of notation, we write $\check{H}_k^{u,v}(X)$ instead of $\check{H}_k^{u,v}(X,\varphi)$.

Corollary 3.1.5. *For every size pair (X,φ), and every $(u,v)\in\Delta^+$, it holds that the value $\ell_{(X,\varphi)}(u,v)$ equals the rank of the 0th persistent Čech homology group $\check{H}_0^{u,v}(X)$.*

Proof. Let us consider the final terms of the long exact sequence of the pair (X_v,X_u):

$$\ldots \to \check{H}_0(X_u) \xrightarrow{\iota_0^{u,v}} \check{H}_0(X_v) \to \check{H}_0(X_v,X_u) \to 0.$$

From the exactness of this sequence we deduce that

$$\operatorname{rank}\check{H}_0^{u,v}(X) = \operatorname{rank}\operatorname{im}\iota_0^{u,v} = \operatorname{rank}\check{H}_0(X_v) - \operatorname{rank}\check{H}_0(X_v,X_u).$$

Applying Theorem 3.1.1 and Lemma 3.1.3, the rank of $\check{H}_0^{u,v}(X)$ is shown to be equal to the number of connected components of X_v that meet X_u, that is $\ell_{(X,\varphi)}(u,v)$. □

3.1.1 Some useful results

In this section we show the link between homological critical values (Definition 1.8) and discontinuities of size functions (Section 1.3.4). Let us recall that homological critical values have been introduced in [16] and intuitively correspond to levels where the lower-level sets undergo a topological change. Discontinuities of size functions have been thoroughly studied in [14, 36].

In particular, we prove that if a point $(u,v)\in\Delta^+$ is a discontinuity point for a size function, then either u or v is a level where the 0-homology of the lower-level set changes (Proposition 3.1.6). Then we show that also the converse is true when the number of homological critical values is finite (Proposition 3.1.7). However, in general, there may exist homological critical values not generating discontinuities for the size function (Remark 2). We conclude the section with a result concerning the surjectivity of the homomorphism induced by inclusion (Proposition 3.1.8).

Analogously to Definition 1.8, we give the following

Definition 3.3. *Let (X,φ) be a size pair. A* homological k-critical value *for (X,φ) is a real number w such that, for every sufficiently small $\varepsilon>0$, the map $\iota_k^{w-\varepsilon,w+\varepsilon}$: $\check{H}_k(X_{w-\varepsilon})\to\check{H}_k(X_{w+\varepsilon})$ induced by inclusion is not an isomorphism.*

The following results show the behavior of a size function according to whether it is calculated in correspondence with homological 0-critical values or not.

Proposition 3.1.6. *If $w \in \mathbb{R}$ is not a homological 0-critical value for the size pair (X, φ), then the following statements are true:*

(i) For every $v > w$, $\lim_{\varepsilon \to 0^+} \left(\ell_{(X,\varphi)}(w+\varepsilon, v) - \ell_{(X,\varphi)}(w-\varepsilon, v)\right) = 0$;

(ii) For every $u < w$, $\lim_{\varepsilon \to 0^+} \left(\ell_{(X,\varphi)}(u, w-\varepsilon) - \ell_{(X,\varphi)}(u, w+\varepsilon)\right) = 0$.

Proof. We begin by proving *(i)*. Let $v > w$. For every $\varepsilon > 0$ such that $v > w + \varepsilon$, we can consider the commutative diagram:

$$\begin{tikzcd}
\cdots \arrow[r] & \check{H}_0(X_{w-\varepsilon}) \arrow[r, "\iota_0^{w-\varepsilon,v}"] \arrow[d, "\iota_0^{w-\varepsilon,w+\varepsilon}"] & \check{H}_0(X_v) \arrow[r, "h"] \arrow[d, "\iota_0^{v,v}"] & \check{H}_0(X_v, X_{w-\varepsilon}) \arrow[r] \arrow[d, "j"] & 0 \arrow[d, "0"'] \\
\cdots \arrow[r] & \check{H}_0(X_{w+\varepsilon}) \arrow[r, "\iota_0^{w+\varepsilon,v}"] & \check{H}_0(X_v) \arrow[r, "k"] & \check{H}_0(X_v, X_{w+\varepsilon}) \arrow[r] & 0
\end{tikzcd} \tag{3.2}$$

where the two horizontal lines are exact homology sequences of the pairs $(X_v, X_{w-\varepsilon})$ and $(X_v, X_{w+\varepsilon})$, respectively, and the vertical maps are homomorphisms induced by inclusions. By the assumption that w is not a homological 0-critical value, there exists an arbitrarily small $\overline{\varepsilon} > 0$ such that $\iota_0^{w-\overline{\varepsilon},w+\overline{\varepsilon}}$ is an isomorphism. Therefore, by applying the Five Lemma in diagram (3.2) with $\varepsilon = \overline{\varepsilon}$, we deduce that also j is an isomorphism. Thus, $\operatorname{rank}\check{H}_0(X_v, X_{w-\overline{\varepsilon}}) = \operatorname{rank}\check{H}_0(X_v, X_{w+\overline{\varepsilon}})$, and consequently, by Corollary 3.1.4, $\ell_{(X,\varphi)}(w+\overline{\varepsilon}, v) = \ell_{(X,\varphi)}(w-\overline{\varepsilon}, v)$. Hence, since size functions are non-decreasing in the first variable, it may be concluded that $\lim_{\varepsilon \to 0^+} \left(\ell_{(X,\varphi)}(w+\varepsilon, v) - \ell_{(X,\varphi)}(w-\varepsilon, v)\right) = 0$.

Now, let us proceed by proving *(ii)*. Let $u < w$. For every $\varepsilon > 0$ such that $u < w - \varepsilon$, let us consider the following commutative diagram:

$$\begin{tikzcd}
\cdots \arrow[r] & \check{H}_0(X_u) \arrow[r, "\iota_0^{u,w-\varepsilon}"] \arrow[d, "\iota_0^{u,u}"] & \check{H}_0(X_{w-\varepsilon}) \arrow[r, "h"] \arrow[d, "\iota_0^{w-\varepsilon,w+\varepsilon}"] & \check{H}_0(X_{w-\varepsilon}, X_u) \arrow[r] \arrow[d, "j"] & 0 \arrow[d, "0"'] \\
\cdots \arrow[r] & \check{H}_0(X_u) \arrow[r, "\iota_0^{u,w+\varepsilon}"] & \check{H}_0(X_{w+\varepsilon}) \arrow[r, "k"] & \check{H}_0(X_{w+\varepsilon}, X_u) \arrow[r] & 0
\end{tikzcd} \tag{3.3}$$

where the vertical maps are homomorphisms induced by inclusions and the two horizontal lines are exact homology sequences of the pairs $(X_{w-\varepsilon}, X_u)$ and $(X_{w+\varepsilon}, X_u)$, respectively. By the assumption that w is not a homological 0-critical value, there exists an arbitrarily small $\overline{\varepsilon} > 0$, for which $\iota_0^{w-\overline{\varepsilon},w+\overline{\varepsilon}} : \check{H}_0(X_{w-\overline{\varepsilon}}) \to \check{H}_0(X_{w+\overline{\varepsilon}})$ is an isomorphism. Therefore, by applying the Five Lemma in diagram (3.3) with $\varepsilon = \overline{\varepsilon}$, we deduce that also j is an isomorphism. Thus, $\operatorname{rank}\check{H}_0(X_{w-\overline{\varepsilon}}, X_u) = \operatorname{rank}\check{H}_0(X_{w+\overline{\varepsilon}}, X_u)$, implying $\ell_{(X,\varphi)}(u, w-\overline{\varepsilon}) = \ell_{(X,\varphi)}(u, w+\overline{\varepsilon})$. Hence, since size functions are non-increasing in the second variable, the desired claim follows. □

Assuming the existence of at most a finite number of homological critical values, we state the converse of Proposition 3.3 saying that homological critical values give rise to discontinuities in size functions.

Proposition 3.1.7. *Let (X,φ) be a size pair with at most a finite number of homological 0-critical values. Let $w \in \mathbb{R}$ be a homological 0-critical value. The following statements hold:*

(i) If $\iota_0^{w-\varepsilon,w+\varepsilon}$ is not surjective for any sufficiently small positive real number ε, then there exists $v > w$ such that w is a discontinuity point for $\ell_{(X,\varphi)}(\cdot, v)$;

(ii) If $\iota_0^{w-\varepsilon,w+\varepsilon}$ is surjective for every sufficiently small positive real number ε, then there exists $u < w$ such that w is a discontinuity point for $\ell_{(X,\varphi)}(u, \cdot)$.

Proof. Let us prove *(i)*, always referring to diagram (3.2) in the proof of Proposition 3.1.6. Let $v > w$. For every $\varepsilon > 0$ such that $v > w+\varepsilon$, the map j of diagram (3.2) is surjective. Indeed, h, k and $\iota_0^{v,v}$ are surjective.

If we prove that there exists $v > w$ for which, for every $\varepsilon > 0$ such that $v > w+\varepsilon$, j is not injective, then, since j is surjective, it necessarily holds that $\operatorname{rank}\check{H}_0(X_v, X_{w-\varepsilon}) > \operatorname{rank}\check{H}_0(X_v, X_{w+\varepsilon})$, for every $\varepsilon > 0$ such that $v > w+\varepsilon$. From this we obtain $\ell_{(X,\varphi)}(w-\varepsilon, v) = \operatorname{rank}\check{H}_0(X_v) - \operatorname{rank}\check{H}_0(X_v, X_{w-\varepsilon}) < \operatorname{rank}\check{H}_0(X_v) - \operatorname{rank}\check{H}_0(X_v, X_{w+\varepsilon}) = \ell_{(X,\varphi)}(w+\varepsilon, v)$, for every $\varepsilon > 0$ such that $v > w+\varepsilon$. Therefore, $\lim\limits_{\varepsilon\to 0^+}\Big(\ell_{(X,\varphi)}(w+\varepsilon, v) - \ell_{(X,\varphi)}(w-\varepsilon, v)\Big) > 0$, that is, w is a discontinuity point for $\ell_{(X,\varphi)}(\cdot, v)$.

Let us see that there exists $v > w$ for which, for every $\varepsilon > 0$ such that $v > w+\varepsilon$, j is not injective.

Since we have hypothesized the presence of at most a finite number of homological 0-critical values for (X,φ), there surely exists $\overline{v} > w$ such that, for every sufficiently small $\varepsilon > 0$, $\overline{v} > w+\varepsilon$ and $\iota_0^{w+\varepsilon,\overline{v}} : \check{H}_0(X_{w+\varepsilon}) \to \check{H}_0(X_{\overline{v}})$ is an isomorphism. Hence, from the exactness of the second row in diagram (3.2), taking such a $\overline{v}$, $\check{H}_0(X_{\overline{v}}, X_{w+\varepsilon})$ results trivial. Now, if j were injective, from the triviality of $\check{H}_0(X_{\overline{v}}, X_{w+\varepsilon})$, it would follow that also $\check{H}_0(X_{\overline{v}}, X_{w-\varepsilon})$ is trivial, and consequently $\iota_0^{w-\varepsilon,\overline{v}}$ surjective. This is a contradiction, since we are assuming $\iota_0^{w-\varepsilon,w+\varepsilon}$ not surjective, and it implies that $\iota_0^{w-\varepsilon,\overline{v}}$ is not surjective because $\iota_0^{w+\varepsilon,\overline{v}}$ and $\iota_0^{\overline{v},\overline{v}}$ are isomorphisms.

As for *(ii)*, we will always refer to diagram (3.3) in the proof of Proposition 3.1.6. In this case, by combining the hypothesis that, for any sufficiently small $\varepsilon > 0$, $\iota_0^{w-\varepsilon,w+\varepsilon}$ is not an isomorphism and $\iota_0^{w-\varepsilon,w+\varepsilon}$ is surjective, it necessarily follows that $\mathrm{rank}\check{H}_0(X_{w-\varepsilon}) > \mathrm{rank}\check{H}_0(X_{w+\varepsilon})$, for every sufficiently small $\varepsilon > 0$. Let $u < w$. For every $\varepsilon > 0$ such that $u + \varepsilon < w$, the map j of diagram (3.3) is surjective. Indeed, h, k and $\iota_0^{w-\varepsilon,w+\varepsilon}$ are surjective.
Now, if we prove the existence of $u < w$, for which, for every $\varepsilon > 0$ such that $u+\varepsilon < w$, j is an isomorphism, it necessarily holds that $\mathrm{rank}\check{H}_0(X_{w-\varepsilon}, X_u) = \mathrm{rank}\check{H}_0(X_{w+\varepsilon}, X_u)$, for every $\varepsilon > 0$ such that $u+\varepsilon < w$. Thus, it follows that $\ell_{(X,\varphi)}(u, w-\varepsilon) = \mathrm{rank}\check{H}_0(X_{w-\varepsilon}) - \mathrm{rank}\check{H}_0(X_{w-\varepsilon}, X_u) > \mathrm{rank}\check{H}_0(X_{w+\varepsilon}) - \mathrm{rank}\check{H}_0(X_{w+\varepsilon}, X_u) = \ell_{(X,\varphi)}(u, w+\varepsilon)$, for every $\varepsilon > 0$ such that $u+\varepsilon < w$, implying $\lim_{\varepsilon\to 0^+}\Big(\ell_{(X,\varphi)}(u, w-\varepsilon) - \ell_{(X,\varphi)}(u, w+\varepsilon)\Big) > 0$, that is, w is a discontinuity point for $\ell_{(X,\varphi)}(u,\cdot)$.

Recalling that j is surjective, let us prove that there exists $u < w$ for which j is injective for every $\varepsilon > 0$ with $u+\varepsilon < w$.
Since we have assumed the presence of at most a finite number of homological 0-critical values for (X,φ), there surely exists $\overline{u} < w$ such that, for every sufficiently small $\varepsilon > 0$, $\overline{u} < w - \varepsilon$ and $\iota_0^{\overline{u},w-\varepsilon} : \check{H}_0(X_{\overline{u}}) \to \check{H}_0(X_{w-\varepsilon})$ is an isomorphism. Hence, for such a $\overline{u}$, $\check{H}_0(X_{w-\varepsilon}, X_{\overline{u}})$ is trivial, implying j injective. $\square$

Dropping the assumption that the number of homological 0-critical values for (X,φ) is finite, the converse of Proposition 3.1.6 is false, as the following remark states.

Remark 2. *From the condition that w is a homological 0-critical value, it does not follow that w is a discontinuity for the function $\ell_{(X,\varphi)}(\cdot, v)$, $v > w$, or for the function $\ell_{(X,\varphi)}(u,\cdot)$, $u < w$.*
In particular, the hypothesis $\mathrm{rank}\check{H}_0(X_{w-\varepsilon}) \neq \mathrm{rank}\check{H}_0(X_{w+\varepsilon})$, *for every sufficiently small* $\varepsilon > 0$, *does not imply the existence of either $v > w$ such that* $\lim_{\varepsilon\to 0^+}\Big(\ell_{(X,\varphi)}(w+\varepsilon, v) -$

$\ell_{(X,\varphi)}(w-\varepsilon,v)\Big) \neq 0$ *or* $u < w$ *such that* $\lim_{\varepsilon\to 0^+}\Big(\ell_{(X,\varphi)}(u,w-\varepsilon)-\ell_{(X,\varphi)}(u,w+\varepsilon)\Big) \neq 0.$

Two different examples, shown in Figures 3.1 and 3.2 support our claim. Let us

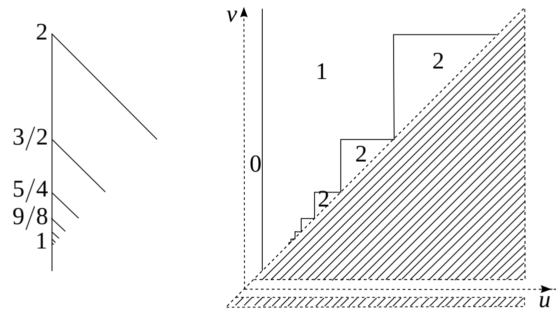

Figure 3.1: An example showing the existence of a real number w that is a homological 0-critical value for (X,φ) but not a discontinuity point for $\ell_{(X,\varphi)}(\cdot,v)$.

describe the first example displayed in Figure 3.1. Let (X,φ) be the size pair where X is the topological space obtained by adding an infinite number of branches to a vertical segment, each one sprouting at the height where the previous expires. These heights are chosen according to the sequence $(1+\frac{1}{2^n})_{n\in\mathbb{N}}$, converging to 1. The measuring function φ is the height function. The size function associated with (X,φ) is displayed on the right side of X. In this setting, $w=1$ is a homological 0-critical value. Indeed, for $w=1$, it holds that $\text{rank}\check{H}_0(X_{w-\varepsilon})=1$ while $\text{rank}\check{H}_0(X_{w+\varepsilon})=2$, for every sufficiently small $\varepsilon>0$. On the other hand, for every $v>w$, and for every small enough $\varepsilon>0$, it holds that $\ell_{(X,\varphi)}(w+\varepsilon,v)=\ell_{(X,\varphi)}(w-\varepsilon,v)=1$. Therefore, $\lim_{\varepsilon\to 0^+}\Big(\ell_{(X,\varphi)}(w+\varepsilon,v)-\ell_{(X,\varphi)}(w-\varepsilon,v)\Big)=0$, for every $v>w$. Moreover, it is immediately verifiable that, for every $u<w$, $\lim_{\varepsilon\to 0^+}\Big(\ell_{(X,\varphi)}(u,w-\varepsilon)-\ell_{(X,\varphi)}(u,w+\varepsilon)\Big)=0$. The second example, shown in Figure 3.2, is built in a similar way. In the chosen size pair (X,φ), φ is again the height function, and X is again obtained by adding an infinite number of branches to a vertical segment, but this time, the sequence of heights of their endpoints is $(2-\frac{1}{2^n})_{n\in\mathbb{N}}$, converging to 2. In this case, $w=2$ is a homological 0-critical value for (X,φ). Indeed, for every sufficiently small $\varepsilon>0$, $\text{rank}\check{H}_0(X_{w-\varepsilon})=2$ while $\text{rank}\check{H}_0(X_{w+\varepsilon})=1$. On the other hand, for every $u<w$, and for every small enough $\varepsilon>0$, it holds that $\ell_{(X,\varphi)}(u,w+\varepsilon)=\ell_{(X,\varphi)}(u,w-\varepsilon)=1$ when $u\geq 1$ and $\ell_{(X,\varphi)}(u,w+\varepsilon)=\ell_{(X,\varphi)}(u,w-\varepsilon)=0$ when $u<1$.

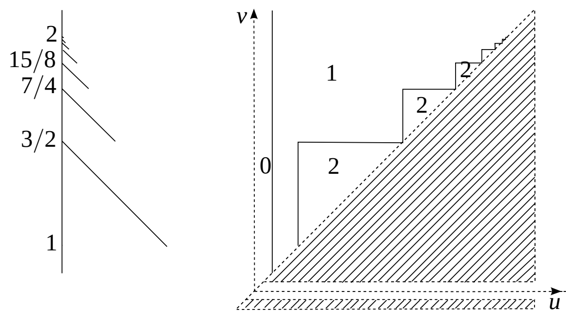

Figure 3.2: An example showing the existence of a real number w that is a homological 0-critical value for (X,φ) but not a discontinuity point for $\ell_{(X,\varphi)}(u,\cdot)$.

Therefore, in both cases, $\lim_{\varepsilon\to 0^+}\Big(\ell_{(X,\varphi)}(u,w-\varepsilon)-\ell_{(X,\varphi)}(u,w+\varepsilon)\Big)=0$ for every $u<w$. Moreover, we can immediately verify that $\lim_{\varepsilon\to 0^+}\Big(\ell_{(X,\varphi)}(w+\varepsilon,v)-\ell_{(X,\varphi)}(w-\varepsilon,v)\Big)=0$ for every $v>w$.

Before concluding this section, we investigate a condition for the surjectivity of the homomorphism between the 0th Čech homology groups induced by the inclusion map of X_u into X_v, $\iota_0^{u,v}:\check{H}_0(X_u)\to\check{H}_0(X_v)$, because it will be needed in Subsection 3.2.3.

Proposition 3.1.8. *Let (X,φ) be a size pair. For every $(u,v)\in\Delta^+$, $\iota_0^{u,v}$ is surjective if and only if $\ell_{(X,\varphi)}(u,v')=\ell_{(X,\varphi)}(v,v')$, for every $v'>v$.*

Proof. For every $v'>v$, let $\frac{X_u}{\sim_{v'}}$ (respectively, $\frac{X_v}{\sim_{v'}}$) be the space obtained quotienting X_u (respectively, X_v) by the relation of $\langle\varphi\le v'\rangle$-connectedness. Let us define the map $F_{v'}:\frac{X_u}{\sim_{v'}}\to\frac{X_v}{\sim_{v'}}$, such that $F_{v'}$ takes the class of $P\in X_u\subseteq X_v$ in $\frac{X_u}{\sim_{v'}}$ into the class of P in $\frac{X_v}{\sim_{v'}}$. $F_{v'}$ is well defined and injective, since $u<v<v'$. The condition that $\ell_{(X,\varphi)}(u,v')=\ell_{(X,\varphi)}(v,v')$ is equivalent to the bijectivity of $F_{v'}$.

Let $\iota_0^{u,v}:\check{H}_0(X_u)\to\check{H}_0(X_v)$ be surjective. By Corollary 3.1.4 and Corollary 3.1.5, this is equivalent to saying that, for every $P\in X_v$, there is $Q\in X_u$ with $P\sim_v Q$. Since $v<v'$, it also holds that $P\sim_{v'} Q$ and this implies $F_{v'}([Q])=[P]$, for all $v'>v$. So, $F_{v'}$ is bijective and $\ell_{(X,\varphi)}(u,v')=\ell_{(X,\varphi)}(v,v')$, for every $v'>v$.

Conversely, let $F_{v'}:\frac{X_u}{\sim_{v'}}\to\frac{X_v}{\sim_{v'}}$ be a surjective map, for all $v'>v$. Let $P\in X_v$. Let (v_n) be a strictly decreasing sequence of real numbers converging to v. The surjectivity of F_{v_n} implies that a $Q_n\in X_u$ exists, such that $F_{v_n}([Q_n])=[P]$, for all $n\in\mathbb{N}$. Thus $P\sim_{v_n} Q_n$, for all $n \in \mathbb{N}$. Since X is compact and X_u is closed in X, there is a subsequence of (Q_n), still denoted by (Q_n), converging in X_u. Let $Q = \lim_{n\to\infty} Q_n \in X_u$. Then, necessarily, $P \sim_{v_n} Q$, for all n. In fact, let us call C_n the connected component of X_{v_n} containing P. Since (v_n) is decreasing, we have $C_n \supseteq C_{n+1}$ for every $n \in \mathbb{N}$. Let us assume that there exists $N \in \mathbb{N}$ such that $P \nsim_{v_N} Q$. Since C_N is closed and $Q \notin C_N$, there exists an open neighborhood $U(Q)$ of Q, such that $U(Q) \cap C_N = \emptyset$. Thus, surely, there exists at least one point $Q_n \in U(Q)$, with $n > N$ and $Q_n \notin C_N$. This is a contradiction, because $Q_n \in C_n \subseteq C_N$, for all $n > N$.

Therefore, $P \sim_{v_n} Q$ for all n, and this implies that $P \sim_v Q$, because of Rem. 3 in [20]. Hence, $\iota_0^{u,v} : \check{H}_0(X_u) \to \check{H}_0(X_v)$ is surjective. $\square$

Remark 3. *The condition that* $\ell_{(X,\varphi)}(u,v') = \ell_{(X,\varphi)}(v,v')$*, for every* $v' > v$*, can be restated saying that* $\ell_{(X,\varphi)}$ *has no points of horizontal discontinuity in the region* $\{(x,y) \in \Delta^+ : u < x \leq v,\ y > v\}$*. In other words, the set* $\{(x,y) \in \Delta^+ : u < x \leq v,\ y > v\}$ *does not contain any cornerpoint (either proper or at infinity) for* $\ell_{(X,\varphi)}$*.*

3.2 The Mayer-Vietoris sequence of persistent Čech homology groups

In this section, we look for a relation expressing the size function associated with the size pair (X,φ) in terms of size functions associated with size pairs $(A,\varphi_{|A})$ and $(B,\varphi_{|B})$, where A and B are closed locally connected subsets of X, such that $X = int(A) \cup int(B)$, and $A \cap B$ is locally connected. The notations $int(A)$ and $int(B)$ stand for the interior of the sets A and B in X, respectively. The previous assumptions on A, B and $A\cap B$, together with the fact that the functions $\varphi_{|A\cap B}$, $\varphi_{|A}$, and $\varphi_{|B}$ are continuous, as restrictions of the continuous function $\varphi : X \to \mathbb{R}$ to spaces endowed with the topology induced from X, ensure that $(A,\varphi_{|A})$, $(B,\varphi_{|B})$, and $(A\cap B,\varphi_{|A\cap B})$ are themselves size pairs. Moreover, in order to apply Corollary 3.1.4 to X, A, B and $A\cap B$ as a tool for our investigation, it is necessary that $\check{H}_0(X_u)$, $\check{H}_0(A_u)$, $\check{H}_0(B_u)$, $\check{H}_0(A\cap B_u)$ are finitely generated groups for every $u \in \mathbb{R}$. These hypotheses on X, A, B and $A\cap B$ will be maintained throughout the chapter.

We find a homological condition guaranteeing a Mayer-Vietoris formula between size functions evaluated at a point $(u,v) \in \Delta^+$, that is, $\ell_{(X,\varphi)}(u,v) = \ell_{(A,\varphi_{|A})}(u,v) + \ell_{(B,\varphi_{|B})}(u,v) - \ell_{(A\cap B,\varphi_{|A\cap B})}(u,v)$ (see Corollary 3.2.6). We shall apply this relation in the next section in order to show that it is possible to match a subset of the cornerpoints for $\ell_{(X,\varphi)}$ to cornerpoints for either $\ell_{(A,\varphi_{|A})}$ or $\ell_{(B,\varphi_{|B})}$.

Our main tools are the Mayer-Vietoris sequence and the homology sequence of the pair, applied to the lower-level sets of X, A, B, and $A \cap B$.

Using the same tools, we show that there exists a Mayer-Vietoris sequence for persistent Čech homology groups that is of order 2. This implies that, under proper assumptions, there is a short exact sequence involving the 0th persistent Čech homology groups of X, A, B, and $A \cap B$ (see Proposition 3.2.7).

We begin by emphasizing some simple properties of the lower-level sets of X, A, B, and $A \cap B$.

Lemma 3.2.1. *Let $u \in \mathbb{R}$. Let us endow X_u with the topology induced by X. Then A_u and B_u are closed sets in X_u. Moreover, $X_u = int(A_u) \cup int(B_u)$ and $A_u \cap B_u = (A\cap B)_u$.*

Proof. A_u is closed in X_u if there exists a set $C \subseteq X$, closed in the topology of X, such that $C \cap X_u = A_u$. It is sufficient to take $C = A$. Analogously for B_u.

About the second statement, the proof that $X_u \supseteq int(A_u) \cup int(B_u)$ is trivial. Let us prove that $X_u \subseteq int(A_u) \cup int(B_u)$. If $x \in X_u$ then $x \in int(A)$ or $x \in int(B)$. Let us suppose that $x \in int(A)$. Then there exists an open neighborhood of x in X contained in A, say $U(x)$. Clearly, $U(x) \cap X_u$ is an open neighborhood of x in X_u and is contained in A_u. Hence $x \in int(A_u)$. The proof is analogous if $x \in int(B)$. The proof that $A_u \cap B_u = (A\cap B)_u$ is trivial. □

Lemma 3.2.1 ensures that, for $(u,v) \in \Delta^+$, we can consider diagram (3.4), where the leftmost vertical line belongs to the Mayer-Vietoris sequence of the triad (X_u, A_u, B_u), the central vertical line belongs to the Mayer-Vietoris sequence of the triad (X_v, A_v, B_v), and the rightmost vertical line belongs to the relative Mayer-Vietoris sequence of the triad $((X_v, X_u), (A_v, A_u), (B_v, B_u))$. For every $k \geq 0$, the horizontal maps f_k, g_k, and h_k are induced by the inclusions of $(A\cap B)_u$ into $(A\cap B)_v$, (A_u, B_u) into (A_v, B_v), and X_u into X_v, respectively. Moreover, f'_k, g'_k and h'_k are induced by the inclusions of $((A\cap B)_v, \emptyset)$ into

$((A\cap B)_v,(A\cap B)_u)$, $((A_v,\emptyset),(B_v,\emptyset))$ into $((A_v,A_u),(B_v,B_u))$, and $(X_v,\emptyset)$ into (X_v,X_u), respectively.

$$
\begin{array}{ccccccc}
 & \vdots & & \vdots & & \vdots & \\
 & \downarrow & & \downarrow & & \downarrow & \\
\cdots\to & \check{H}_{k+1}(X_u) & \stackrel{h_{k+1}}{\to} & \check{H}_{k+1}(X_v) & \stackrel{h'_{k+1}}{\to} & \check{H}_{k+1}(X_v,X_u) & \to\cdots \\
 & \downarrow\Delta_u & & \downarrow\Delta_v & & \downarrow\Delta_{v,u} & \\
\cdots\to & \check{H}_k((A\cap B)_u) & \stackrel{f_k}{\to} & \check{H}_k((A\cap B)_v) & \stackrel{f'_k}{\to} & \check{H}_k((A\cap B)_v,(A\cap B)_u) & \to\cdots \\
 & \downarrow\alpha_u & & \downarrow\alpha_v & & \downarrow\alpha_{v,u} & \\
\cdots\to & \check{H}_k(A_u)\oplus\check{H}_k(B_u) & \stackrel{g_k}{\to} & \check{H}_k(A_v)\oplus\check{H}_k(B_v) & \stackrel{g'_k}{\to} & \check{H}_k(A_v,A_u)\oplus\check{H}_k(B_v,B_u) & \to\cdots \\
 & \downarrow\beta_u & & \downarrow\beta_v & & \downarrow\beta_{v,u} & \\
\cdots\to & \check{H}_k(X_u) & \stackrel{h_k}{\to} & \check{H}_k(X_v) & \stackrel{h'_k}{\to} & \check{H}_k(X_v,X_u) & \to\cdots \\
 & \downarrow & & \downarrow & & \downarrow & \\
 & \vdots & & \vdots & & \vdots &
\end{array}
\tag{3.4}
$$

Lemma 3.2.2. *Each horizontal and vertical line in diagram* (3.4) *is exact. Moreover, each square in the same diagram is commutative.*

Proof. We recall that we are assuming that X is compact and φ continuous, therefore X_u and X_v are compact, as are A_u, A_v, B_u and B_v by Lemma 3.2.1. Therefore, since we are also assuming that the coefficient group G is a vector space over a field, it holds that the

homology sequences of the pairs (X_v, X_u), $((A\cap B)_v, (A\cap B)_u)$, (A_v, A_u), (B_v, B_u) (horizontal lines) are exact (cf. Theorem B.1 in Appendix B).
Analogously, the Mayer-Vietoris sequences of (X_u, A_u, B_u) and (X_v, A_v, B_v), and the relative Mayer-Vietoris sequence of $((X_v, X_u), (A_v, A_u), (B_v, B_u))$ (vertical lines) are exact (cf. Theorems B.2 and B.4 in Appendix B).

About the commutativity of the top squares, it is sufficient to apply Theorem B.3 in Appendix B. The same conclusion can be drawn for the commutativity of the bottom squares, with X_v replaced by $(X_v, \emptyset)$, A_v by $(A_v, \emptyset)$ and B_v by $(B_v, \emptyset)$, respectively, applying Theorem B.5. $\square$

The image of the maps f_k, g_k, and h_k of diagram (3.4) are related to the kth persistent Čech homology groups. In particular, when $k = 0$, they are related to size functions, as the following lemma formally states.

Lemma 3.2.3. *For $(u,v) \in \Delta^+$, let f_k, g_k, h_k be the maps induced by the inclusions of $(A\cap B)_u$ into $(A\cap B)_v$, (A_u, B_u) into (A_v, B_v), and X_u into X_v, respectively. Then $\operatorname{im} f_k = \check{H}_k^{u,v}(A\cap B)$, $\operatorname{im} g_k = \check{H}_k^{u,v}(A) \oplus \check{H}_k^{u,v}(B)$, and $\operatorname{im} h_k = \check{H}_k^{u,v}(X)$. In particular, $\operatorname{rank} \operatorname{im} f_0 = \ell_{(A\cap B, \varphi_{|A\cap B})}(u,v)$, $\operatorname{rank} \operatorname{im} g_0 = \ell_{(A,\varphi_{|A})}(u,v) + \ell_{(B,\varphi_{|B})}(u,v)$ and $\operatorname{rank} \operatorname{im} h_0 = \ell_{(X,\varphi)}(u,v)$.*

Proof. The proof trivially follows from the definition of kth persistent Čech homology group (Definition 3.2) and from Corollary 3.1.5. $\square$

The following proposition proves that the commutativity of squares in diagram (3.4) induces a sequence of Mayer-Vietoris of order 2 involving the kth persistent Čech homology groups of X, A, B, and $A\cap B$, for every integer $k \geq 0$.

Proposition 3.2.4. *Let us consider the sequence of homomorphisms of persistent Čech homology groups*

$$\cdots \to \check{H}_{k+1}^{u,v}(X) \xrightarrow{\Delta} \check{H}_k^{u,v}(A\cap B) \xrightarrow{\alpha} \check{H}_k^{u,v}(A) \oplus \check{H}_k^{u,v}(B) \xrightarrow{\beta} \check{H}_k^{u,v}(X) \to \cdots \to \check{H}_0^{u,v}(X) \to 0$$

where $\Delta = \Delta_{v|\operatorname{im} h_{k+1}}$, $\alpha = \alpha_{v|\operatorname{im} f_k}$, and $\beta = \beta_{v|\operatorname{im} g_k}$. For every integer $k \geq 0$, the following statements hold:

(i) $\operatorname{im}\Delta \subseteq \ker\alpha$*;*

(ii) $\operatorname{im}\alpha \subseteq \ker\beta$;

(iii) $\operatorname{im}\beta \subseteq \ker\Delta$,

that is, the sequence is of order 2.

Proof. First of all, we observe that, by Lemma 3.2.2, $\operatorname{im}\Delta \subseteq \operatorname{im} f_k$, $\operatorname{im}\alpha \subseteq \operatorname{im} g_k$ and $\operatorname{im}\beta \subseteq \operatorname{im} h_k$. Now we prove only claim *(i)*, considering that *(ii)* and *(iii)* can be deduced analogously.

(i) Let $c \in \operatorname{im}\Delta$. Then $c \in \operatorname{im} f_k$ and $c \in \operatorname{im}\Delta_v = \ker\alpha_v$ in diagram (3.4). Therefore $c \in \ker\alpha$. □

3.2.1 The size function of the union of two spaces

In the rest of the section, we focus on the ending part of diagram (3.4), that is on diagram (3.5), and, in the rest of the chapter, the notations we use always refer to diagram (3.5).

We are now ready to deduce the relation among $\ell_{(X,\varphi)}$, $\ell_{(A,\varphi_{|A})}$ and $\ell_{(B,\varphi_{|B})}$.

Theorem 3.2.5. *For every* $(u,v) \in \Delta^+$, *it holds that*

$$\begin{aligned}\ell_{(X,\varphi)}(u,v) &= \ell_{(A,\varphi_{|A})}(u,v) + \ell_{(B,\varphi_{|B})}(u,v) - \ell_{(A\cap B,\varphi_{|A\cap B})}(u,v)\\ &\quad + \operatorname{rank}\ker\alpha_v - \operatorname{rank}\ker\alpha_{v,u}.\end{aligned}$$

Proof. By the exactness of the central vertical line of diagram (3.5) and by the surjectivity of the homomorphism β_v, repeatedly using the dimensional relation between the domain of a homomorphism, its kernel and its image, we obtain

$$\begin{aligned}\operatorname{rank}\check{H}_0(X_v) &= \operatorname{rank}\operatorname{im}\beta_v\\ &= \operatorname{rank}\check{H}_0(A_v)\oplus\check{H}_0(B_v) - \operatorname{rank}\ker\beta_v\\ &= \operatorname{rank}\check{H}_0(A_v)\oplus\check{H}_0(B_v) - \operatorname{rank}\operatorname{im}\alpha_v \qquad (3.6)\\ &= \operatorname{rank}\check{H}_0(A_v) + \operatorname{rank}\check{H}_0(B_v)\\ &\quad -\operatorname{rank}\check{H}_0((A\cap B)_v) + \operatorname{rank}\ker\alpha_v.\end{aligned}$$

$$
\begin{array}{ccccccccc}
 & & \vdots & & \vdots & & \vdots & & \\
 & & \downarrow & & \downarrow & & \downarrow & & \\
\cdots \to & & \check{H}_1(X_u) & \xrightarrow{h_1} & \check{H}_1(X_v) & \xrightarrow{h'_1} & \check{H}_1(X_v, X_u) & & \to \cdots \\
 & & \downarrow \Delta_u & & \downarrow \Delta_v & & \downarrow \Delta_{v,u} & & \\
\cdots \to & & \check{H}_0((A\cap B)_u) & \xrightarrow{f_0} & \check{H}_0((A\cap B)_v) & \xrightarrow{f'_0} & \check{H}_0((A\cap B)_v, (A\cap B)_u) & & \to 0 \\
 & & \downarrow \alpha_u & & \downarrow \alpha_v & & \downarrow \alpha_{v,u} & & \\
\cdots \to & & \check{H}_0(A_u)\oplus\check{H}_0(B_u) & \xrightarrow{g_0} & \check{H}_0(A_v)\oplus\check{H}_0(B_v) & \xrightarrow{g'_0} & \check{H}_0(A_v, A_u)\oplus\check{H}_0(B_v, B_u) & & \to 0 \\
 & & \downarrow \beta_u & & \downarrow \beta_v & & \downarrow \beta_{v,u} & & \\
\cdots \to & & \check{H}_0(X_u) & \xrightarrow{h_0} & \check{H}_0(X_v) & \xrightarrow{h'_0} & \check{H}_0(X_v, X_u) & & \to 0 \\
 & & \downarrow & & \downarrow & & \downarrow & & \\
 & & 0 & & 0 & & 0 & &
\end{array}
\tag{3.5}
$$

Similarly, by the exactness of the rightmost vertical line of the same diagram and by the surjectivity of $\beta_{v,u}$, it holds that

$$\begin{aligned} \mathrm{rank}\check{H}_0(X_v,X_u) &= \mathrm{rank}\check{H}_0(A_v,A_u)+\mathrm{rank}\check{H}_0(B_v,B_u) \\ &\quad -\mathrm{rank}\check{H}_0((A\cap B)_v,(A\cap B)_u)+\mathrm{rank}\ker\alpha_{v,u}. \end{aligned} \tag{3.7}$$

Now, subtracting equality (3.7) from equality (3.6), we have

$$\begin{aligned} \mathrm{rank}\check{H}_0(X_v)-\mathrm{rank}\check{H}_0(X_v,X_u) &= \mathrm{rank}\check{H}_0(A_v)-\mathrm{rank}\check{H}_0(A_v,A_u) \\ &\quad +\mathrm{rank}\check{H}_0(B_v)-\mathrm{rank}\check{H}_0(B_v,B_u) \\ &\quad -\mathrm{rank}\check{H}_0((A\cap B)_v)+\mathrm{rank}\check{H}_0((A\cap B)_v,(A\cap B)_u) \\ &\quad +\mathrm{rank}\ker\alpha_v-\mathrm{rank}\ker\alpha_{v,u}, \end{aligned}$$

which is equivalent, in terms of size functions, to the relation claimed, because of Corollary 3.1.5. □

Corollary 3.2.6. *For every $(u,v)\in\Delta^+$, it holds that*

$$\ell_{(X,\varphi)}(u,v)=\ell_{(A,\varphi_{|A})}(u,v)+\ell_{(B,\varphi_{|B})}(u,v)-\ell_{(A\cap B,\varphi_{|A\cap B})}(u,v)$$

if and only if $\mathrm{rank}\ker\alpha_v=\mathrm{rank}\ker\alpha_{v,u}$.

Proof. Immediate from Theorem 3.2.5. □

We now show that combining the assumption that α_v and $\alpha_{v,u}$ are both injective with Proposition 3.2.4, there is a short exact sequence involving the 0th persistent Čech homology groups of X, A, B, and $A\cap B$.

Proposition 3.2.7. *For every $(u,v)\in\Delta^+$, such that the maps α_v and $\alpha_{v,u}$ are injective, the sequence of maps*

$$0\to\check{H}_0^{u,v}(A\cap B)\xrightarrow{\alpha}\check{H}_0^{u,v}(A)\oplus\check{H}_0^{u,v}(B)\xrightarrow{\beta}\check{H}_0^{u,v}(X)\to 0, \tag{3.8}$$

where $\alpha=\alpha_{v|\mathrm{im}\,f_0}$ and $\beta=\beta_{v|\mathrm{im}\,g_0}$, is exact.

Proof. By Proposition 3.2.4, we only have to show that β is surjective, α is injective, and $\operatorname{rank}\operatorname{im}\alpha = \operatorname{rank}\ker\beta$.

We recall that $\check{H}_0^{u,v}(A\cap B) = \operatorname{im} f_0$, $\check{H}_0^{u,v}(A)\oplus\check{H}_0^{u,v}(B) = \operatorname{im} g_0$, and $\check{H}_0^{u,v}(X) = \operatorname{im} h_0$ (Lemma 3.2.3).

We begin by showing that β is surjective, going through diagram (3.5). Let $c \in \operatorname{im} h_0$. There exists $d \in \check{H}_0(X_u)$ such that $h_0(d) = c$. Since β_u is surjective, there exists $d' \in \check{H}_0(A_u)\oplus\check{H}_0(B_u)$ such that $h_0\circ\beta_u(d') = c$. By Lemma 3.2.2, $\beta_v\circ g_0(d') = c$. Thus, taking $c' = g_0(d')$, we immediately have $\beta(c') = c$.

As for the injectivity of α, the claim is immediate because $\ker\alpha \subseteq \ker\alpha_v$ and we are assuming α_v injective.

Now we have to show that $\operatorname{rank}\operatorname{im}\alpha = \operatorname{rank}\ker\beta$. In order to do so, we observe that for every $(u,v)\in\Delta^+$ it holds that

$$\begin{aligned}
\ell_{(X,\varphi)}(u,v) &= \operatorname{rank}\check{H}_0^{u,v}(X)\\
&= \operatorname{rank}\operatorname{im}\beta\\
&= \operatorname{rank}H_0^{u,v}(A)\oplus\check{H}_0^{u,v}(B) - \operatorname{rank}\ker\beta \qquad (3.9)\\
&= \ell_{(A,\varphi_{|A})}(u,v) + \ell_{(B,\varphi_{|B})}(u,v) - \operatorname{rank}\ker\beta.
\end{aligned}$$

On the other hand, by Corollary 3.2.6, when $\operatorname{rank}\ker\alpha_v = \operatorname{rank}\ker\alpha_{v,u}$ it holds that

$$\ell_{(X,\varphi)}(u,v) = \ell_{(A,\varphi_{|A})}(u,v) + \ell_{(B,\varphi_{|B})}(u,v) - \ell_{(A\cap B,\varphi_{|A\cap B})}(u,v).$$

Hence, if $\operatorname{rank}\ker\alpha_v = \operatorname{rank}\ker\alpha_{v,u}$, then $\operatorname{rank}\ker\beta = \ell_{(A\cap B,\varphi_{|A\cap B})}(u,v)$. Moreover, since $\ell_{(A\cap B,\varphi_{|A\cap B})}(u,v) = \operatorname{rank}\check{H}_0^{u,v}(A\cap B) = \operatorname{rank}\ker\alpha + \operatorname{rank}\operatorname{im}\alpha$, when $\operatorname{rank}\ker\alpha_v = \operatorname{rank}\ker\alpha_{v,u}$ we have $\operatorname{rank}\ker\beta = \operatorname{rank}\ker\alpha + \operatorname{rank}\operatorname{im}\alpha$. Therefore, when $\operatorname{rank}\ker\alpha_v = \operatorname{rank}\ker\alpha_{v,u} = 0$, it follows that $\operatorname{rank}\ker\beta = \operatorname{rank}\operatorname{im}\alpha$. □

The condition $\operatorname{rank}\ker\alpha_v = \operatorname{rank}\ker\alpha_{v,u} = 0$ in the previous Proposition 3.2.7 cannot be weakened, in fact:

Remark 4. *The equality* $\operatorname{rank}\ker\alpha_v = \operatorname{rank}\ker\alpha_{v,u}$ *does not imply the injectivity of* α.

Indeed, Figure 3.3 shows an example of a topological space $X = A\cup B$ on which, taking the height function as measuring function and $u,v\in\mathbb{R}$ as displayed, it holds that

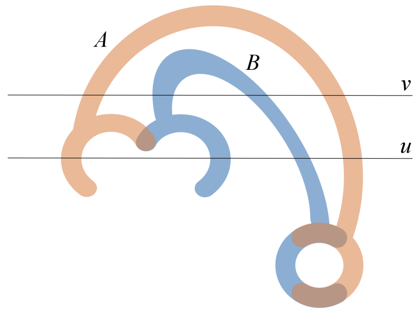

Figure 3.3: The sets A and B used in Remark 4.

$\operatorname{rank}\ker\alpha_v = \operatorname{rank}\ker\alpha_{v,u} \neq 0$, but $\operatorname{rank}\ker\alpha > 0$, making the sequence (3.8) not exact. To see that $\operatorname{rank}\ker\alpha_v = \operatorname{rank}\ker\alpha_{v,u} \neq 0$, we note that the equalities (3.6) and (3.7) imply $\operatorname{rank}\ker\alpha_v = \operatorname{rank}\check{H}_0(X_v) - \operatorname{rank}\check{H}_0(A_v) - \operatorname{rank}\check{H}_0(B_v) + \operatorname{rank}\check{H}_0((A\cap B)_v) = 2 - 2 - 2 + 3 = 1$ and $\operatorname{rank}\ker\alpha_{v,u} = \operatorname{rank}\check{H}_0(X_v, X_u) - \operatorname{rank}\check{H}_0(A_v, A_u) - \operatorname{rank}\check{H}_0(B_v, B_u) + \operatorname{rank}\check{H}_0((A\cap B)_v, (A\cap B)_u) = 0 - 0 - 0 + 1 = 1$, respectively. To see that $\operatorname{rank}\ker\alpha = 1$, let us consider the homology sequence of the pair (X_v, X_u)

$$\cdots \to \check{H}_2(X_v, X_u) \to \check{H}_1(X_u) \xrightarrow{h_1} \check{H}_1(X_v) \xrightarrow{h_1'} \check{H}_1(X_v, X_u) \to \cdots$$

that is the first horizontal line in diagram (3.5). In this instance, $\check{H}_2(X_v, X_u) = 0$, so it follows that h_1 is injective. Moreover, $\operatorname{rank}\check{H}_1(X_u) = \operatorname{rank}\check{H}_1(X_v) = 1$ implies the surjectivity of h_1. Recalling from Proposition 3.2.4 that $\Delta = \Delta_{v|\operatorname{im} h_1}$, we have that $\Delta = \Delta_v$. Then, since $\operatorname{im}\Delta \subseteq \ker\alpha \subseteq \ker\alpha_v = \operatorname{im}\Delta_v$ and $\operatorname{rank}\operatorname{im}\Delta = \operatorname{rank}\operatorname{im}\Delta_v = 1$, it follows that $\operatorname{rank}\ker\alpha = 1$.

As shown in the proof of Proposition 3.2.7, for every $(u,v) \in \Delta^+$, it holds that $\ell_{(X,\varphi)}(u,v) = \ell_{(A,\varphi_{|A})}(u,v) + \ell_{(B,\varphi_{|B})}(u,v) - \operatorname{rank}\ker\beta$ (see equality (3.9)). So, as an immediate consequence, we observe that

Remark 5. *$\ell_{(X,\varphi)}(u,v) \leq \ell_{(A,\varphi_{|A})}(u,v) + \ell_{(B,\varphi_{|B})}(u,v)$ holds for every $(u,v) \in \Delta^+$.*

3.2.2 Examples

In this section, we give two examples illustrating the previous results.

In both these examples, we consider a "double open-end wrench" shaped object A, partially occluded by another object B, resulting in different shapes $X = A \cup B \subset \mathbb{R}^2$. The size functions $\ell_{(A,\varphi_{|A})}$, $\ell_{(B,\varphi_{|B})}$, $\ell_{(A\cap B,\varphi_{|A\cap B})}$, $\ell_{(X,\varphi)}$ are computed taking $\varphi : X \to \mathbb{R}$, $\varphi(P) = -\|P - H\|$, with H a fixed point in $\mathbb{R}^2$.

In the first example, shown in Figure 3.4, it is easy to check that the relation given in Corollary 3.2.6, $\ell_{(X,\varphi)}(u,v) = \ell_{(A,\varphi_{|A})}(u,v) + \ell_{(B,\varphi_{|B})}(u,v) - \ell_{(A\cap B,\varphi_{|A\cap B})}(u,v)$, holds for every $(u,v) \in \Delta^+$.

In the second example, shown in Figure 3.5, a deformation of the occluding object B in Figure 3.4 makes the relation given in Corollary 3.2.6 not everywhere valid in Δ^+. More precisely, the condition $\operatorname{rank}\ker\alpha_v = \operatorname{rank}\ker\alpha_{v,u} = 1$ holds for every $(u,v) \in \Delta^+$, with $-a \le u < -b$ and $-c \le v$, whereas the condition $\operatorname{rank}\ker\alpha_v = \operatorname{rank}\ker\alpha_{v,u} = 0$ holds for every $(u,v) \in \Delta^+$ with $u < -a$, for every $(u,v) \in \Delta^+$ with $-a \le u < v < -b$, and for every $(u,v) \in \Delta^+$ with $-b \le u < v < -c$. Therefore, in these regions, $\ell_{(X,\varphi)}(u,v) = \ell_{(A,\varphi_{|A})}(u,v) + \ell_{(B,\varphi_{|B})}(u,v) - \ell_{(A\cap B,\varphi_{|A\cap B})}(u,v)$. In the remaining regions of Δ^+, this relation does not hold. To be more precise, $\ell_{(X,\varphi)}(u,v) < \ell_{(A,\varphi_{|A})}(u,v) + \ell_{(B,\varphi_{|B})}(u,v) - \ell_{(A\cap B,\varphi_{|A\cap B})}(u,v)$ for every $(u,v) \in \Delta^+$ with $-a \le u < -b$ and $-b \le v < -c$, because $\operatorname{rank}\ker\alpha_v = 0$ and $\operatorname{rank}\ker\alpha_{v,u} = 1$; while, $\ell_{(X,\varphi)}(u,v) > \ell_{(A,\varphi_{|A})}(u,v) + \ell_{(B,\varphi_{|B})}(u,v) - \ell_{(A\cap B,\varphi_{|A\cap B})}(u,v)$ for every $(u,v) \in \Delta^+$ with $-b \le u$ and $-c \le v$ because $\operatorname{rank}\ker\alpha_v = 1$ and $\operatorname{rank}\ker\alpha_{v,u} = 0$. To simplify the visualization of the regions of Δ^+ in which the equality holds, the reader can refer to Figure 3.5 (b), where $\ell_{(X,\varphi)}$ is displayed using white for points $(u,v) \in \Delta^+$ that verify $\ell_{(X,\varphi)}(u,v) = \ell_{(A,\varphi_{|A})}(u,v) + \ell_{(B,\varphi_{|B})}(u,v) - \ell_{(A\cap B,\varphi_{|A\cap B})}(u,v)$ and red for the other ones.

3.2.3 Conditions for the exactness of $0 \to \check{H}_0^{u,v}(A\cap B) \to \check{H}_0^{u,v}(A) \oplus \check{H}_0^{u,v}(B) \to \check{H}_0^{u,v}(X) \to 0$

In this section we look for sufficient conditions in order that α_v and $\alpha_{v,u}$ are injective, so that the sequence

$$0 \;\to\; \check{H}_0^{u,v}(A\cap B) \;\overset{\alpha}{\to}\; \check{H}_0^{u,v}(A) \oplus \check{H}_0^{u,v}(B) \;\overset{\beta}{\to}\; \check{H}_0^{u,v}(X) \to 0 \tag{3.10}$$

is exact (cf. Proposition 3.2.7), and the relation $\ell_{(X,\varphi)}(u,v) = \ell_{(A,\varphi_{|A})}(u,v) + \ell_{(B,\varphi_{|B})}(u,v) - \ell_{(A\cap B,\varphi_{|A\cap B})}(u,v)$ of Corollary 3.2.6 is satisfied.

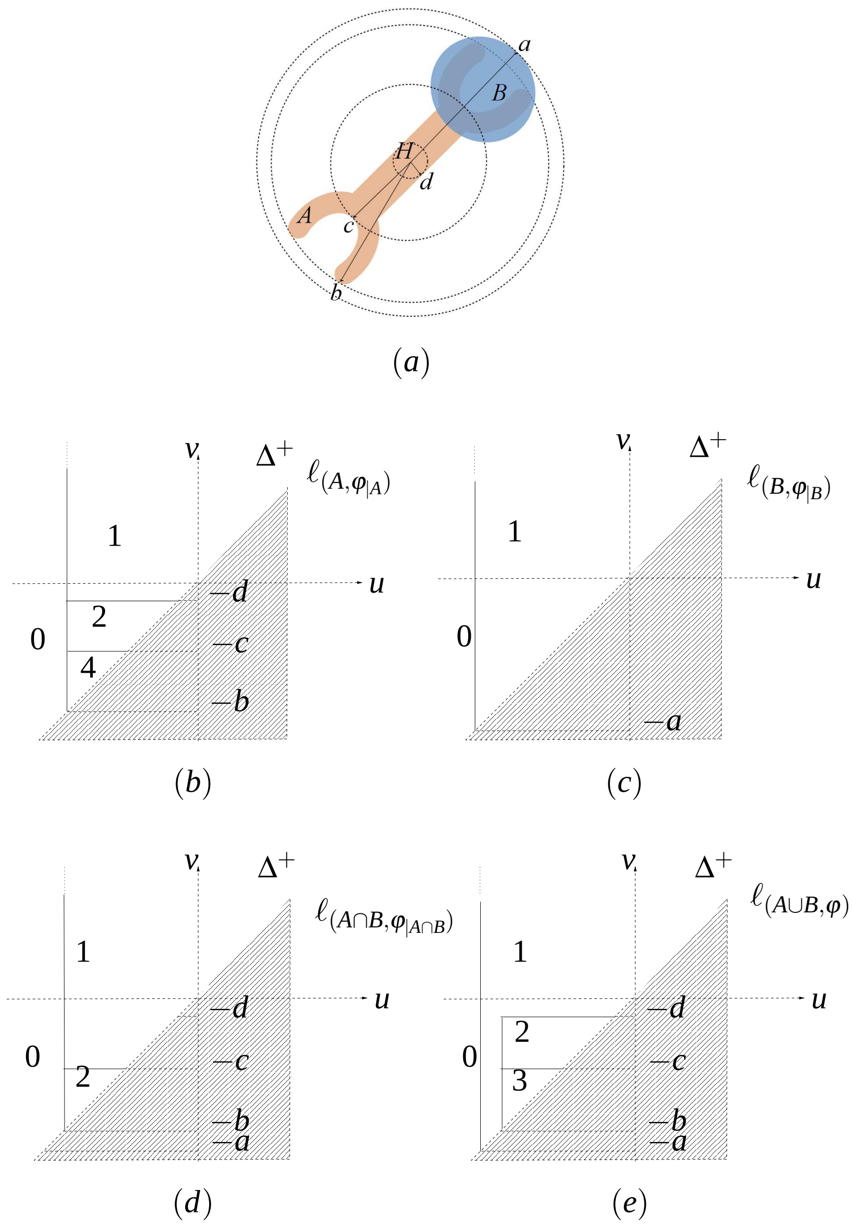

Figure 3.4: In (a) a "double open-end wrench" shaped object A is occluded by another object B. In (b), (c), (d) and (e) we show the size functions of $(A, \varphi_{|A})$, $(B, \varphi_{|B})$, $(A \cap B, \varphi_{|A\cap B})$ and $(A \cup B, \varphi)$, respectively, computed taking $\varphi : X \to \mathbb{R}$, $\varphi(P) = -\|P - H\|$. In this example the relation $\ell_{(X,\varphi)} = \ell_{(A,\varphi_{|A})} + \ell_{(B,\varphi_{|B})} - \ell_{(A\cap B,\varphi_{|A\cap B})}$ of Corollary 3.2.6 holds everywhere in Δ^+.

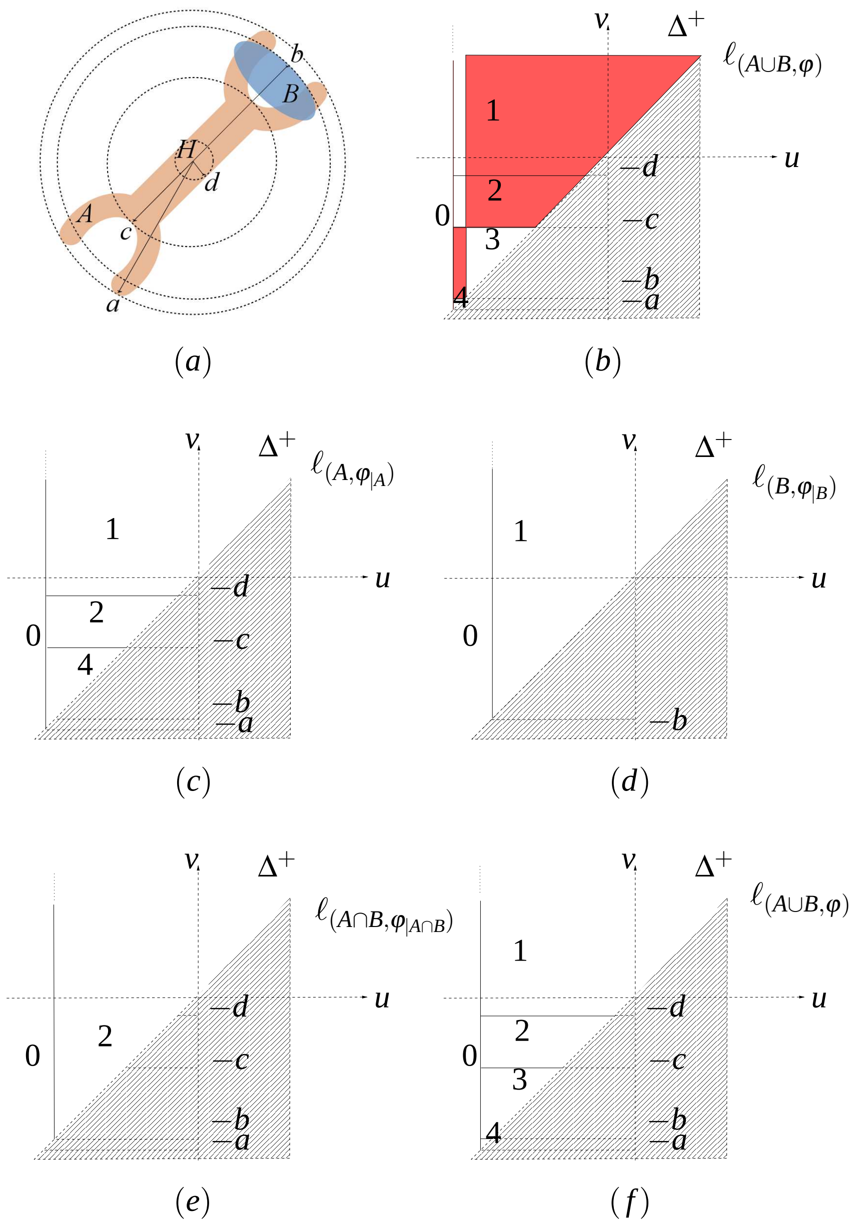

Figure 3.5: In (a) the same "double open-end wrench" shaped object A as in Figure 3.4 is considered together with a different occluding object B. In (c), (d), (e), (f) we display the size functions of $(A,\varphi_{|A})$, $(B,\varphi_{|B})$, $(A\cap B,\varphi_{|A\cap B})$ and $(A\cup B,\varphi)$, respectively, computed taking $\varphi : X \to \mathbb{R}$, $\varphi(P) = -\|P-H\|$. In this case the relation $\ell_{(X,\varphi)} = \ell_{(A,\varphi_{|A})} + \ell_{(B,\varphi_{|B})} - \ell_{(A\cap B,\varphi_{|A\cap B})}$ of Corollary 3.2.6 does not hold everywhere in Δ^+. In (b) we underline the regions of Δ^+ where the equality is not valid by coloring them.

The reason for looking for these conditions lies in the fact that they can be used as a guidance in choosing the most appropriate measuring function in order to study the shape of a partially occluded object.

Remark 6. *If we require the surjectivity in addition to the injectivity of α_v and α_{vu}, sequence (3.10) is trivial.*

Indeed, as stated by the following Proposition 3.2.9, the bijectivity of α_v and α_{vu} implies that $\ell_{(X,\varphi)}(u,v) = \mathrm{rank} H_0^{u,v}(X)$ vanishes, and hence all the homology groups involved in sequence (3.10) are trivial.

Lemma 3.2.8. *For every $(u,v) \in \Delta^+$, α_v is surjective if and only if $\alpha_{v,u}$ is surjective.*

Proof. It is immediate by the surjectivity of the homomorphisms f_0' and g_0' and by the commutativity of the squares in diagram (3.5). □

Proposition 3.2.9. *For every $(u,v) \in \Delta^+$ such that at least one among α_u, α_v, $\alpha_{v,u}$ is surjective, we have $\ell_{(X,\varphi)}(u,v) = 0$.*

Proof. Let us suppose α_u surjective. In diagram (3.5), it follows that, by surjectivity of β_u, $\check{H}_0(X_u)$ is trivial, and by the exactness of the last horizontal sequence and the surjectivity of h_0', it holds that $\mathrm{rank}\check{H}_0(X_v) = \mathrm{rank}\check{H}_0(X_v, X_u)$ making $\ell_{(X,\varphi)}(u,v)$ trivial. Let α_v be surjective. In diagram (3.5), it follows that, by surjectivity of β_v, $\check{H}_0(X_v)$ is trivial. Moreover, by the previous Lemma 3.2.8, α_v is surjective if and only if so is $\alpha_{v,u}$. The surjectivity of $\alpha_{v,u}$ and that of $\beta_{v,u}$ imply $\check{H}_0(X_v, X_u) = 0$ and hence the claim. □

The first condition ensuring the injectivity of α_v and $\alpha_{v,u}$ that we exhibit (Theorem 3.2.11), relates the exactness of the sequence (3.10) to the values taken by the size function $\ell_{(A\cap B, \varphi_{|A\cap B})}$. Roughly speaking, it indicates that the fewer the number of cornerpoints in the size function of $A\cap B$, the larger the region of Δ^+ where the sequence (3.10) is necessarily exact. We underline that this is only a sufficient condition, as the examples in Section 3.2.2 easily show.

The sketch of proof is the following. We begin by showing that the surjectivity of f_0 in diagram (3.5) is a sufficient condition, ensuring that $\alpha_{v,u}$ is injective. Then we note that, for points $(u,v) \in \Delta^+$ where the size function of $A\cap B$ has no cornerpoints in the upper right region $\{(u',v') \in \Delta^+ :\ u \le u' \le v, v' > v\}$, f_0 is necessarily surjective. So we obtain a condition on $\ell_{(A\cap B,\varphi_{|A\cap B})}(u,v)$ such that $\alpha_{v,u}$ is injective. Finally, showing that if $\ell_{(A\cap B,\varphi_{|A\cap B})}(u,v) \le 1$, then α_v is injective, we prove the claim of Theorem 3.2.11.

Lemma 3.2.10. *Let* $\alpha = \alpha_{v|\mathrm{im}\, f_0}$ *and* $\beta = \beta_{v|\mathrm{im}\, g_0}$. *If* f_0 *is surjective, then* $\mathrm{im}\, \alpha = \ker \beta$ *and* $\alpha_{v,u} = 0$.

Proof. By Proposition 3.2.4 *(ii)*, $\mathrm{im}\, \alpha \subseteq \ker \beta$, so we need to prove that $\ker \beta \subseteq \mathrm{im}\, \alpha$. Let $c \in \ker \beta \subseteq \ker \beta_v$ and consider diagram (3.5). Since $\mathrm{im}\, \alpha_v = \ker \beta_v$, there exists $d \in \check{H}_0((A\cap B)_v)$ such that $\alpha_v(d) = c$. By hypothesis, f_0 is surjective, so $\check{H}_0((A\cap B)_v) = \mathrm{im}\, f_0$. Hence $d \in \mathrm{im}\, f_0$, implying $\alpha(d) = c$. Thus, $c \in \mathrm{im}\, \alpha$, and hence $\mathrm{im}\, \alpha = \ker \beta$.

Let us now show that $\alpha_{v,u}$ is trivial. By observing again diagram (3.5), we see that f_0 is surjective if and only if f_0' is trivial. Since f_0' is surjective, it holds that f_0 is surjective if and only if $\check{H}_0((A\cap B)_v,(A\cap B)_u) = 0$. Therefore, if f_0 is surjective, then $\alpha_{v,u} = 0$. □

Theorem 3.2.11. *Let* $(u,v) \in \Delta^+$. *The following statements hold*

(i) *If* $\ell_{(A\cap B,\varphi_{|A\cap B})}(u,v') = \ell_{(A\cap B,\varphi_{|A\cap B})}(v,v')$ *for every* $(v,v') \in \Delta^+$, *then* $\alpha_{v,u} = 0$.

(ii) *If* $\ell_{(A\cap B,\varphi_{|A\cap B})}(v,v') \le 1$ *for every* $(v,v') \in \Delta^+$, *then* $\ker \alpha_v = 0$.

Proof. Let us prove *(i)*. If $\ell_{(A\cap B,\varphi_{|A\cap B})}(u,v') = \ell_{(A\cap B,\varphi_{|A\cap B})}(v,v')$ for every $(v,v') \in \Delta^+$, applying Proposition 3.1.8 with $A\cap B$ in place of X and f_0 in place of $\iota_0^{u,v}$, it follows that f_0 is surjective. Hence, by Lemma 3.2.10, we have $\alpha_{v,u}$ trivial.

Let us now prove *(ii)*. From the assumption $\ell_{(A\cap B,\varphi_{|A\cap B})}(v,v') \le 1$, for every $(v,v') \in \Delta^+$, we deduce that either $(A\cap B)_v$ is empty or $(A\cap B)_v$ is non-empty and connected. If $(A\cap B)_v$ is empty, then $\check{H}_0((A\cap B)_v)$ is trivial and the claim is proved. Let us consider the case when $(A\cap B)_v$ is non-empty and connected. Let $z_0 = \{z_0(\mathcal{U}_{(A\cap B)_v})\} \in \check{H}_0((A\cap B)_v)$. If $z_0 \in \ker \alpha_v = \mathrm{im}\, \Delta_v$, for each $z_0(\mathcal{U}_{(A\cap B)_v}) \in H_0(\mathcal{U}_{(A\cap B)_v})$ there is a 1-chain $c_1(\mathcal{U}_{A_v})$ on A_v and a 1-chain $c_1(\mathcal{U}_{B_v})$ on B_v, such that the homology class of $\partial c_1(\mathcal{U}_{A_v}) = -\partial c_1(\mathcal{U}_{B_v})$ is equal to $z_0(\mathcal{U}_{(A\cap B)_v})$, up to homomorphisms induced by the inclusion. We now show that $\partial c_1(\mathcal{U}_{A_v})$ is a boundary on $(A\cap B)_v$. This will prove that $z_0(\mathcal{U}_{(A\cap B)_v})$ is trivial, yielding the injectivity of α_v. If $c_1(\mathcal{U}_{A_v}) = \sum_{i=1}^n a_i \cdot < U_i^0, U_i^1 >$, then $\partial c_1(\mathcal{U}_{A_v}) = \sum_{i=1}^n a_i \cdot U_i^1 - \sum_{i=1}^n a_i \cdot U_i^0$. From $\partial c_1(\mathcal{U}_{A_v}) = -\partial c_1(\mathcal{U}_{B_v})$, we deduce that, for $i = 1,\dots,n$,

U_i^0 and U_i^1 have non-empty intersection with $(A \cap B)_v$. By Proposition 3.1.2, the connectedness of $(A \cap B)_v$ implies that there is a simple chain on $(A \cap B)_v$ connecting U_i^0 and U_i^1, for $i = 1, \dots, n$. Therefore $\partial c_1(\mathcal{U}_{A_v})$ is a boundary on $(A \cap B)_v$. □

We conclude by observing that other sufficient conditions exist, implying that both α_v and $\alpha_{v,u}$ are injective. An example is given by the following result.

Proposition 3.2.12. *If* $\mathrm{rank}\check{H}_1(X_v) = 0$ *and* $\mathrm{rank}\check{H}_0(X_u) = \ell_{(X,\varphi)}(u,v)$, *then* $\ker \alpha_v = \ker \alpha_{v,u} = 0$.

Proof. The condition $\mathrm{rank}\check{H}_1(X_v) = 0$ trivially implies that $\ker \alpha_v = 0$. On the other hand, it implies the injectivity of the homomorphism h in the following exact sequence:

$$\cdots \to \check{H}_1(X_v) \xrightarrow{h_1'} \check{H}_1(X_v, X_u) \xrightarrow{h} \check{H}_0(X_u) \xrightarrow{h_0} \check{H}_0(X_v) \xrightarrow{h_0'} \check{H}_0(X_v, X_u) \to 0,$$

which is the first horizontal sequence in diagram (3.5). Therefore, by the assumption $\mathrm{rank}\check{H}_0(X_u) = \ell_{(X,\varphi)}(u,v)$, it follows that

$$\mathrm{rank}\check{H}_1(X_v, X_u) = \mathrm{rank}\,\mathrm{im}\,h = \mathrm{rank}\,\ker h_0 = \mathrm{rank}\check{H}_0(X_u) - \ell_{(X,\varphi)}(u,v) = 0,$$

and, consequently, the triviality of $\ker \alpha_{v,u}$ has been proved. □

3.3 Partial matching of cornerpoints in size functions of occluded shapes

As recalled in Subsection 1.3.4, in [36] it was shown that size functions can be concisely represented by collections of points, called cornerpoints, with multiplicities.

This representation by cornerpoints has the important property of being stable against continuous deformations of the considered objects. For this reason, in dealing with the shape comparison problem, via size functions, one actually compares the sets of cornerpoints using the Hausdorff distance or the matching distance (Definitions 1.6 and 1.7). The Hausdorff distance and the matching distance differ in that the former does not take into account the multiplicities of cornerpoints, while the latter does.

The aim of this section is to show what happens to cornerpoints in the presence of occlusions.

We prove that each cornerpoint for the size function of an occluded shape X is a cornerpoint for the size function of the original shape A, or the occluding shape B, or their intersection $A \cap B$, providing that a certain condition holds (Corollary 3.3.2). However, even when this condition is not verified, it holds that the coordinates of cornerpoints of $\ell_{(X,\varphi)}$ are always related to those of the cornerpoints of $\ell_{(A,\varphi|_A)}$ or $\ell_{(B,\varphi|_B)}$ or $\ell_{(A\cap B,\varphi|_{A\cap B})}$ (Theorems 3.3.3 and 3.3.4).

We begin by proving a relation between multiplicities of points for the size functions associated with X, A and B. Since cornerpoints are points with positive multiplicity (Definitions 1.4 and 1.5), we obtain conditions for cornerpoints of the size functions of A and B to persist in $A \cup B$. This fact suggests that in size theory the partial matching of an occluded shape with the original shape can be translated into the partial matching of cornerpoints of the corresponding size functions. This intuition will be developed in the experimental Section 3.4.

In the next proposition we obtain a relation involving the multiplicities of points in the size functions associated with X, A and B.

Proposition 3.3.1. *For every $p = (\bar{u}, \bar{v}) \in \Delta^+$, it holds that*

$$\mu_X(p) - \mu_A(p) - \mu_B(p) + \mu_{A\cap B}(p) = \lim_{\varepsilon \to 0^+} \big(\operatorname{rank}\ker \alpha_{\bar{v}-\varepsilon,\bar{u}-\varepsilon} - \operatorname{rank}\ker \alpha_{\bar{v}-\varepsilon,\bar{u}+\varepsilon} \\ + \operatorname{rank}\ker \alpha_{\bar{v}+\varepsilon,\bar{u}+\varepsilon} - \operatorname{rank}\ker \alpha_{\bar{v}+\varepsilon,\bar{u}-\varepsilon}\big).$$

Proof. Applying Theorem 3.2.5 four times with $(u,v) = (\bar{u}+\varepsilon, \bar{v}-\varepsilon)$, $(u,v) = (\bar{u}-\varepsilon, \bar{v}-\varepsilon)$, $(u,v) = (\bar{u}+\varepsilon, \bar{v}+\varepsilon)$, $(u,v) = (\bar{u}-\varepsilon, \bar{v}+\varepsilon)$, and ε a positive real number so small that $\bar{u}+\varepsilon < \bar{v}-\varepsilon$, we get

$$
\begin{aligned}
&\ell_{(X,\varphi)}(\bar{u}+\varepsilon,\bar{v}-\varepsilon)-\ell_{(X,\varphi)}(\bar{u}-\varepsilon,\bar{v}-\varepsilon)-\ell_{(X,\varphi)}(\bar{u}+\varepsilon,\bar{v}+\varepsilon)+\ell_{(X,\varphi)}(\bar{u}-\varepsilon,\bar{v}+\varepsilon)\\
&\quad= \ell_{(A,\varphi_{|A})}(\bar{u}+\varepsilon,\bar{v}-\varepsilon)+\ell_{(B,\varphi_{|B})}(\bar{u}+\varepsilon,\bar{v}-\varepsilon)-\ell_{(A\cap B,\varphi_{|A\cap B})}(\bar{u}+\varepsilon,\bar{v}-\varepsilon)\\
&\qquad+\operatorname{rank}\ker\alpha_{\bar{v}-\varepsilon}-\operatorname{rank}\ker\alpha_{\bar{v}-\varepsilon,\bar{u}+\varepsilon}\\
&\qquad-\Big(\ell_{(A,\varphi_{|A})}(\bar{u}-\varepsilon,\bar{v}-\varepsilon)+\ell_{(B,\varphi_{|B})}(\bar{u}-\varepsilon,\bar{v}-\varepsilon)-\ell_{(A\cap B,\varphi_{|A\cap B})}(\bar{u}-\varepsilon,\bar{v}-\varepsilon)\\
&\qquad+\operatorname{rank}\ker\alpha_{\bar{v}-\varepsilon}-\operatorname{rank}\ker\alpha_{\bar{v}-\varepsilon,\bar{u}-\varepsilon}\Big)\\
&\qquad-\Big(\ell_{(A,\varphi_{|A})}(\bar{u}+\varepsilon,\bar{v}+\varepsilon)+\ell_{(B,\varphi_{|B})}(\bar{u}+\varepsilon,\bar{v}+\varepsilon)-\ell_{(A\cap B,\varphi_{|A\cap B})}(\bar{u}+\varepsilon,\bar{v}+\varepsilon)\\
&\qquad+\operatorname{rank}\ker\alpha_{\bar{v}+\varepsilon}-\operatorname{rank}\ker\alpha_{\bar{v}+\varepsilon,\bar{u}+\varepsilon}\Big)\\
&\qquad+\ell_{(A,\varphi_{|A})}(\bar{u}-\varepsilon,\bar{v}+\varepsilon)+\ell_{(B,\varphi_{|B})}(\bar{u}-\varepsilon,\bar{v}+\varepsilon)-\ell_{(A\cap B,\varphi_{|A\cap B})}(\bar{u}-\varepsilon,\bar{v}+\varepsilon)\\
&\qquad+\operatorname{rank}\ker\alpha_{\bar{v}+\varepsilon}-\operatorname{rank}\ker\alpha_{\bar{v}+\varepsilon,\bar{u}-\varepsilon}\\
&\quad= \ell_{(A,\varphi_{|A})}(\bar{u}+\varepsilon,\bar{v}-\varepsilon)-\ell_{(A,\varphi_{|A})}(\bar{u}-\varepsilon,\bar{v}-\varepsilon)\\
&\qquad-\ell_{(A,\varphi_{|A})}(\bar{u}+\varepsilon,\bar{v}+\varepsilon)+\ell_{(A,\varphi_{|A})}(\bar{u}-\varepsilon,\bar{v}+\varepsilon)\\
&\qquad+\ell_{(B,\varphi_{|B})}(\bar{u}+\varepsilon,\bar{v}-\varepsilon)-\ell_{(B,\varphi_{|B})}(\bar{u}-\varepsilon,\bar{v}-\varepsilon)\\
&\qquad-\ell_{(B,\varphi_{|B})}(\bar{u}+\varepsilon,\bar{v}+\varepsilon)+\ell_{(B,\varphi_{|B})}(\bar{u}-\varepsilon,\bar{v}+\varepsilon)\\
&\qquad-\ell_{(A\cap B,\varphi_{|A\cap B})}(\bar{u}+\varepsilon,\bar{v}-\varepsilon)+\ell_{(A\cap B,\varphi_{|A\cap B})}(\bar{u}-\varepsilon,\bar{v}-\varepsilon)\\
&\qquad+\ell_{(A\cap B,\varphi_{|A\cap B})}(\bar{u}+\varepsilon,\bar{v}+\varepsilon)-\ell_{(A\cap B,\varphi_{|A\cap B})}(\bar{u}-\varepsilon,\bar{v}+\varepsilon)\\
&\qquad+\operatorname{rank}\ker\alpha_{\bar{v}-\varepsilon,\bar{u}-\varepsilon}-\operatorname{rank}\ker\alpha_{\bar{v}-\varepsilon,\bar{u}+\varepsilon}+\operatorname{rank}\ker\alpha_{\bar{v}+\varepsilon,\bar{u}+\varepsilon}-\operatorname{rank}\ker\alpha_{\bar{v}+\varepsilon,\bar{u}-\varepsilon}.
\end{aligned}
$$

Hence, by definition of multiplicity of a point of Δ^+ (Definition 1.4), we have that

$$\begin{aligned}
&\lim_{\varepsilon\to 0^+}\big(\operatorname{rank}\ker\alpha_{\bar v-\varepsilon,\bar u-\varepsilon}-\operatorname{rank}\ker\alpha_{\bar v-\varepsilon,\bar u+\varepsilon}\\
&\qquad+\operatorname{rank}\ker\alpha_{\bar v+\varepsilon,\bar u+\varepsilon}-\operatorname{rank}\ker\alpha_{\bar v+\varepsilon,\bar u-\varepsilon}\big)\\
&=\ \lim_{\varepsilon\to 0^+}\Big(\ell_{(X,\varphi)}(\bar u+\varepsilon,\bar v-\varepsilon)-\ell_{(X,\varphi)}(\bar u-\varepsilon,\bar v-\varepsilon)\\
&\qquad-\ell_{(X,\varphi)}(\bar u+\varepsilon,\bar v+\varepsilon)+\ell_{(X,\varphi)}(\bar u-\varepsilon,\bar v+\varepsilon)\Big)\\
&\qquad-\lim_{\varepsilon\to 0^+}\Big(\ell_{(A,\varphi_{|A})}(\bar u+\varepsilon,\bar v-\varepsilon)-\ell_{(A,\varphi_{|A})}(\bar u-\varepsilon,\bar v-\varepsilon)\\
&\qquad-\ell_{(A,\varphi_{|A})}(\bar u+\varepsilon,\bar v+\varepsilon)+\ell_{(A,\varphi_{|A})}(\bar u-\varepsilon,\bar v+\varepsilon)\Big)\\
&\qquad-\lim_{\varepsilon\to 0^+}\Big(\ell_{(B,\varphi_{|B})}(\bar u+\varepsilon,\bar v-\varepsilon)-\ell_{(B,\varphi_{|B})}(\bar u-\varepsilon,\bar v-\varepsilon)\\
&\qquad-\ell_{(B,\varphi_{|B})}(\bar u+\varepsilon,\bar v+\varepsilon)+\ell_{(B,\varphi_{|B})}(\bar u-\varepsilon,\bar v+\varepsilon)\Big)\\
&\qquad+\lim_{\varepsilon\to 0^+}\Big(\ell_{(A\cap B,\varphi_{|A\cap B})}(\bar u+\varepsilon,\bar v-\varepsilon)-\ell_{(A\cap B,\varphi_{|A\cap B})}(\bar u-\varepsilon,\bar v-\varepsilon)\\
&\qquad-\ell_{(A\cap B,\varphi_{|A\cap B})}(\bar u+\varepsilon,\bar v+\varepsilon)+\ell_{(A\cap B,\varphi_{|A\cap B})}(\bar u-\varepsilon,\bar v+\varepsilon)\Big)\\
&=\ \lim_{\varepsilon\to 0^+}(\mu^{\varepsilon}_{(X,\varphi)}(p)-\mu^{\varepsilon}_{(A,\varphi_{|A})}(p)-\mu^{\varepsilon}_{(B,\varphi_{|B})}(p)+\mu^{\varepsilon}_{(A\cap B,\varphi_{|A\cap B})}(p))\\
&=\ \mu_{(X,\varphi)}(p)-\mu_{(A,\varphi_{|A})}(p)-\mu_{(B,\varphi_{|B})}(p)+\mu_{(A\cap B,\varphi_{|A\cap B})}(p).
\end{aligned}$$

□

Using the previous Proposition 3.3.1, we find a condition ensuring that proper cornerpoints for the size function of X are also proper cornerpoints for the size function of A or B.

Corollary 3.3.2. *Let $p=(\bar u,\bar v)$ be a proper cornerpoint for $\ell_{(X,\varphi)}$ and*

$$\begin{aligned}
&\lim_{\varepsilon\to 0^+}\big(\operatorname{rank}\ker\alpha_{\bar v-\varepsilon,\bar u-\varepsilon}-\operatorname{rank}\ker\alpha_{\bar v-\varepsilon,\bar u+\varepsilon}\\
&\qquad+\operatorname{rank}\ker\alpha_{\bar v+\varepsilon,\bar u+\varepsilon}-\operatorname{rank}\ker\alpha_{\bar v+\varepsilon,\bar u-\varepsilon}\big)\le 0.
\end{aligned}$$

Then p is a proper cornerpoint for either $\ell_{(A,\varphi_{|A})}$ or $\ell_{(B,\varphi_{|B})}$ or both.

Proof. By Proposition 3.3.1, the assumption $\lim_{\varepsilon\to 0^+}\big(\operatorname{rank}\ker\alpha_{\bar v-\varepsilon,\bar u-\varepsilon}-\operatorname{rank}\ker\alpha_{\bar v-\varepsilon,\bar u+\varepsilon}$ $+\operatorname{rank}\ker\alpha_{\bar v+\varepsilon,\bar u+\varepsilon}-\operatorname{rank}\ker\alpha_{\bar v+\varepsilon,\bar u-\varepsilon}\big)\le 0$ implies $\mu_X(p)\le\mu_A(p)+\mu_B(p)-\mu_{A\cap B}(p)$. Since p is a cornerpoint for $\ell_{(X,\varphi)}$, it holds that $\mu_X(p)>0$. Since multiplicities are always non-negative, this easily implies that either $\mu_A(p) > 0$ or $\mu_B(p) > 0$ (or both), proving the statement. $\square$

Remark 7. *If $p = (\overline{u}, \overline{v})$ is a proper cornerpoint for $\ell_{(X,\varphi)}$ and $\ell_{(A\cap B),\varphi_{|A\cap B}}(\overline{v}, v') \leq 1$ for every $v' > \overline{v}$, then it is a proper cornerpoint for either $\ell_{(A,\varphi|_A)}$ or $\ell_{(B,\varphi|_B)}$ or both.*

This is easily seen by combining Lemma 3.2.10 with Proposition 3.1.8. Indeed, by the right-continuity of size functions and the fact that they are non-decreasing in the first variable, for a sufficiently small ε it holds that $\ker \alpha_{\overline{v}-\varepsilon,\overline{u}-\varepsilon} = 0$, $\ker \alpha_{\overline{v}-\varepsilon,\overline{u}+\varepsilon} = 0$, $\ker \alpha_{\overline{v}+\varepsilon,\overline{u}+\varepsilon} = 0$, $\ker \alpha_{\overline{v}+\varepsilon,\overline{u}-\varepsilon} = 0$.

The following two theorems state that the abscissas of the cornerpoints for $\ell_{(X,\varphi)}$ are abscissas of cornerpoints for $\ell_{(A,\varphi|_A)}$ or $\ell_{(B,\varphi|_B)}$ or $\ell_{(A\cap B,\varphi|_{A\cap B})}$; the ordinates of the cornerpoints for $\ell_{(X,\varphi)}$ are, in general, homological 0-critical values for $(A, \varphi_{|A})$ or $(B, \varphi_{|B})$ or $(A \cap B, \varphi_{|A\cap B})$, and, under restrictive conditions, abscissas or ordinates of cornerpoints for $\ell_{(A,\varphi|_A)}$ or $\ell_{(B,\varphi|_B)}$ or $\ell_{(A\cap B,\varphi|_{A\cap B})}$, respectively.

These facts can easily be seen in the examples illustrated in Figures 3.4–3.5. In particular, in Figure 3.5, the size function $\ell_{(X,\varphi)}$ presents the proper cornerpoint $(-a, -b)$, which is neither a cornerpoint for $\ell_{(A,\varphi|_A)}$ nor $\ell_{(B,\varphi|_B)}$ nor $\ell_{(A\cap B,\varphi|_{A\cap B})}$. Nevertheless, its abscissa $-a$ is the abscissa of all cornerpoints for $\ell_{(A,\varphi|_A)}$, while its ordinate $-b$ is the abscissa of the cornerpoint at infinity for both $\ell_{(B,\varphi|_B)}$ and $\ell_{(A\cap B,\varphi|_{A\cap B})}$.

Theorem 3.3.3. *If $p = (\overline{u}, \overline{v}) \in \Delta^+$ is a proper cornerpoint for $\ell_{(X,\varphi)}$, then there exists at least one proper cornerpoint for $\ell_{(A,\varphi|_A)}$ or $\ell_{(B,\varphi|_B)}$ or $\ell_{(A\cap B,\varphi|_{A\cap B})}$ having $\overline{u}$ as abscissa. Moreover, if $(\overline{u}, \infty) \in \Delta^*$ is a cornerpoint at infinity for $\ell_{(X,\varphi)}$, then it is a cornerpoint at infinity for $\ell_{(A,\varphi|_A)}$ or $\ell_{(B,\varphi|_B)}$.*

Proof. As for the first assertion, we prove the contrapositive statement.

Let $\overline{u} \in \mathbb{R}$, and let us suppose that there are no proper cornerpoints for $\ell_{(A,\varphi|_A)}$, $\ell_{(B,\varphi|_B)}$ and $\ell_{(A\cap B,\varphi|_{A\cap B})}$ having $\overline{u}$ as abscissa. Then it follows that, for every $v > \overline{u}$:

$$\lim_{\varepsilon\to 0^+} \left(\ell_{(A\cap B,\varphi|_{A\cap B})}(\overline{u}+\varepsilon, v) - \ell_{(A\cap B,\varphi|_{A\cap B})}(\overline{u}-\varepsilon, v) \right) = 0,$$
$$\lim_{\varepsilon\to 0^+} \left(\ell_{(A,\varphi|_A)}(\overline{u}+\varepsilon, v) - \ell_{(A,\varphi|_A)}(\overline{u}-\varepsilon, v) \right) = 0,$$
$$\lim_{\varepsilon\to 0^+} \left(\ell_{(B,\varphi|_B)}(\overline{u}+\varepsilon, v) - \ell_{(B,\varphi|_B)}(\overline{u}-\varepsilon, v) \right) = 0.$$

Indeed, if there exists $v > \overline{u}$, such that

$$\lim_{\varepsilon\to 0^+}\Big(\ell_{(A\cap B,\varphi|_{A\cap B})}(\overline{u}+\varepsilon,v)-\ell_{(A\cap B,\varphi|_{A\cap B})}(\overline{u}-\varepsilon,v)\Big)\neq 0,$$

then $\overline{u}$ is a discontinuity point for $\ell_{(A\cap B,\varphi|_{A\cap B})}(\cdot,v)$, implying the presence of at least one proper cornerpoint having $\overline{u}$ as abscissa [36, Lemma 3]. Analogously for $\ell_{(A,\varphi|_A)}$ and $\ell_{(B,\varphi|_B)}$.

Moreover, since size functions are natural valued functions and are non-decreasing in the first variable, for every $v > \overline{u}$, there exists $\overline{\varepsilon} > 0$ small enough such that $v-\overline{\varepsilon} > \overline{u}+\overline{\varepsilon}$, and

$$\begin{aligned} 0 &= \lim_{\varepsilon\to 0^+}\Big(\ell_{(A\cap B,\varphi|_{A\cap B})}(\overline{u}+\varepsilon,v)-\ell_{(A\cap B,\varphi|_{A\cap B})}(\overline{u}-\varepsilon,v)\Big)\\ &= \ell_{(A\cap B,\varphi|_{A\cap B})}(\overline{u}+\overline{\varepsilon},v)-\ell_{(A\cap B,\varphi|_{A\cap B})}(\overline{u}-\overline{\varepsilon},v). \end{aligned}$$

So, for every $\eta < \overline{\varepsilon}$, we have $\ell_{(A\cap B,\varphi|_{A\cap B})}(\overline{u}+\eta,v) = \ell_{(A\cap B,\varphi|_{A\cap B})}(\overline{u}-\eta,v)$. This is equivalent to saying that $\mathrm{rank}\check{H}_0((A\cap B)_v) - \mathrm{rank}\check{H}_0((A\cap B)_v,(A\cap B)_{\overline{u}+\eta}) = \mathrm{rank}\check{H}_0((A\cap B)_v) - \mathrm{rank}\check{H}_0((A\cap B)_v,(A\cap B)_{\overline{u}-\eta})$, that is, $\mathrm{rank}\check{H}_0((A\cap B)_v,(A\cap B)_{\overline{u}+\eta}) = \mathrm{rank}\check{H}_0((A\cap B)_v,(A\cap B)_{\overline{u}-\eta})$. Thus, proceeding in a similar way for $\ell_{(A,\varphi|_A)}$ and $\ell_{(B,\varphi|_B)}$, we obtain $\mathrm{rank}\check{H}_0(A_v,A_{\overline{u}+\eta}) = \mathrm{rank}\check{H}_0(A_v,A_{\overline{u}-\eta})$ and $\mathrm{rank}\check{H}_0(B_v,B_{\overline{u}+\eta}) = \mathrm{rank}\check{H}_0(B_v,B_{\overline{u}-\eta})$. Now, observing that, by the conditions on v, the same results shown above also hold taking $v+\eta$ or $v-\eta$ in place of v for every $\eta < \varepsilon$, let us consider the following diagram:

$$\begin{array}{ccc} \check{H}_0((A\cap B)_{v-\eta},(A\cap B)_{\overline{u}-\eta}) & \xrightarrow{\alpha_{v-\eta,\overline{u}-\eta}} & \check{H}_0(A_{v-\eta},A_{\overline{u}-\eta})\oplus\check{H}_0(B_{v-\eta},B_{\overline{u}-\eta}) \\ \downarrow{\scriptstyle j_1} & & {\scriptstyle j_2}\downarrow \\ \check{H}_0((A\cap B)_{v-\eta},(A\cap B)_{\overline{u}+\eta}) & \xrightarrow{\alpha_{v-\eta,\overline{u}+\eta}} & \check{H}_0(A_{v-\eta},A_{\overline{u}+\eta})\oplus\check{H}_0(B_{v-\eta},B_{\overline{u}+\eta}), \end{array}$$

where the homomorphisms j_1 and j_2 are induced by inclusions. Since they are surjective and their respective domain and codomain have the same rank, we deduce that j_1 and j_2 are isomorphisms. So, we obtain that $\ker\alpha_{v-\eta,\overline{u}-\eta} \simeq \ker\alpha_{v-\eta,\overline{u}+\eta}$.

Analogously, from the diagram

$$\begin{array}{ccc} \check{H}_0((A\cap B)_{v+\eta},(A\cap B)_{\overline{u}-\eta}) & \xrightarrow{\alpha_{v+\eta,\overline{u}-\eta}} & \check{H}_0(A_{v+\eta},A_{\overline{u}-\eta})\oplus\check{H}_0(B_{v+\eta},B_{\overline{u}-\eta}) \\ \downarrow{\scriptstyle k_1} & & {\scriptstyle k_2}\downarrow \\ \check{H}_0((A\cap B)_{v+\eta},(A\cap B)_{\overline{u}+\eta}) & \xrightarrow{\alpha_{v+\eta,\overline{u}+\eta}} & \check{H}_0(A_{v+\eta},A_{\overline{u}+\eta})\oplus\check{H}_0(B_{v+\eta},B_{\overline{u}+\eta}), \end{array}$$

we can deduce that $\ker \alpha_{v+\eta,\overline{u}-\eta} \simeq \ker \alpha_{v+\eta,\overline{u}+\eta}$. Thus, since η can be chosen arbitrarily small, it follows that

$$\lim_{\eta\to 0^+}\left(\ker \alpha_{v-\eta,\overline{u}-\eta} - \ker \alpha_{v-\eta,\overline{u}+\eta}\right) = 0,$$
$$\lim_{\eta\to 0^+}\left(\ker \alpha_{v+\eta,\overline{u}-\eta} - \ker \alpha_{v+\eta,\overline{u}+\eta}\right) = 0.$$

Therefore, applying Proposition 3.3.1, we have

$$\mu_X(p) - \mu_A(p) - \mu_B(p) + \mu_{A\cap B}(p) = 0$$

and, in particular, by the hypothesis that $p = (\overline{u}, v)$ is not a proper cornerpoint for $\ell_{(A\cap B,\varphi|_{A\cap B})}$, or $\ell_{(A,\varphi|_A)}$, or $\ell_{(B,\varphi|_B)}$ for any $v > \overline{u}$, it holds that $\mu_X(p) = 0$.

In the case of cornerpoints at infinity, we observe that, if $(\overline{u},\infty)$ is a cornerpoint at infinity for $\ell_{(X,\varphi)}$, then $\overline{u} = \min_{P\in C}\varphi(P)$, for at least one connected component C of X [36, Prop. 9]. Furthermore, since $X = A\cup B$, it follows that $\overline{u} = \min_{P\in C\cap A}\varphi_{|A}(P)$ or $\overline{u} = \min_{P\in C\cap B}\varphi_{|B}(P)$, from which (by [36, Prop. 9]), $(\overline{u},\infty)$ is shown to be a cornerpoint at infinity for $\ell_{(A,\varphi|_A)}$ or $\ell_{(B,\varphi|_B)}$. □

Theorem 3.3.4. *If $p = (\overline{u},\overline{v}) \in \Delta^+$ is a proper cornerpoint for $\ell_{(X,\varphi)}$, then $\overline{v}$ is a homological 0-critical value for $(A,\varphi_{|A})$ or $(B,\varphi_{|B})$ or $(A\cap B,\varphi_{|A\cap B})$. Furthermore, if there exists at most a finite number of homological 0-critical values for $(A,\varphi_{|A})$, $(B,\varphi_{|B})$, and $(A\cap B,\varphi_{|A\cap B})$, then $\overline{v}$ is the abscissa of a cornerpoint (proper or at infinity) or the ordinate of a proper cornerpoint for $\ell_{(A,\varphi|_A)}$ or $\ell_{(B,\varphi|_B)}$ or $\ell_{(A\cap B,\varphi|_{A\cap B})}$.*

Proof. Regarding the first assertion, we prove the contrapositive statement.

Let $\overline{v} \in \mathbb{R}$, and let us suppose that $\overline{v}$ is not a homological 0-critical value for the size pairs $(A,\varphi_{|A})$, $(B,\varphi_{|B})$ and $(A\cap B,\varphi_{|A\cap B})$. Then, by Definition 3.3, for every $\overline{\varepsilon} > 0$, there exists ε with $0 < \varepsilon < \overline{\varepsilon}$, such that the vertical homomorphisms h and k induced by inclusions in the following commutative diagram

$$\begin{array}{ccccccccc}
\cdots \longrightarrow & \check{H}_0((A\cap B)_{\overline{v}-\varepsilon}) & \longrightarrow & \check{H}_0(A_{\overline{v}-\varepsilon})\oplus \check{H}_0(B_{\overline{v}-\varepsilon}) & \longrightarrow & \check{H}_0(X_{\overline{v}-\varepsilon}) & \longrightarrow & 0 \\
 & \downarrow h & & \downarrow k & & \downarrow \iota_0^{\overline{v}-\varepsilon,\overline{v}+\varepsilon} & & \downarrow 0 \\
\cdots \longrightarrow & \check{H}_0((A\cap B)_{\overline{v}+\varepsilon}) & \longrightarrow & \check{H}_0(A_{\overline{v}+\varepsilon})\oplus \check{H}_0(B_{\overline{v}+\varepsilon}) & \longrightarrow & \check{H}_0(X_{\overline{v}+\varepsilon}) & \longrightarrow & 0
\end{array}$$

are isomorphisms. Hence, using the Five Lemma, we can deduce that also $\iota_0^{\overline{v}-\varepsilon,\overline{v}+\varepsilon}$ is an isomorphism, implying that $\overline{v}$ is not a homological 0-critical value for (X,φ).

Consequently, from Proposition 3.1.6, $\lim_{\varepsilon\to 0^+}\Big(\ell_{(X,\varphi)}(u,\bar{v}-\varepsilon)-\ell_{(X,\varphi)}(u,\bar{v}+\varepsilon)\Big)=0$, for every $u<\bar{v}$. Hence, it follows that, choosing $u=\bar{u}-\varepsilon$, $\lim_{\varepsilon\to 0^+}\Big(\ell_{(X,\varphi)}(\bar{u}-\varepsilon,\bar{v}-\varepsilon)-\ell_{(X,\varphi)}(\bar{u}-\varepsilon,\bar{v}+\varepsilon)\Big)=0$, and $\lim_{\varepsilon\to 0^+}\Big(\ell_{(X,\varphi)}(\bar{u}+\varepsilon,\bar{v}-\varepsilon)-\ell_{(X,\varphi)}(\bar{u}+\varepsilon,\bar{v}+\varepsilon)\Big)=0$, choosing $u=\bar{u}+\varepsilon$. Therefore, by Definition 1.4, we obtain $\mu_X(p)=0$.

Now, let us proceed with the proof of the second statement, assuming that $\bar{v}$ is a homological 0-critical value for $(A,\varphi_{|A})$. It is analogous for $(B,\varphi_{|B})$ and $(A\cap B,\varphi_{|A\cap B})$. For such a $\bar{v}$, by Definition 3.3, it holds that, for every sufficiently small $\varepsilon>0$, $\iota_0^{\bar{v}-\varepsilon,\bar{v}+\varepsilon}:\check{H}_0(A_{\bar{v}-\varepsilon})\to\check{H}_0(A_{\bar{v}+\varepsilon})$ is not an isomorphism. In particular, if $\iota_0^{\bar{v}-\varepsilon,\bar{v}+\varepsilon}$ is not surjective for any sufficiently small $\varepsilon>0$, then, by Proposition 3.1.7 *(i)*, there exists $v>\bar{v}$, such that $\bar{v}$ is a discontinuity point for $\ell_{(A,\varphi_{|A})}(\cdot,v)$. This condition necessarily implies the existence of a cornerpoint (proper or at infinity) for $\ell_{(A,\varphi_{|A})}$, having $\bar{v}$ as abscissa [36, Lemma 3].

On the other hand, if $\iota_0^{\bar{v}-\varepsilon,\bar{v}+\varepsilon}$ is surjective for every sufficiently small $\varepsilon>0$, then, by Proposition 3.1.7 *(ii)*, there exists $u<\bar{v}$ such that $\bar{v}$ is a discontinuity point for $\ell_{(A,\varphi_{|A})}(u,\cdot)$. This condition necessarily implies the existence of a proper cornerpoint for $\ell_{(A,\varphi_{|A})}$, having $\bar{v}$ as ordinate [36, Lemma 3]. □

3.4 Experimental results

In this section we are going to describe the results we have achieved in some preliminary experiments concerning the analysis of size functions behavior under partial occlusions.

Psychophysical observations indicate that human and monkey perception of partially occluded shapes changes according to whether, or not, the occluding pattern is visible to the observer, and whether the occluded shape is a filled figure or an outline [49]. In particular, discrimination performance is higher for filled shapes than for outlines, and in both cases it significantly improves when shapes are occluded by a visible rather than invisible object.

In computer vision experiments, researchers usually work with invisible occluding patterns, both on outlines (see, e.g., [15, 40, 53, 55, 56]) and on filled shapes (see, e.g.,

[43]).

In order to analyze the potential of our approach in the recognition of occluded shapes, we have considered both visible and invisible occlusions. To perform our tests we have worked with filled images from the MPEG-7 dataset [52]. In all the experiments, the occluding pattern is a rectangular shape occluding from the top, or the left, by an area we increasingly vary from 10% to 60% of the height or width of the bounding box of the original shape. For both the original shapes and the occluded ones, size functions are always computed with respect to a family of eight measuring functions having only the set of black pixels as domain. They are defined as follows: four of them as the distance from the line passing through the origin (top left point of the bounding box), rotated by an angle of 0, $\frac{\pi}{4}$, $\frac{\pi}{2}$ and $\frac{3\pi}{4}$ radians, respectively, with respect to the horizontal position; the other four as minus the distance from the same lines, respectively. This family of measuring functions is chosen only for demonstrative purposes, since the associated size functions are simple in terms of the number of cornerpoints, but, at the same time, non-trivial in terms of shape information.

3.4.1 Visible occlusions

In the case of visible occlusions, with reference to the notation used in our theoretical setting, we are considering A as the original shape, B as a black rectangle, and X as the occluded shape generated by their union.

The first experiment aims to show how a trace of the size function describing the shape of an object is contained in the size function related to the occluded shape when the occluding pattern is visible. In order to do that, we work with 70 filled images, each chosen from a different class of the MPEG-7 dataset (see Table 3.1).

In Table 3.2, for different levels of occlusion, each 3D bar chart displays, along the z-axis, the percentage of common cornerpoints between the set of size functions associated with the 70 occluded shapes (x-axis), and the set of size functions associated with the 70 original ones (y-axis). Note that, for each occluded shape, the highest bar is always on the diagonal, that is, where the occluded object is compared with the corresponding original one.

Three particular instances of our dataset images are shown in Tables 3.3–3.5 (first

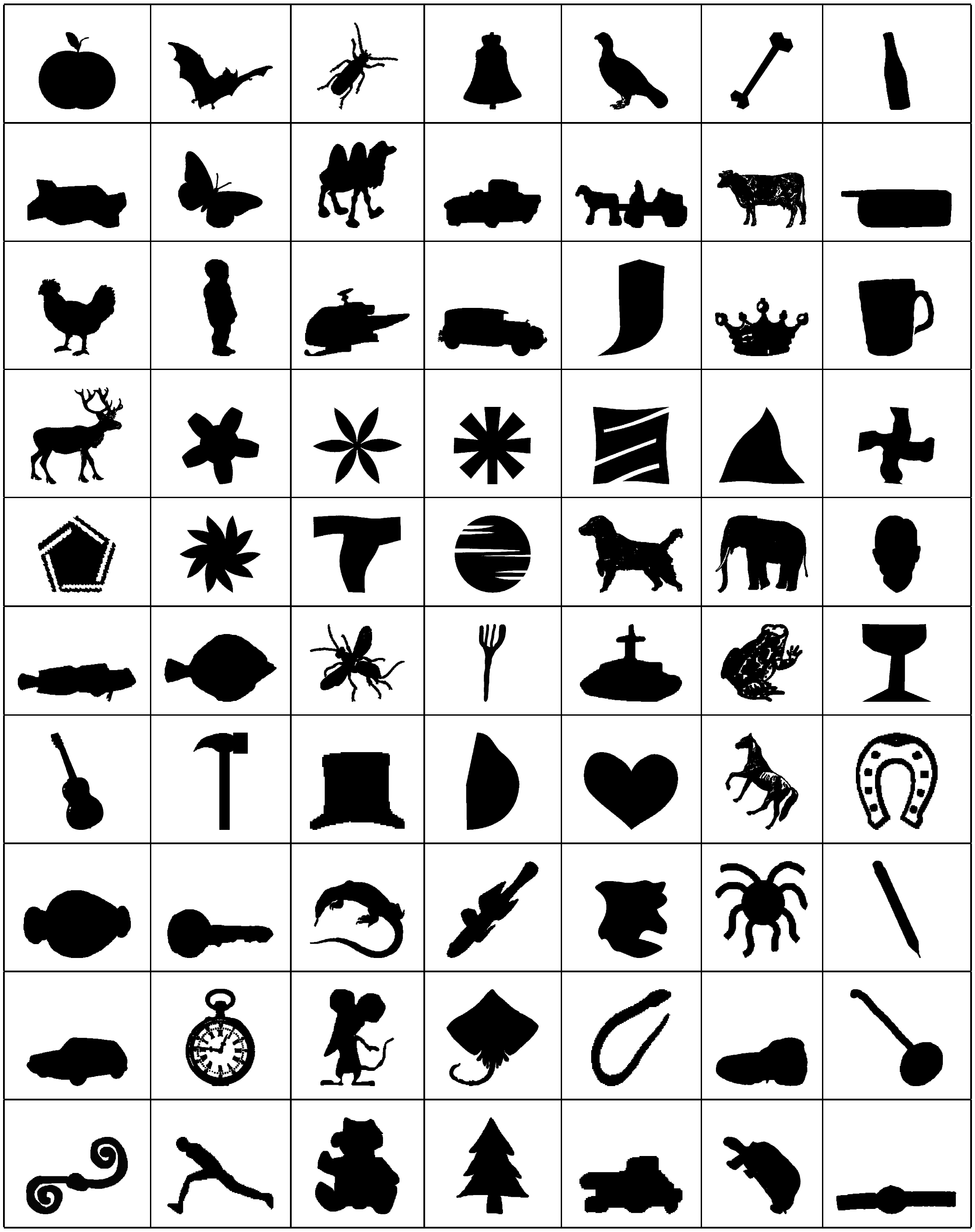

Table 3.1: The training set used in our experiment described in Table 3.2, involving visible occlusions, and in all the experiments with invisible occlusions: 70 images, each one belonging to a different class of the MPEG-7 dataset.

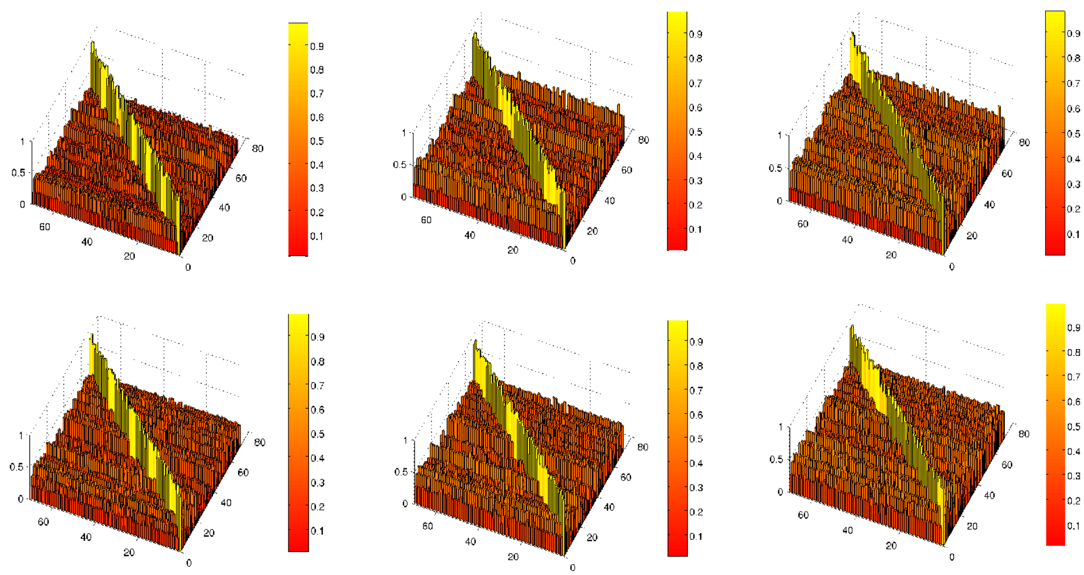

Table 3.2: 3D bar charts displaying, in the case of visible occlusions, the percentage of common corner-points (z-axis) between the 70 occluded shapes (x-axis) and the 70 original ones (y-axis) correspondingly ordered. First row: Shapes are occluded from top by 20% (column 1), by 40% (column 2), by 60% (column 3). Second row: Shapes are occluded from the left by 20% (column 1), by 40% (column 2), by 60% (column 3).

column) with their size functions with respect to the second group of four measuring functions (the next-to-last column). The chosen images are characterized by different homological features, which will be changed in the presence of occlusion. For example, the “camel” in Table 3.3 is a connected shape without holes, but the first homological group may turn out non-trivial because of the occlusion (see second row, first column). On the other hand, Table 3.4 shows a “frog”, which is a connected shape with several holes. The different percentages of occlusion can create some new holes or destroy them (see rows 3–4). Finally, the “pocket watch”, represented in Table 3.5, is primarily characterized by several connected components, whose number decreases as the occluding area increases. This results in a reduction of the number of cornerpoints at infinity in its size functions. In spite of these topological changes, it can easily be seen that, given a measuring function, even if the size function related to a shape and the size function related to the occluded shape are defined by different cornerpoints, because of occlusion, a common subset of these is present, making a partial matching possible between them. This result raises a question: what does happen when a shape is not only occluded, but also deformed?

It has to be expected that, in a situation characterized by the presence of both occlusions and deformations, it will not be possible to find a common subset of cornerpoints between the original shape and the occluded one, since the deformation has slightly changed the cornerpoints position.

As an example, in Table 3.6 (row 3, from left to right) a “device1” shape is depicted with four of its eight size functions. By comparison with the size functions of the same shape occluded from the top (row 1), or from the left (row 2), with respect to the same measuring functions, it is easily seen that they present common substructures, since some cornerpoints are preserved after occlusions. In the first column, rows 4–5, two different instances of “device1” are illustrated, and can be considered as perturbations of the shape in row 3; the respective size functions present similar structures if compared with those associated with the shape in row 3.

To test the behavior of size functions when both occlusions and deformations are introduced, we perform a retrieval test with a training set consisting of 75 images: three instances chosen from 25 different classes. The test set contains 25 occluded images,

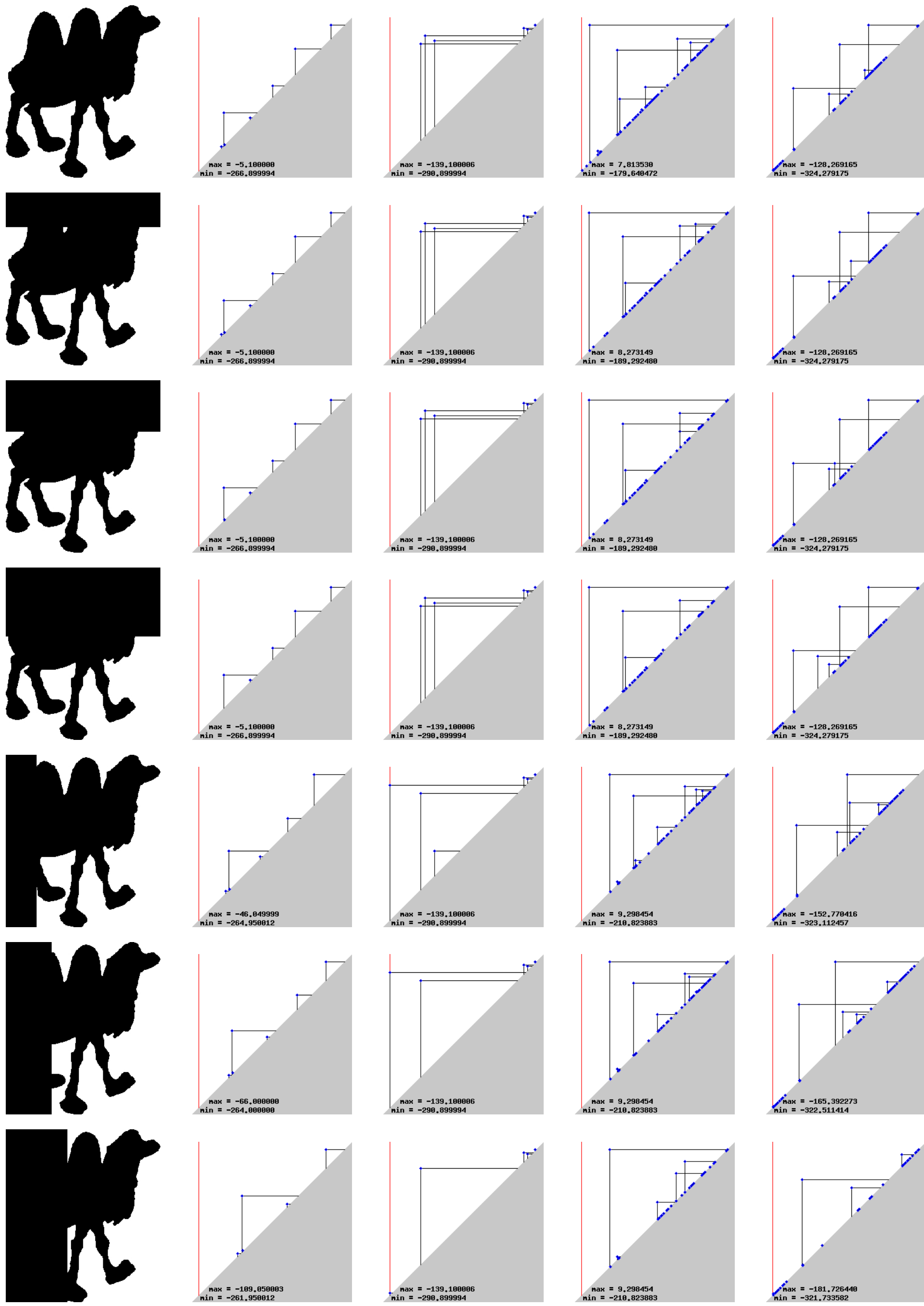

Table 3.3: The first column: (row 1) original “camel” shape, (rows 2–4) occluded from top by 20%, 30%, 40%, (row 5–7) occluded from left by 20%, 30%, 40%. From second column onwards: corresponding size functions related to measuring functions defined as minus distances from four lines rotated by 0, $\pi/4$, $\pi/2$, $3\pi/4$, with respect to the horizontal position.

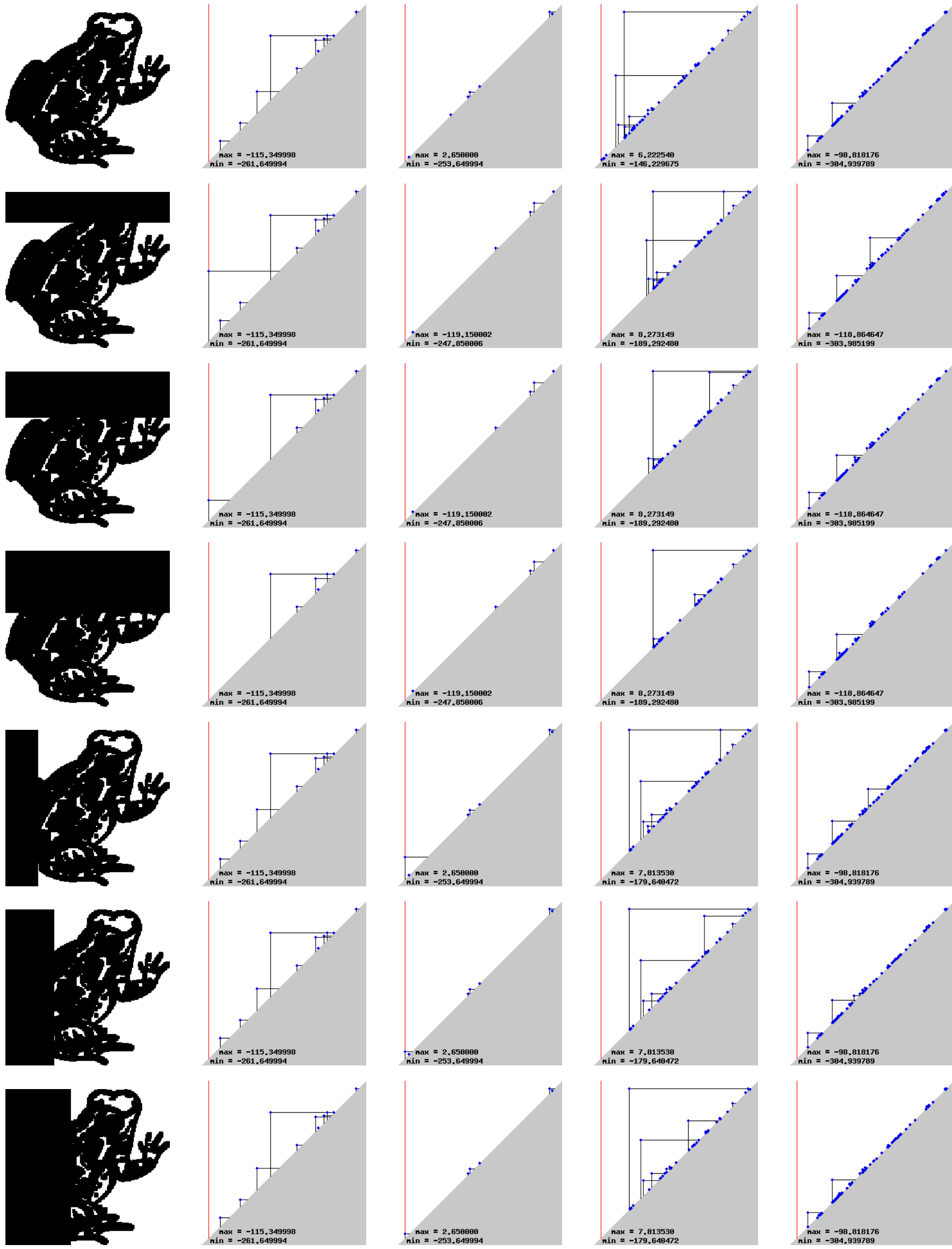

Table 3.4: The first column: (row 1) original “frog” shape, (rows 2–4) occluded from top by 20%, 30%, 40%, (row 5–7) occluded from left by 20%, 30%, 40%. From second column onwards: corresponding size functions related to measuring functions defined as minus distances from four lines rotated by 0, $\pi/4$, $\pi/2$, $3\pi/4$, with respect to the horizontal position.

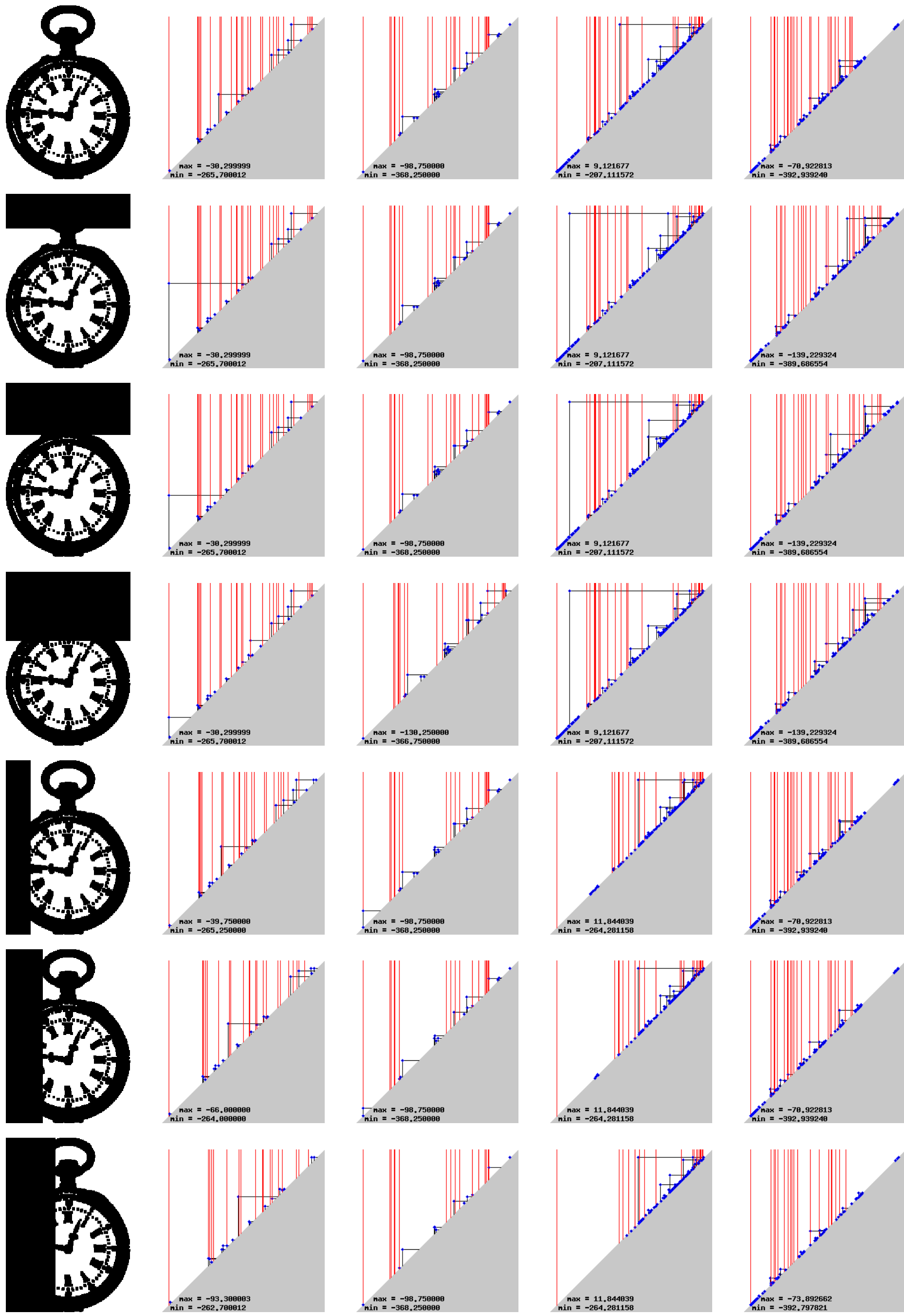

Table 3.5: The first column: (row 1) original “pocket watch” shape, (rows 2–4) occluded from top by 20%, 30%, 40%, (row 5–7) occluded from left by 20%, 30%, 40%. From second column onwards: corresponding size functions related to measuring functions defined as minus distances from four lines rotated by 0, $\pi/4$, $\pi/2$, $3\pi/4$, with respect to the horizontal position.

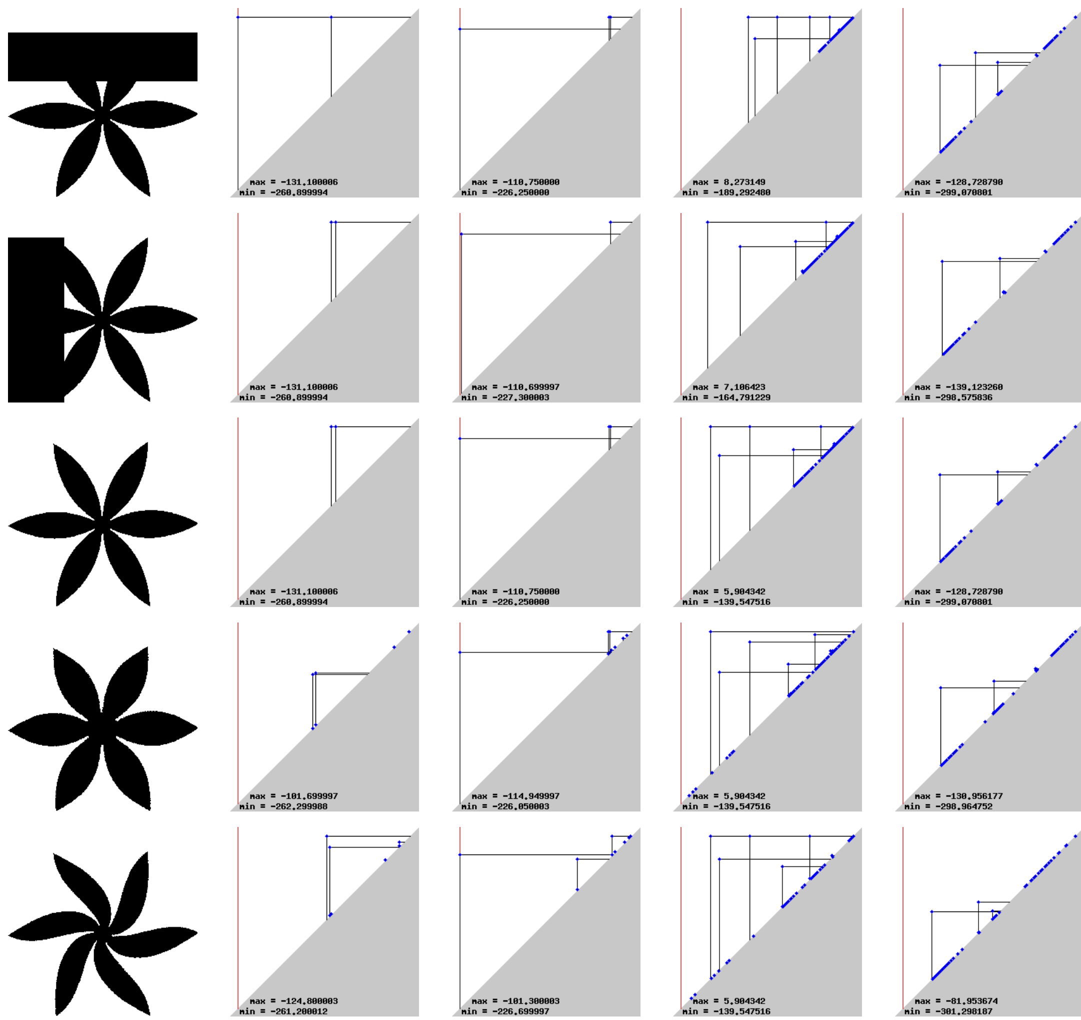

Table 3.6: Column 1: in rows 3–5, three “device1” shapes; in rows 1–2, the same “device1” shape depicted in row 3, occluded from the top and from the left, respectively. Columns 2–4: corresponding size functions related to measuring functions defined as minus distances from four lines rotated by 0, $\pi/4$, $\pi/2$, $3\pi/4$, with respect to the horizontal position.

each taken from a different class. Each of them is taken as a query and is matched with all the images in the training set. Comparison is performed by calculating the sum of the eight Hausdorff distances between the sets of cornerpoints for the size functions associated with the corresponding eight measuring functions. The retrieval is evaluated using the *Bull's Eye Performance* (BEP) criterion. The BEP is measured by computing the correct retrievals among the top $2N$ retrievals, where N is the number of relevant (or similar) shapes to the query in the database. The effect of an increasing occlusion by an horizontal rectangle (vertical, respectively) on the retrieval performance is described by the graph in Table 3.7 (a) ((b), respectively).

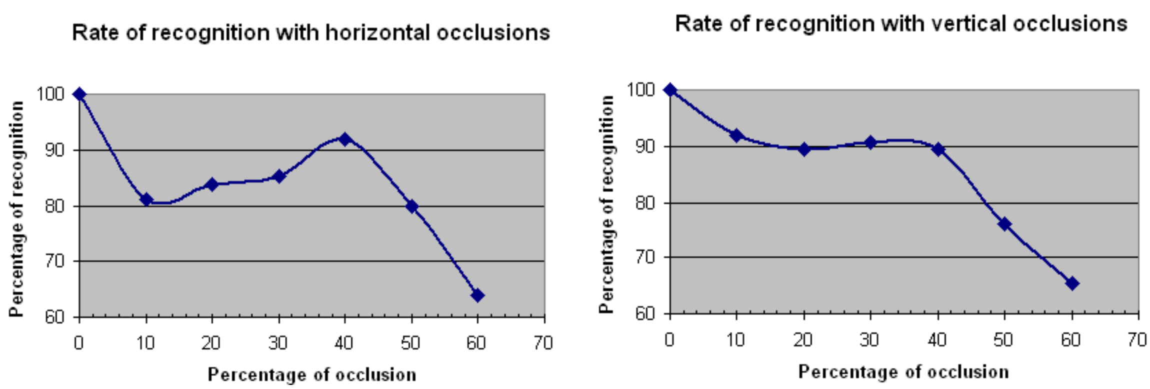

(a) (b)

Table 3.7: Two graphs describing the variation of retrieval performance when the occlusion area increases from the left (a) and from the top (b).

The atypical trend of the above graphs may be explained looking at Table 3.8, where examples of query tests, with an incremental percentage of occluded area from the left are illustrated. As it can be observed, when a low percentage of the "dog" is hidden by the black rectangle, the occluded dog looks more similar to an elephant than to a dog. Indeed, there the rectangle is seen as a shape feature (a proboscis) rather than an occluding pattern. In general, this fact improves the results in correspondence of higher percentage of occlusion (30–40%) than when the percentage of occlusion is low (10–20%).

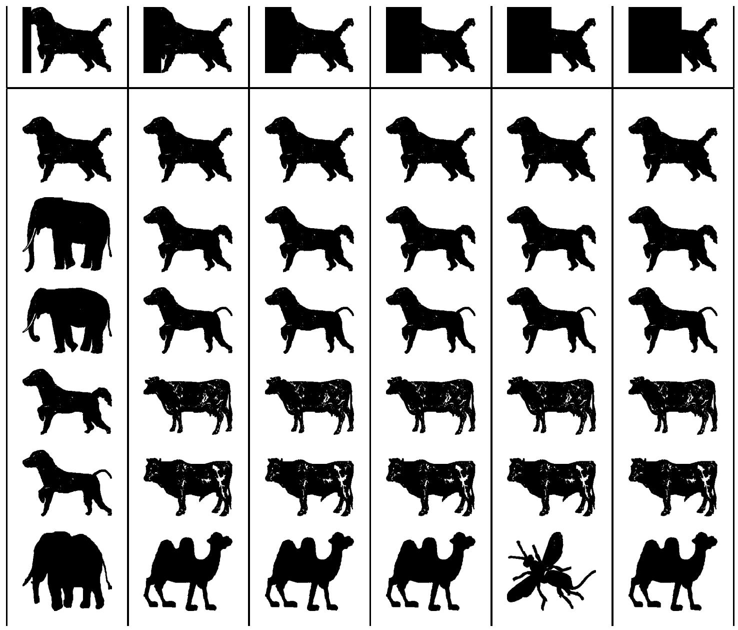

Table 3.8: Top retrieval results for a "dog" shape partially occluded from the left. Results are depicted in every column in increasing order of distance from the query.

3.4.2 Invisible occlusions

When invisible occluding patterns are considered, with reference to the notation used in our theoretical setting, we take X as the original shape, A as the the occluded shape, and B as the invisible part of X. In this case, using again the database shown in Table 3.1, a comparison between cornerpoints of size functions, analogous to that of Table 3.2, has been performed and the results are exhibited in Table 3.9. The percentages of occlusion, from the top (first row) and from the left (second row), here vary from 20 to 40 (columns 1–3).

Moreover, we have also performed a recognition test for occluded shapes by comparison of size functions. By varying the amount of occluded area, we compare each occluded shape with each of the 70 original shapes. Comparison is performed by calculating the sum of the eight Hausdorff distances between the sets of cornerpoints for the size functions associated with the corresponding eight measuring functions. Then each occluded shape is assigned to the class of its nearest neighbor among the original

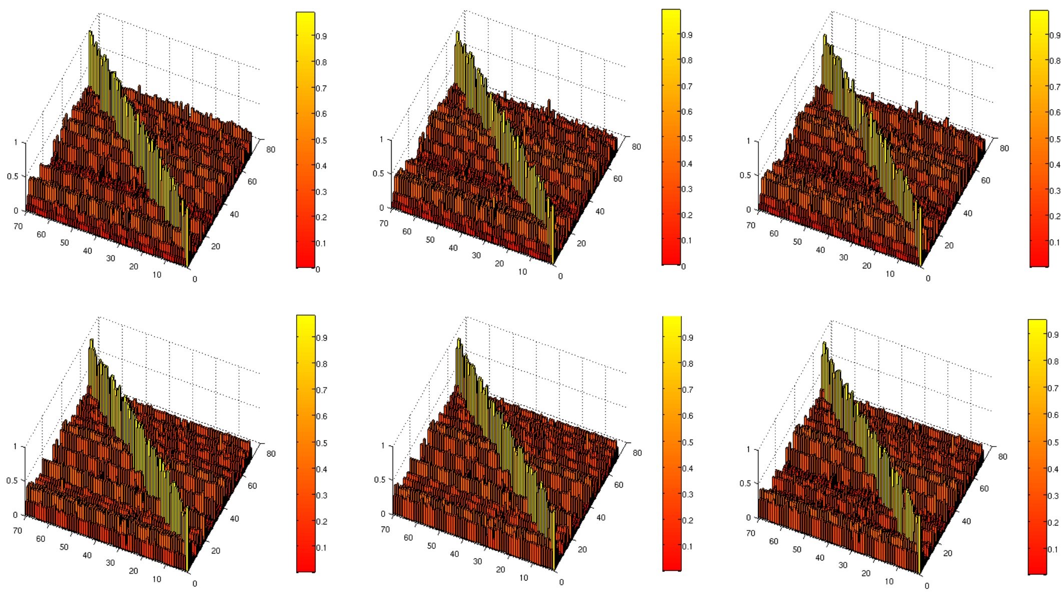

Table 3.9: 3D bar charts displaying, in the case of invisible occlusions, the percentage of common cornerpoints (z-axis) between 70 occluded shapes (y-axis) and the 70 original ones (x-axis) correspondingly ordered. First row: Shapes are occluded from top by 20% (column 1), by 30% (column 2), by 40% (column 3). Second row: Shapes are occluded from the left by 20% (column 1), by 30% (column 2), by 40% (column 3).

shapes. Comparison through the Hausdorff distance is computed under the following convention. When the original shape is disconnected by the occlusion, we retain only the connected component of greatest area (see some instances in Table 3.10). This choice allows us to obtain always a finite Hausdorff distance, but determines a high loss of shape information even when the percentage of occlusion is low.

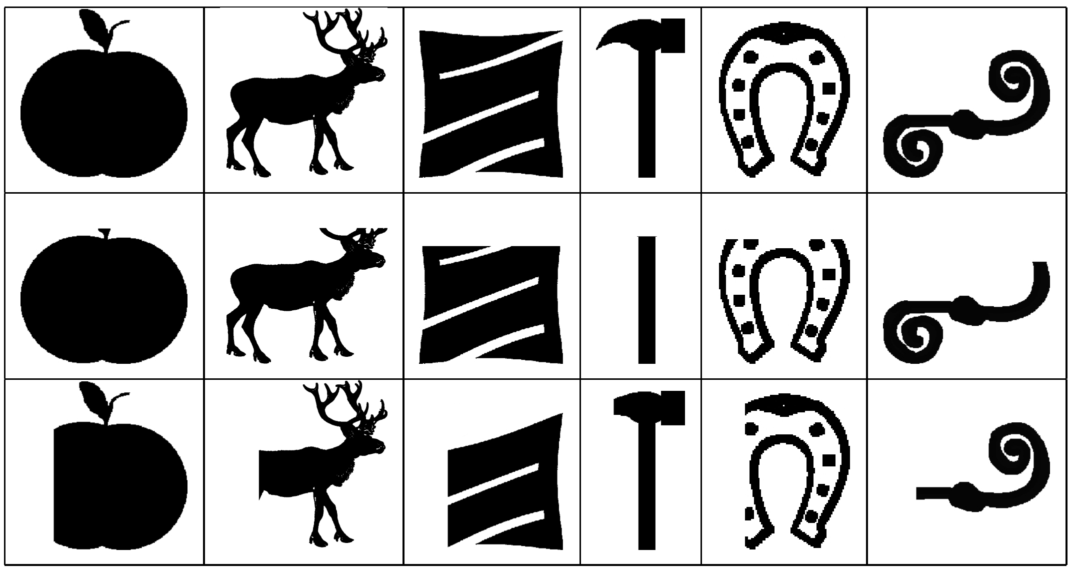

Table 3.10: The first row: some instances from the MPEG-7 dataset; the second and third rows: by 20% occluded from the top and from the left, respectively.

In Table 3.11, two graphs describe the rate of correct recognition in the presence of an increasing percentage of invisible occlusion. The leftmost graph is related to the occlusion from the top, the rightmost one is related to the same occlusion from the left.

3.5 Discussion

The main contribution of this part of our research work is the analysis of the behavior of size functions in the presence of occlusions.

Specifically we have proved that size functions can assess a partial matching between shapes by showing common subsets of cornerpoints. Therefore, using size functions, recognizing a shape which is partially occluded by a foreground shape, becomes an easy task. Indeed, recognition is achieved simply by associating with the occluded shape

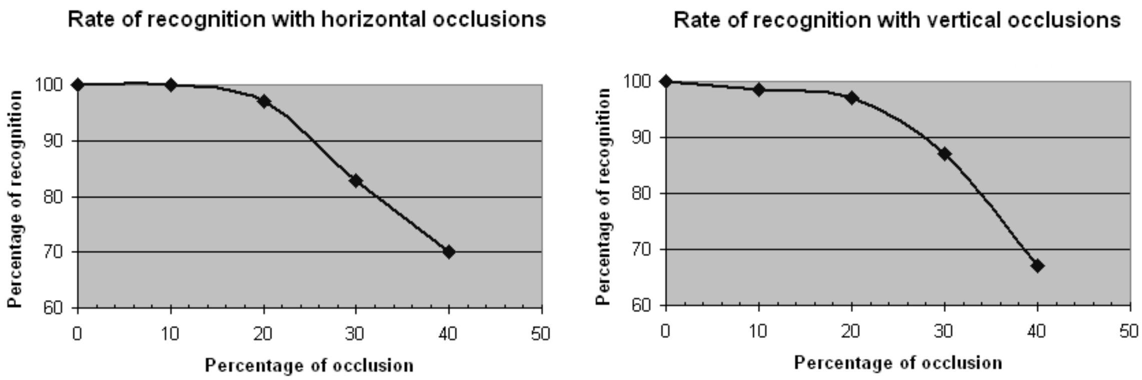

Table 3.11: The leftmost (rightmost, respectively) graph describes the recognition trend when the occluded area from the top (left, respectively) increases.

that form whose size function presents the largest common subset of cornerpoints (as in the experiments in Table 3.2–3.9). The experimental results show that this method is effective both with visible and invisible occlusions.

In practice, however, shapes may undergo other deformations due to e.g. perspective, articulations, noise. As a consequence of these alterations, cornerpoints may move. Anyway, small continuous changes in shape induce small displacements in cornerpoints configuration. However, when deformations are added to occlusions, the Hausdorff distance between size functions seems not robust enough for recognition or retrieval tasks. The reason is that it works globally on the whole set of cornerpoints and therefore it is not able to detect substructures. As a consequence, an important open question is how to automatically detect similar substructures in size functions when cornerpoints can be distorted. This question will be addressed in a future research combining the results shown here with the polynomial representation of size functions [31].

Conclusions and future work

This thesis illustrates the main results on shape-from-functions methods obtained during my Ph. D study.

Summarizing, we have shown an approach to the problem of multidimensional Persistent Homology Theory, alternative to that given in [12].

Our strategy is based on the idea to reduce the computation of a multidimensional persistent homology module to the 1-dimensional setting by partitioning into half-planes the domain of the associated rank invariant. This procedure leads to the definition of a stable bottleneck distance between multidimensional rank invariants, D_B, as the supremum, over all admissible vector pairs, of the bottleneck distances between 1-dimensional rank invariants, d_B. Eventually, it has been proved that D_B has a higher discriminatory power than d_B, verifying that the former constitutes a better lower bound for the natural pseudo-distance than the latter.

In Section 2.5, we have discussed some questions arisen from our investigation in multidimensional Persistent Homology Theory, while, at the present time, our short term goal is to weaken the conditions imposed on the pair $(X, \vec{\varphi})$. To be more precise, we are looking for analogous results that involve triangulable spaces endowed with continuous multi-valued functions, instead of max-tame size pairs.

Furthermore, we have exposed a theoretical construction based on Mayer-Vietoris sequences of Čech homology groups to prove the robustness of size functions against occlusions.

The relation among the size functions associated with an occluded object, the original object and the occluding pattern proved in this thesis, respectively, endowed with the same measuring function, can be translated into a relation among their cornerpoints.

In particular, we have proved that, in general, under occlusion, the coordinates of cornerpoints are maintained; in addition, a subset of cornerpoints is preserved if and only if an algebraic condition holds. Various experiments, involving both visible and invisible occlusions, confirm our theoretical results.

In this setting, the only remaining crucial point concerns the behavior of size functions when both occlusions and deformations alter the description of a shape. A strategy planned to tackle this problem is to represent a size function as a complex polynomial whose roots are the cornerpoints counted with multiplicities [31]. In this way, a small perturbation in a shape can be translated into a small variation of the roots of the polynomial.

Finally, with regard to further developments in the field of shape-from-functions methods, our present research is concentrated on another kind of shape descriptor: the Reeb graph.

Reeb graphs are very popular shape descriptors in computational frameworks, especially in applications such as 3D shape matching, shape coding and comparison. Today, even if, in experimental results, they have shown themselves to be stable under small perturbations of mapping functions, theoretical results proving this stability with respect to a suitable distance are not yet available. Our purpose is to define such a metric to enhance the theory beside these topological graphs.

Appendix

A A brief review on Čech homology

In this description of Čech homology theory, we follow [42].

Given a compact Hausdorff space X, let $\Sigma(X)$ denote the family of all finite coverings of X by open sets. The coverings in $\Sigma(X)$ will be denoted by script letters $\mathcal{U}$, $\mathcal{V}$, $\ldots$ and the open sets in a covering by italic capitals U, V, $\ldots$ An element $\mathcal{U}$ of $\Sigma(X)$ may be considered as a simplicial complex if we define *vertex* to mean *open set U in* $\mathcal{U}$ and agree that a subcollection $U_0, \ldots, U_k$ of such vertices constitutes a k-simplex if and only if the intersection $\bigcap_{i=0}^{k} U_i$ is not empty. The resulting complex is known as the *nerve of the covering* $\mathcal{U}$.

Given a covering $\mathcal{U}$ in $\Sigma(X)$, we may define the chain groups $C_k(\mathcal{U}, G)$, the cycle groups $Z_k(\mathcal{U}, G)$, the boundary groups $B_k(\mathcal{U}, G)$, and the homology groups $H_k(\mathcal{U}, G)$.

The collection $\Sigma(X)$ of finite open coverings of a space X may be partially ordered by refinement. A covering $\mathcal{V}$ refines the covering $\mathcal{U}$, and we write $\mathcal{U} < \mathcal{V}$, if every element of $\mathcal{V}$ is contained in some element of $\mathcal{U}$. It turns out that $\Sigma(X)$ is a direct set under refinement.

If $\mathcal{U} < \mathcal{V}$ in $\Sigma(X)$, then there is a simplicial mapping $\pi_{\mathcal{U}\mathcal{V}}$ of $\mathcal{V}$ into $\mathcal{U}$ called a *projection*. This is defined by taking $\pi_{\mathcal{U}\mathcal{V}}(V)$, $V \in \mathcal{V}$, to be any (fixed) element U of $\mathcal{U}$ such that V is contained in U. There may be many projections of $\mathcal{V}$ into $\mathcal{U}$. Each projection $\pi_{\mathcal{U}\mathcal{V}}$ induces a chain mapping of $C_k(\mathcal{V}, G)$ into $C_k(\mathcal{U}, G)$, still denoted by $\pi_{\mathcal{U}\mathcal{V}}$, and this in turn induces homomorphisms ${}_*\pi_{\mathcal{U}\mathcal{V}}$ of $H_k(\mathcal{V}, G)$ into $H_k(\mathcal{U}, G)$. If $\mathcal{U} < \mathcal{V}$ in $\Sigma(X)$, then it can be proved that any two projections of $\mathcal{V}$ into $\mathcal{U}$ induce the same homomorphism of $H_k(\mathcal{V}, G)$ into $H_k(\mathcal{U}, G)$.

Now we are ready to define a Čech cycle. A *k-dimensional Čech cycle* of the space X is a collection $z_k = \{z_k(\mathcal{U})\}$ of k-cycles $z_k(\mathcal{U})$, one for each and every cycle group $Z_k(\mathcal{U},G)$, $\mathcal{U} \in \Sigma(X)$, with the property that if $\mathcal{U} < \mathcal{V}$, then $\pi_{\mathcal{U}\mathcal{V}} z_k(\mathcal{V})$ is homologous to $z_k(\mathcal{U})$. Each cycle $z_k(\mathcal{U})$ in the collection z_k is called a *coordinate of the Čech cycle.* Hence a Čech cycle has a coordinate on every covering of the space X. The addition of Čech cycles is defined by setting $\{z_k(\mathcal{U})\} + \{z'_k(\mathcal{U})\} = \{z_k(\mathcal{U}) + z'_k(\mathcal{U})\}$. The homology relation is defined as follows. A Čech cycle $z_k = \{z_k(\mathcal{U})\}$ is homologous to zero (or is a *bounding Čech cycle*) if each coordinate $z_k(\mathcal{U})$ is homologous to zero on the covering $\mathcal{U}$, for all $\mathcal{U}$ in $\Sigma(X)$. Then two Čech cycles z_k and z'_k are *homologous Čech cycles* if their difference $z_k - z'_k$ is homologous to zero. This homology relation is an equivalence relation. The corresponding equivalence classes $[z_k]$ are the elements of the *kth Čech homology group* $\check{H}(X,G)$, where $[z_k] + [z'_k] = [z_k + z'_k]$.

Let us now see how continuous mappings between spaces induce homomorphisms on Čech homology groups. Let $f : X \to Y$ be a continuous mapping of X into Y, where both X and Y are compact Hausdorff spaces. Then each open covering $\mathcal{U} \in \Sigma(Y)$ can be associated with an open covering $f^{-1}(\mathcal{U}) \in \Sigma(X)$. In particular, we may define a simplicial mapping $f_{\mathcal{U}}$ of $f^{-1}(\mathcal{U})$ into $\mathcal{U}$ by setting $f_{\mathcal{U}}(f^{-1}(U)) = U$ for each non-empty set $f^{-1}(U), U \in \mathcal{U}$. If $\mathcal{U} < \mathcal{V}$, then the maps $f_{\mathcal{U}}$ and $f_{\mathcal{V}}$ commute with the projection of $f^{-1}(\mathcal{V})$ into $f^{-1}(\mathcal{U})$ and the projection of $\mathcal{V}$ into $\mathcal{U}$. Now we can define the *homomorphism induced by the continuous mapping* f as the map $f_* : \check{H}_k(X,G) \to \check{H}_k(Y,G)$ by setting, for every $z_k \in \check{H}_k(X,G)$, $f_*(z_k) = \{f_{\mathcal{U}}(z_k(f^{-1}(\mathcal{U}))\}$.

It is also possible to define relative Čech cycles in the following way. If A is a closed subset of X, we say that a *simplex* $\langle U_0, \ldots, U_k \rangle$ of $\mathcal{U} \in \Sigma(X)$ is *on* A if and only if the intersection $\bigcap_{i=0}^{k} U_i$ meets A. The collection of all simplexes of $\mathcal{U}$ on A is a closed subcomplex $\mathcal{U}_A$ of $\mathcal{U}$. Therefore, we may consider the relative simplicial groups $H_k(\mathcal{U},\mathcal{U}_A,G)$ over a coefficient group G. Since for $\mathcal{V} > \mathcal{U}$ in $\Sigma(X)$, the projection $\pi_{\mathcal{U}\mathcal{V}}$ of $\mathcal{V}$ into $\mathcal{U}$ projects $\mathcal{V}_A$ into $\mathcal{U}_A$, each projection $\pi_{\mathcal{U}\mathcal{V}}$ is a simplicial mapping of the pair $(\mathcal{V},\mathcal{V}_A)$ into the pair $(\mathcal{U},\mathcal{U}_A)$. We may define a *k-dimensional Čech cycle* of the space X *relative to* A as a collection $z_k = \{z_k(\mathcal{U})\}$ of k-chains $z_k(\mathcal{U})$, $\mathcal{U} \in \Sigma(X)$, with the property that $z_k(\mathcal{U})$ is a k-cycle on $\mathcal{U}$ relative to $\mathcal{U}_A$, and if $\mathcal{U} < \mathcal{V}$, then $\pi_{\mathcal{U}\mathcal{V}} z_k(\mathcal{V})$ is homologous to $z_k(\mathcal{U})$ relative to $\mathcal{U}_A$. Evidently, $\check{H}_k(X,\emptyset) = \check{H}_k(X)$ and $\check{H}_k(X,X) = 0$, for each integer k.

B Exactness axiom in Čech homology and Mayer-Vietoris sequence

In Čech homology theory all the Eilenberg-Steenrod axioms hold, except the exactness axiom. However, if some assumptions are made on the considered spaces and coefficients, this axiom also holds. Indeed, in [30], Chap. IX, Thm. 7.6 (see also [47]), we read the following result concerning the sequence of a pair (X,A)

$$\cdots \to \check{H}_{k+1}(X,A) \xrightarrow{\partial} \check{H}_k(A) \xrightarrow{i_*} \check{H}_k(X) \xrightarrow{j_*} \check{H}_k(X,A) \to \cdots \to \check{H}_0(X,A) \to 0$$

which, in general, is only of order 2 (this means that the composition of any two successive homomorphisms of the sequence is zero, i.e. im $\subseteq$ ker).

Theorem B.1. [30, Chap. IX, Thm. 7.6] *If (X,A) is compact and G is a vector space over a field, then the homology sequence of the pair (X,A) is exact.*

It follows that, if (X,A) is compact and G is a vector space over a field, Čech homology satisfies all the axioms of homology theories, and therefore all the general theorems in Chap. I of [30] also hold for Čech homology. In particular, using [30, Chap. I, Thm. 15.3], we have the exactness of the Mayer-Vietoris sequence in Čech homology:

Theorem B.2. *Let (X,A,B) be a compact proper triad and G be a vector space over a field. The Mayer-Vietoris sequence of (X,A,B) with $X = A \cup B$*

$$\cdots \to \check{H}_{k+1}(X) \xrightarrow{\Delta} \check{H}_k(A \cap B) \xrightarrow{\alpha} \check{H}_k(A) \oplus \check{H}_k(B) \xrightarrow{\beta} \check{H}_k(X) \to \cdots \to \check{H}_0(X) \to 0$$

is exact.

Concerning homomorphisms between Mayer-Vietoris sequences, from [30, Chap. I, Thm. 15.4], we deduce the following result.

Theorem B.3. *If (X,A,B) and (Y,C,D) are proper triads, $X = A \cup B$, $Y = C \cup D$, and $f : (X,A,B) \to (Y,C,D)$ is a map of one proper triad into another, then f induces a homomorphism of the Mayer-Vietoris sequence of (X,A,B) into that of (Y,C,D) such* *that commutativity holds in the diagram*

$$\begin{array}{ccccccccc} \cdots \to & \check{H}_{k+1}(X) & \to & \check{H}_k(A\cap B) & \to & \check{H}_k(A)\oplus\check{H}_k(B) & \to & \check{H}_k(X) & \to \cdots \\ & \downarrow & & \downarrow & & \downarrow & & \downarrow & \\ \cdots \to & \check{H}_{k+1}(Y) & \to & \check{H}_k(C\cap D) & \to & \check{H}_k(C)\oplus\check{H}_k(D) & \to & \check{H}_k(Y) & \to \cdots \end{array}$$

A relative form of the Mayer-Vietoris sequence, different from the one proposed in [30], is useful in Chapter 3. In order to obtain this sequence, we can adapt the construction explained in [41] to Čech homology and obtain the following result.

Theorem B.4. *If* (X,A,B) *and* (Y,C,D) *are compact proper triads with* $X = A\cup B$, $Y = C\cup D$, $Y \subseteq X$, $C \subseteq A$, $D \subseteq B$, *then there is a relative Mayer-Vietoris sequence of homology groups with coefficients in a vector space G over a field*

$$\cdots \to \check{H}_{k+1}(X,Y) \to \check{H}_k(A\cap B, C\cap D) \to \check{H}_k(A,C)\oplus\check{H}_k(B,D) \to \check{H}_k(X,Y) \to \cdots$$
$$\cdots \to \check{H}_0(X,Y) \to 0$$

that is exact.

Proof. Given a covering $\mathcal{U}$ of $\Sigma(X)$, we may consider the relative simplicial homology groups $H_k(\mathcal{U},\mathcal{U}_Y)$, $H_k(\mathcal{U}_A,\mathcal{U}_C)$, $H_k(\mathcal{U}_B,\mathcal{U}_D)$, $H_k(\mathcal{U}_{A\cap B},\mathcal{U}_{C\cap D})$, for every $k \geq 0$. For these groups the relative Mayer-Vietoris sequence

$$\cdots \to H_{k+1}(\mathcal{U},\mathcal{U}_Y) \to H_k(\mathcal{U}_{A\cap B},\mathcal{U}_{C\cap D}) \to H_k(\mathcal{U}_A,\mathcal{U}_C)\oplus H_k(\mathcal{U}_B,\mathcal{U}_D) \to H_k(\mathcal{U},\mathcal{U}_Y) \to \cdots$$

is exact (cf. [41, page 152]).

We now recall that the kth Čech homology group of a pair of spaces (X,Y) over G is the inverse limit of the system of groups $\{H_k(\mathcal{U},\mathcal{U}_Y,G),\pi_{\mathcal{U}\mathcal{V}}\}$ defined on the direct set of all open coverings of the pair (X,Y) (cf. [30, Chap. IX, Thm. 3.2 and Def. 3.3]). Since, given an inverse system of exact lower sequences, where all the terms of the sequence belong to the category of vector spaces over a field, the limit sequence is also exact (cf. [30, Chap. VII, Thm. 5.7] and [47]), the claim is proved. $\square$

The following result, concerning homomorphisms of relative Mayer-Vietoris exact sequences, holds. We omit the proof, which can be obtained in a standard way.

Theorem B.5. *If* (X,A,B), (Y,C,D), (X',A',B'), (Y',C',D') *are compact proper triads with* $X = A \cup B$, $Y = C \cup D$, $Y \subseteq X$, $C \subseteq A$, $D \subseteq B$, *and* $X' = A' \cup B'$, $Y' = C' \cup D'$, $Y' \subseteq X'$, $C' \subseteq A'$, $D' \subseteq B'$, *and* $f : X \to X'$ *is a map such that* $f(Y) \subseteq Y'$, $f(A) \subseteq A'$, $f(B) \subseteq B'$, $f(C) \subseteq C'$, $f(D) \subseteq D'$, *then* f *induces a homomorphism of the relative Mayer-Vietoris sequences such that commutativity holds in the diagram*

$$\begin{array}{ccccccccc}
\cdots \to & \check{H}_{k+1}(X,Y) & \to & \check{H}_k(A\cap B, C\cap D) & \to & \check{H}_k(A,C)\oplus\check{H}_k(B,D) & \to & \check{H}_k(X,Y) & \to \cdots \\
& \downarrow & & \downarrow & & \downarrow & & \downarrow & \\
\cdots \to & \check{H}_{k+1}(X',Y') & \to & \check{H}_k(A'\cap B', C'\cap D') & \to & \check{H}_k(A',C')\oplus\check{H}_k(B',D') & \to & \check{H}_k(X',Y') & \to \cdots
\end{array}$$

Bibliography

[1] M. Allili and D. Corriveau, *Topological analysis of shapes using Morse theory*, Comput. Vis. Image Underst. **105** (2007), 188–199.

[2] Y. A. Ban, H. Edelsbrunner and J. Rudolph, *Interface surfaces for protein-protein complexes*, Journal of the ACM **53** (2008), 361–378.

[3] S. Biasotti, D. Giorgi, B. Falcidieno and M.Spagnuolo, *Reeb graphs for shape analysis and applications*, Theorical Computer Science **392** 1-3 (2008), 5–22.

[4] S. Biasotti, A. Cerri, P. Frosini, D. Giorgi, C. Landi, *Multidimensional size functions for shape comparison*, Journal of Mathematical Imaging and Vision, **32** (2008), 161–179.

[5] T. K. Dey, H. Edelsbrunner and S. Guha, *Computational Topology*, in Advances in Discrete and Computational Geometry, **233**, Providence (1999), 109–143.

[6] S. Biasotti, L. De Floriani, B. Falcidieno, P. Frosini, D. Giorgi, C. Landi, L. Papaleo, M. Spagnuolo, *Describing shapes by geometrical-topological properties of real functions*, ACM Computing Surveys, **40** (4) (2008), 12:1–12:87.

[7] Biasotti S., Marini S., Spagnuolo M., Falcidieno B.: Sub-part correspondence by structural descriptors of 3D shapes. Computer-Aided Design **38** (9) (2006), 1002–1019.

[8] F. Cagliari, M. Ferri and P. Pozzi, *Size functions from a categorical viewpoint*, Acta Appl. Math. **67** (2001), 225–235.

[9] F. Cagliari, B. Di Fabio and M. Ferri, *One-Dimensional Reduction of Multidimensional Persistent Homology* (preprint), arXiv:math/0702713.

[10] F. Cagliari, L. Grasselli and C. Landi, *Presentations of morse homology for studying shape of manifolds*, Tech. Report, DISMI, Univ. di Modema e Reggio Emilia **10** (2001).

[11] G. Carlsson, A. Zomorodian, A. Collins, and L. Guibas, *Persistence barcodes for shapes*, International Journal of Shape Modeling **11** (2005), 149–187.

[12] G. Carlsson and A. Zomorodian, *The Theory of Multidimensional Persistence*, Symposium on Computational Geometry, June 6–8, 2007, Gyeongiu, South Korea (2007), 184–193.

[13] A. Cerri, M. Ferri and D. Giorgi, *Retrieval of trademark images by means of size functions*, Graph. Models **68** (5) (2006), 451–471.

[14] A. Cerri, P. Frosini *Necessary conditions for discontinuities of multidimensional size functions* (preprint), arXiv:0811.1868.

[15] J.S. Cho and J. Choi, *Contour-based partial object recognition using symmetry in image databases*, in SAC ’05: Proceedings of the 2005 ACM Symposium on Applied computing, Santa Fe, New Mexico (2005), 1190–1194.

[16] D. Cohen-Steiner, H. Edelsbrunner and J. Harer, *Stability of persistence diagrams*, Discrete and Computational Geometry **37** (1) (2007), 103–120.

[17] M. d’Amico, Δ^* *reduction of size graphs as a new algorithm for computing size functions of shapes* In: Proc. Internat. Conf. on Computer Vision, Pattern Recognition and Image Processing, Feb. 27-Mar. 3, 2000, Atlantic City, **2** (2000), 107–110.

[18] M. d’Amico, P. Frosini and C. Landi, *Optimal matching between reduced size functions*, Technical Report **35** (2003).

[19] M. d’Amico, P. Frosini, C. Landi, *Natural pseudo-distance and optimal matching between reduced size functions*, Acta Applicandae Mathematicae (in press).

[20] M. d'Amico, P. Frosini and C. Landi, *Using matching distance in size theory: A survey*, International Journal of Imaging Systems and Technology **16** (5) (2006), 154–161.

[21] F. Dibos, P. Frosini and D. Pasquignon, *The use of Size Functions for Comparison of Shapes through Differential Invariants*, Journal of Mathematical Imaging and Vision **21** (2) (2004), 107–118.

[22] B. Di Fabio, C. Landi, *Čech homology for shape recognition in the presence of occlusions* (preprint), arXiv:0807.0796.

[23] P. Donatini and P. Frosini, *Lower bounds for natural pseudodistances via size functions*, Archives of Inequalities and Applications **2** (2004), 1–12.

[24] P. Donatini, P. Frosini and C. Landi, *Deformation energy for size functions*, in Energy Minimization Methods in Computer Vision and Pattern Recognition, E.R. Hancock, M. Pelillo eds., Lecture Notes in Computer Science, **1654** Springer-Verlag (1999), 44–53.

[25] P. Donatini, P. Frosini and A. Lovato, *Size functions for signature recognition*, Proc. of the SPIE's Workshop "Vision Geometry VII", 3454 (1998), 178–183.

[26] H. Edelsbrunner, J. Harer. *Jacobi sets of multiple Morse functions*, Foundations of Computational Mathematics, Minneapolis 2002, Cambridge Univ. Press, England, 37–57.

[27] H. Edelsbrunner and J. Harer. *Persistent homology — a survey*, Contemporary Mathematics, **453** (2008), 257–282.

[28] H. Edelsbrunner, D. Letscher and A. Zomorodian, *Topological Persistence and Simplification*, Proc. 41st Ann. IEEE Sympos. Found Comput. Sci. (2000), 454–463.

[29] H. Edelsbrunner, D. Letscher and A. Zomorodian, *Topological Persistence and Simplification*, Discrete Comput. Geom. **28** (2002), 511–533.

[30] S. Eilenberg and N. Steenrod, *Foundations of algebraic topology*, Princeton University Press (1952).

[31] M. Ferri, C. Landi, *Representing size functions by complex polynomials*, Proc. Math. Met. in Pattern Recognition **9**, Moskow, November (1999), 16–19.

[32] M. Ferri, S. Lombardini, C. Pallotti, *Leukocyte classifications by size functions*, WACV94, (1994), 223–229.

[33] P. Frosini, *A distance for similarity classes of submanifolds of a Euclidean space*, Bulletin of the Australian Mathematical Society, **42** (3) (1990), 407–416.

[34] P. Frosini, *Measuring shapes by size functions*, in Proc. of SPIE, Intelligent Robots and Computer Vision X: Algorithms and Techniques, D. P. Casasent Ed., Boston, MA **1607** (1991), 122–133.

[35] C. Landi and P. Frosini, *New pseudodistances for the size function space*, Proc. SPIE **3168**, Vision Geometry VI, Robert A. Melter, Angela Y. Wu, Longin J. Latecki (eds.) (1997), 52–60.

[36] P. Frosini and C. Landi, *Size functions and formal series*, Appl. Algebra Engrg. Comm. Comput. **12** (2001), 327–349.

[37] P. Frosini and C. Landi, *Size functions as complete invariants for image recognition*, In: Proc. SPIE 4794 Vision Geometry XI, L. J. Latecki, D. M. Mount and A. Y. Wu eds. (2002), 101–109.

[38] P. Frosini and M. Mulazzani, *Size homotopy groups for computation of natural size distances*, Bull. Belg. Math. Soc. **6** (1999), 455–464.

[39] R. Ghrist, *Barcodes: The persistent topology of data*, Bull. Amer. Math. Soc. **45** (2008), 61–75.

[40] A. Ghosh and N. Petkov, *Robustness of shape descriptors to incomplete contour representations*, IEEE Trans. on Pattern Analysis and Machine Intelligence **27** (1) (2005), 1793–1804.

[41] A. Hatcher, *Algebraic topology*, Cambridge University Press (2002).

[42] J.G. Hocking and G.S. Young, *Topology*, Addison–Wesley Publishing Company (1961).

[43] M. Hoynck and J.-R. Ohm, *Shape retrieval with robustness against partial occlusion*, in IEEE Int. Conf. on Acoustics, Speech, and Signal Processing, Proceedings. (ICASSP '03), **3** (2003), III–593–6.

[44] D.P. Huttenlocher, G.A. Klanderman and W.J. Rucklidge, *Comparing images using the Hausdorff distance* IEEE Transactions on Pattern Analysis and Machine Intelligence, **15**(1993), 850–863

[45] A. Jaklic, A. Leonardis and F. Solina, *Segmentation and Recovery of Superquadrics*, Computational imaging and vision, Kluwer, Dordrecht, **20** (2000), ISBN 0-7923-6601-8.

[46] T. Kaczynski, K. Mischaikow and M. Mrozek, *Computational Homology*, Applied Mathematical Sciences, Springer-Verlag, New York **157** (2004).

[47] G. M. Kelly, *The exactness of Čech homology over a vector space*, Proc. Cambridge Philos. Soc. **57** (1961), 428–429.

[48] D. Kelly, J. McDonald, T. Lysaght and C. Markham, *Analysis of sign language gestures using size functions and principal component analysis*, Proc. 2008 Int. Machine Vision and Image Processing Conf. (2008), 31–36.

[49] G. Kovács, R. Vogels and G. A. Orban, *Selectivity of macaque inferior temporal neurons for partially occluded shapes*, The Journal of Neuroscience **15** (3) (1995), 1984–1997.

[50] L.J. Latecki, R. Lakämper, D. Wolter, *Optimal partial shape similarity*. Image Vision Comput. **23** (2) (2005), 227–236 .

[51] J. Milnor, *Morse Theory*, Princeton University Press, Princeton, NJ (1963).

[52] $http://www.imageprocessingplace.com/root\_files\_V3/image\_databases.htm$.

[53] G. Mori, S. Belongie and H. Malik, *Shape contexts enable efficient retrieval of similar shapes*, CVPR **1** (2001), 723–730.

[54] I. Stanganelli, A. Brucale, L. Calori, R. Gori, A. Lovato, S. Magi, B. Kopf, R. Bacchilega, V. Rapisarda, A. Testori, P.A. Ascierto, E. Simeone, M. Ferri, *Computer-aided diagnosis of melanocytic lesions*, Anticancer Res. **25** (2005), 4577–4582.

[55] K. B. Sun and B. J. Super, *Classification of Contour Shapes Using Class Segment Sets*, in CVPR '05: Proceedings of the 2005 IEEE Computer Society Conference on Computer Vision and Pattern Recognition (CVPR'05) **2** (2005), 727–733.

[56] M. Tanase and R. C. Veltkamp, *Part-based shape retrieval*, in MULTIMEDIA '05: Proceedings of the 13th annual ACM international conference on Multimedia, Hilton, Singapore (2005), 543–546.

[57] R.C. Veltkamp and M. Hagedoorn, *State-of-the-art in shape matching*, in M. Lew (Ed.), Principles of Visual Information Retrieval, Springer (2001), 87–119.

[58] C. Uras and A. Verri, *Invariant size functions*, Applications of Invariance in Computer Vision, J. L. Mundy, A. Zisserman, and D. Forsyth eds., Springer LNCS **825** (1994), 215–234.

[59] C. Uras and A. Verri, *Sign language recognition: an application of the theory of size functions*, Proceedings of the 6th British conference on Machine vision **2** (1995), 711–720.

[60] C. Uras and A. Verri, *Metric-topological approach to shape representation and recognition*, Image Vision Comput. **14** (1996), 189–207.

[61] C. Uras and A. Verri, *Aspect-based object recognition with size functions*, Proceedings of the 13th International Conference on Pattern Recognition **1** (1996), 682–686.

[62] C. Uras and A. Verri, *Computing size functions from edge maps*, Internat. J. Comput. Vision **23** (2) (1997), 169–183.

[63] R.C. Veltkamp, *Shape matching:similarity measures and algorithms* In Shape Modeling International (2001), 188–197.

[64] A. Verri, C. Uras, P. Frosini and M. Ferri, *On the use of size functions for shape analysis*, Biol. Cybern. **70** (1993), 99–107.

[65] R.L. Wilder, *Topology of manifolds*, American Mathematical Society (1949).

[66] H.J. Wolfson and I. Rigoutsos, *Geometric Hashing: An Overview*, IEEE Computational Science and Engineering, **4** (4) (1997), 10–21.